Published for SISSA by Springer

Received: *June 17, 2014*
Accepted: *August 6, 2014*
Published: *September 24, 2014*

Measurement of the Z/γ^* boson transverse momentum distribution in pp collisions at $\sqrt{s} = 7$ TeV with the ATLAS detector

The ATLAS collaboration

E-mail: atlas.publications@cern.ch

Abstract: This paper describes a measurement of the Z/γ^* boson transverse momentum spectrum using ATLAS proton-proton collision data at a centre-of-mass energy of $\sqrt{s} = 7$ TeV at the LHC. The measurement is performed in the $Z/\gamma^* \to e^+e^-$ and $Z/\gamma^* \to \mu^+\mu^-$ channels, using data corresponding to an integrated luminosity of 4.7 fb^{-1}. Normalized differential cross sections as a function of the Z/γ^* boson transverse momentum are measured for transverse momenta up to 800 GeV. The measurement is performed inclusively for Z/γ^* rapidities up to 2.4, as well as in three rapidity bins. The channel results are combined, compared to perturbative and resummed QCD calculations and used to constrain the parton shower parameters of Monte Carlo generators.

Keywords: Hadron-Hadron Scattering

ArXiv ePrint: 1406.3660

doi:10.1007/JHEP09(2014)145

JHEP09(2014)145

Contents

JHEP09(2014)145

1 Introduction

The transverse momentum distribution of W and Z bosons produced in hadronic collisions is a traditional probe of strong interaction dynamics. The low transverse momentum (p_{T}) range is governed by initial-state parton radiation (ISR) and the intrinsic transverse momentum of the initial-state partons inside the proton, and modeled using soft-gluon resummation [1] or parton shower models [2, 3]. Quark-gluon scattering dominates at high p_{T} and is described by perturbative QCD [4–6]. The correct modelling of the vector boson p_{T} distribution is important in many physics analyses at the LHC for which the production of W or Z bosons constitutes a significant background. Moreover, it is crucial for a precise measurement of the W boson mass. The transverse momentum distribution also probes the gluon density of the proton [7]. Vector boson p_{T} distribution measurements were published by ATLAS [8, 9] and CMS [10] based on 35–40 pb^{-1} of proton-proton collisions at a centre-of-mass energy of $\sqrt{s} = 7$ TeV. The typical precision of these measurements is 4% to 10%.

This paper presents a measurement of the normalized Z boson transverse momentum distribution (p_{T}^{Z}) with the ATLAS detector, in the $Z/\gamma^{*} \to e^{+}e^{-}$ and $Z/\gamma^{*} \to \mu^{+}\mu^{-}$ channels, using LHC proton-proton collision data taken in 2011 at a centre-of-mass energy of $\sqrt{s} = 7\,\mathrm{TeV}$ and corresponding to an integrated luminosity of 4.7 fb^{-1} [11]. The large integrated luminosity allows the measurement to be performed in three different Z boson rapidity (y_Z) bins, probing the transverse momentum dynamics over a wide range of the initial-state parton momentum fraction. With respect to previous results, the present analysis aims at reduced uncertainties, finer binning and extended measurement range.

Reconstructed from the final-state lepton kinematics, p_{T}^{Z} is affected by lepton energy and momentum measurement uncertainties. To minimize the impact of these uncertainties, the $\phi_{\eta}^{\star}$ observable[1] was introduced as an alternative probe of p_{T}^{Z} [12], pioneered at the Tevatron [13–15], and studied by ATLAS using the present data set [16] and LHCb [17]. The correlation between $\phi_{\eta}^{\star}$ and p_{T}^{Z} is, however, only partial and the good experimental resolution on $\phi_{\eta}^{\star}$ is counterbalanced by a reduced sensitivity to the underlying transverse momentum distribution; in addition, interpreting $\phi_{\eta}^{\star}$ as a probe of p_{T}^{Z} assumes that the final-state lepton angular correlations are correctly modeled. The measurement presented in this paper allows the effects of the Z boson transverse momentum and the lepton angular correlations to be disentangled unambiguously.

QCD predictions for the p_{T}^{Z} distribution are described in the next section. After a brief description of the experiment in section 3, the measurement is presented in sections 4–8. The results are compared to available QCD predictions in section 9 and used to constrain phenomenological models describing the low-p_{T}^{Z} region in section 10; the compatibility of the $\phi_{\eta}^{\star}$ measurement with the p_{T}^{Z}-constrained models is also tested. Section 11 concludes the paper.

2 QCD predictions

The measurements are compared to a representative set of theoretical predictions. They rely on perturbative QCD (pQCD) only, or include resummation of soft-gluon emissions. Resummation is treated either analytically, or using Monte Carlo methods.

Fully differential inclusive boson-production cross sections can be obtained to second order in the strong coupling constant α_{S} (NNLO) using the FEWZ3.1 [4–6] and DYNNLO1.3 [18, 19] programs. The $\mathcal{O}(\alpha_{\mathrm{S}}^{2})$ cross-section predictions are valid at large p_{T}^{Z}, where the cross section is dominated by the radiation of high-p_{T} gluons. At low p_{T}^{Z}, multiple soft-gluon emissions predominate and fixed-order pQCD predictions are not appropriate.

The RESBOS calculation relies on soft-gluon resummation at low p_{T}^{Z} and matches the $\mathcal{O}(\alpha_{\mathrm{S}}^{2})$ cross section at high p_{T}^{Z}. It simulates the vector boson decays but does not include a description of the hadronic activity in the event. Two versions are used here, which differ in the non-perturbative parameterization used to perform the resummation. The

[1] $\phi_{\eta}^{\star}$ is defined as $\tan(\phi_{\mathrm{acop}}/2)\sin\theta_{\eta}^{\star}$, with $\phi_{\mathrm{acop}} = \pi - \Delta\phi$ and $\theta_{\eta}^{\star} = \tanh[\Delta\eta/2]$, $\Delta\phi$ the opening angle between the Z boson decay leptons in the transverse plane, and $\Delta\eta = \eta^{-} - \eta^{+}$ the difference in pseudorapidity between the negatively and positively charged lepton.

JHEP09(2014)145

original parameterization [1] and a recent development [20] are referred to as ResBos-BLNY (NLO+NNLL) and ResBos-GNW (NNLO+NNLL), respectively, in this paper. Further predictions at $\mathcal{O}(\alpha_S^2)$ and including resummation terms at next-to-next-to-leading-logarithmic accuracy (NNLO+NNLL) were also obtained [21], primarily focusing on the $\phi_\eta^\star$ observable.

The Pythia [2] and Herwig [3] generators use the parton shower approach to describe the low-p_T^Z region and include an $\mathcal{O}(\alpha_S)$ matrix element for the emission of one hard parton. The NLO Monte Carlo generators Mc@nlo [22] and Powheg [23] consistently incorporate NLO QCD matrix elements into the parton shower frameworks of Herwig or Pythia. The Alpgen [24] and Sherpa [25] generators implement tree-level matrix elements for the generation of multiple hard partons in association with the boson for various parton multiplicities. The generators listed above are used in performing the measurement, as described in section 4.

The generators contain phenomenological parameters which are not constrained by the theory but can be adjusted to improve their description of the measured distributions. The ATLAS measurement is thus compared to the current state-of-the-art models. In section 10, the low-p_T^Z region is used to adjust the parton shower parameters in Pythia, used as full event generator or interfaced to Powheg.

3 The ATLAS detector

ATLAS [26] is a multipurpose detector[2] consisting of an inner tracking system (ID) inside a 2 T superconducting solenoid, electromagnetic and hadronic calorimeters and, outermost, a toroidal large acceptance muon spectrometer (MS), surrounding the interaction point with almost full coverage.

The ID allows precision tracking of charged particles for $|\eta| < 2.5$. The three innermost layers constitute the pixel detector. The semiconductor tracker, at intermediate radii, consists of four double-sided silicon strip layers allowing reconstruction of three-dimensional space points. The outer layers, made of straw tubes sensitive to transition radiation, complete the momentum measurement for $|\eta| < 2$ and provide ability to distinguish electrons from pions.

The calorimeters between the ID and the MS measure the energy of particles in the range $|\eta| < 4.9$. The high-granularity electromagnetic (EM) calorimeter is made of lead absorbers immersed in a liquid-argon active medium, and is divided into barrel ($|\eta| < 1.5$) and end-cap ($1.4 < |\eta| < 3.2$) regions. For $|\eta| < 2.5$, it is finely segmented in η and ϕ for position measurement and particle identification purposes, and has three layers in depth to enable longitudinal EM-shower reconstruction. The hadronic calorimeter surrounding the EM calorimeter is divided into a central part covering $|\eta| < 1.7$, made of alternating

[2] ATLAS uses a right-handed coordinate system with its origin at the nominal interaction point (IP) in the centre of the detector and the z-axis along the beam pipe. The x-axis points from the IP to the centre of the LHC ring, and the y-axis points upward. Cylindrical coordinates (r, ϕ) are used in the transverse plane, ϕ being the azimuthal angle around the beam pipe. The pseudorapidity is defined in terms of the polar angle θ as $\eta = -\ln\tan(\theta/2)$.

JHEP09(2014)145

steel and plastic scintillator tiles, and end-cap ($1.5 < |\eta| < 3.2$) and forward ($|\eta| < 4.9$) sections included in the liquid argon end-cap cryostats, and using copper and tungsten as absorbing material, respectively.

The MS, covering a range of $|\eta| < 2.7$, consists of three stations of drift tubes and cathode-strip chambers, which allow precise muon track measurements and of resistive-plate and thin-gap chambers for muon triggers and additional measurements of the ϕ coordinate.

4 Event simulation

The response of the ATLAS detector to generated Monte Carlo (MC) events is simulated [27] using GEANT4 [28] for the description of the ATLAS detector geometry, and the interaction of particles with the material defined by that geometry. These samples are used to model the signal, estimate the backgrounds and to correct the observed p_{T}^{Z} spectrum for detector effects back to the particle level, a procedure hereafter referred to as unfolding.

The MC signal samples used as baseline for the measurement are obtained using the POWHEG generator version r1556 interfaced with PYTHIA6.425 to model the parton shower, hadronization and underlying event with parameters set according to tune AUET2B [29]. POWHEG events are generated using the CT10 parton distribution function (PDF) set [30]. The predicted p_{T}^{Z} distribution is then modified to match that of PYTHIA6.425 with the AMBT1 tune [31], denoted by PYTHIA6-AMBT1, which agrees with the data within 5% accuracy [8]. These samples are referred to as POWHEG+PYTHIA6.

Additional signal samples, used for comparison, are based on PYTHIA6.425 with tune AUET2B and PDF set MRSTMCal [32] (referred to as PYTHIA6-AUET2B); MC@NLO4.01 with the CT10 PDF set, interfaced to HERWIG6.520 to model the parton shower and hadronization, and to JIMMY4.31 [33] for the simulation of multiple interactions, with parameters set according to tune AUET2 [34]; and finally SHERPA1.4.0 with the CT10 PDFs. The MC generators used in tuning studies described in section 10 are PYTHIA version 8.176 [35, 36] and POWHEG version r2314.

Background processes include $W^{\pm} \to \ell^{\pm}\nu$, $Z \to \tau^{+}\tau^{-}$ and $b\bar{b}, c\bar{c} \to \ell^{\pm} + X$ and are generated with PYTHIA6-AUET2B. The $t\bar{t}$ background sample is based on MC@NLO interfaced to HERWIG+JIMMY. Backgrounds from weak boson pair production are simulated using HERWIG+JIMMY, tuned with AUET2. All generators are interfaced to PHOTOS2.154 [37] and TAUOLA2.4 [38] to simulate QED final-state radiation (FSR) and τ-lepton decays, except SHERPA and PYTHIA8, which rely on their internal treatment. Photon-induced dilepton production, i.e. the double dissociative process $q\bar{q} \to \ell^{+}\ell^{-}$ and inelastic photon-induced $pp \to \ell^{+}\ell^{-}$, is simulated using HORACE [39] and HERWIG++ [40], interfaced to the MRST2004qed PDFs [41].

The MC events are simulated with additional interactions in the same or neighbouring bunch crossings to match the pile-up conditions during LHC operation, and are weighted to reproduce the distribution of the average number of interactions per bunch crossing in data.

JHEP09(2014)145

5 Event reconstruction and selection

Electrons are reconstructed from energy deposits measured in the EM calorimeter and matched to ID tracks. They are required to have $p_{\mathrm{T}} > 20\,\mathrm{GeV}$ and $|\eta| < 2.47$ excluding $1.37 < |\eta| < 1.52$, which corresponds to the transition region between the barrel and end-cap EM calorimeters. The electrons are identified using shower shape, track-cluster matching and transition radiation criteria [42]. The $Z/\gamma^* \to e^+e^-$ event trigger requires two such electrons with $p_{\mathrm{T}} > 12$ GeV. Muons are reconstructed from high-quality MS segments matched to ID tracks. They are required to have $p_{\mathrm{T}} > 20$ GeV, $|\eta| < 2.4$ and to be isolated to suppress background from heavy-flavour decays. The isolation requires the sum of transverse momenta of additional tracks with $p_{\mathrm{T}} > 1$ GeV and within a cone of size $\Delta R \equiv \sqrt{(\Delta\eta)^2 + (\Delta\phi)^2} = 0.2$ around the muon to be less than 10% of the muon p_{T}. The $Z/\gamma^* \to \mu^+\mu^-$ event trigger requires one muon with $p_{\mathrm{T}} > 18$ GeV.

Events are required to have at least one primary vertex reconstructed from at least three tracks with $p_{\mathrm{T}} > 500\,\mathrm{MeV}$, and to contain exactly two oppositely charged same flavour leptons, selected as described above, with invariant mass satisfying $66\ \mathrm{GeV} < m_{\ell\ell} < 116\ \mathrm{GeV}$ ($\ell = e, \mu$). This broad interval is chosen to minimize the impact of QED FSR on the signal acceptance. The total selected sample consists of 1228863 $Z/\gamma^* \to e^+e^-$ and 1816784 $Z/\gamma^* \to \mu^+\mu^-$ candidate events.

Monte Carlo events are corrected to take into account differences with data in lepton reconstruction, identification and trigger efficiencies, as well as energy and momentum scale and resolution. The efficiencies are determined using a tag-and-probe method based on reconstructed Z and W events [42]. The isolation requirement used in the muon channel induces significant p_{T}^Z dependence in the muon selection efficiency, and the efficiency determination is repeated in each p_{T}^Z bin. The energy resolution and scale corrections are obtained comparing the lepton pair invariant mass distribution in data and simulation [43, 44].

6 Background estimation

The background to the observed Z signal includes contributions from $Z/\gamma^* \to \tau^+\tau^-$, $W \to \ell\nu$, gauge boson pair production, single top quark and $t\bar{t}$ production, and multijet production. The electroweak and top quark background contributions are estimated from simulation and normalized using theoretical cross sections calculated at NNLO accuracy. For the multijet background, which dominates at low p_{T}^Z, the leptons originate from semileptonic decays or from hadrons or photons misidentified as electrons, which cannot be simulated accurately and are determined using data-driven methods.

In the electron channel, the multijet background fraction is determined from the electron isolation distribution observed in data. The isolation variable, x, is defined as the transverse energy contained in a cone of size $\Delta R = 0.3$ around the electron energy cluster (excluding the electron itself), divided by the electron transverse energy. On average, isolated electrons from $Z/\gamma^* \to e^+e^-$ decays are expected at lower values of x than multijet background events. The signal distribution, $S(x)$, is given by the simulation and shifted to

JHEP09(2014)145

match the data in the signal-dominated low-x region. A jet-enriched sample is extracted from data by requiring electron candidates to fail the track-cluster matching or shower shape criteria in the first EM calorimeter layer, but otherwise pass the analysis selections, giving $B(x)$. This distribution is corrected for the residual contribution from electroweak and top quark backgrounds, which are estimated using simulation. The multijet background normalization is then given by a fit of $D(x) = qB(x) + (1-q)S(x)$, where $D(x)$ is the isolation distribution observed in data and q is the fitted background fraction. The above procedure is repeated, separating events with same charge sign (SS) and opposite charge sign (OS) leptons in the background-enriched sample, and varying ΔR between 0.2 and 0.4. The average of the results and their envelope define the multijet background fraction and its uncertainty, yielding $q = (0.14^{+0.10}_{-0.05})\%$. The p_{T}^{Z} shape of the background is assumed to follow that of the background-enriched sample; this assumption is verified by repeating the procedure in three coarse p_{T}^{Z} bins. The uncertainty on the shape is defined from the difference between the SS and OS samples.

In the muon channel, the multijet background is estimated using muon isolation information in signal- and background-dominated invariant-mass regions. Four two-dimensional regions are defined, characterized by a mass window and according to whether both muons pass or fail the isolation cut described in section 5. The signal region (region A), the two control regions (regions B and C) and the multijet region (region D) are defined as follows:

Region A (signal region):	66 GeV $< m_{\mu\mu} <$ 116 GeV,	isolated
Region B:	47 GeV $< m_{\mu\mu} <$ 60 GeV,	isolated
Region C:	66 GeV $< m_{\mu\mu} <$ 116 GeV,	non-isolated
Region D (multijet region):	47 GeV $< m_{\mu\mu} <$ 60 GeV,	non-isolated

Assuming the $m_{\mu\mu}$ and isolation distributions are not correlated, the number of multijet events in the signal region is determined from the number of events observed in regions B, C and D, as $n_{\mathrm{A}} = n_{\mathrm{B}} \times n_{\mathrm{C}}/n_{\mathrm{D}}$, where n_{B}, n_{C} and n_{D} are corrected for the residual contribution from electroweak and top processes. In an alternative method, the multijet background is assumed to be dominated by heavy-flavour decays, and its normalization is derived from the number of observed SS muon pairs, corrected by the expected OS/SS ratio in heavy-flavour jet events, as predicted by Pythia. Since the results of the two methods differ by more than their estimated uncertainty, the background normalization used for this channel is defined as the average of the two computations, and its uncertainty as their half difference, giving an expected fraction of $(0.11 \pm 0.06)\%$. The p_{T}^{Z} shape of the multijet background is defined from the control sample with the inverted isolation cut (region D); using that obtained from the SS sample instead has negligible impact on the measurement result.

Figure 1 shows the p_{T}^{Z} distributions for data and Monte Carlo samples including the experimental corrections discussed in section 5 as well as the background estimates, in the electron and muon channels.

JHEP09(2014)145

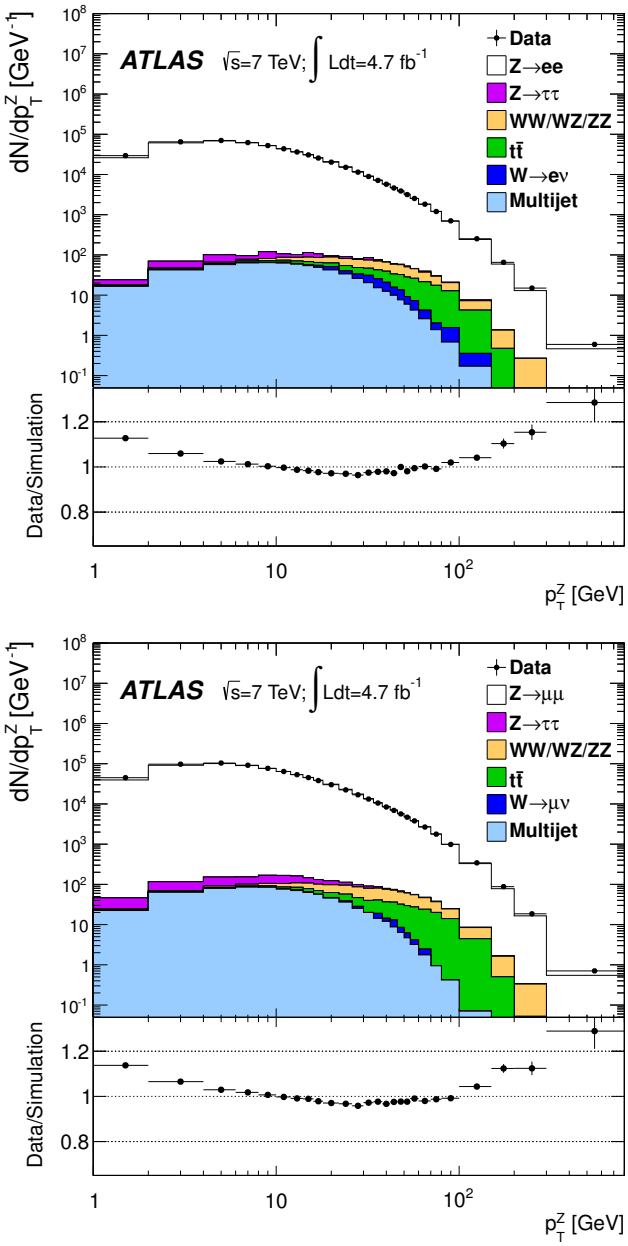

Figure 1. Distributions of p_{T}^{Z} for data and simulation, and their ratios, in the electron channel (top) and muon channel (bottom). The plots show statistical uncertainties only.

7 Unfolding and systematic uncertainties

The normalized differential cross section as a function of p_{T}^{Z} is defined as $(1/\sigma^{\mathrm{fid}})(\mathrm{d}\sigma^{\mathrm{fid}}/\mathrm{d}p_{\mathrm{T}}^{Z})$, where σ^{fid} is the inclusive $pp \to Z/\gamma^{*}$ cross section measured within the fiducial acceptance defined by requiring $p_{\mathrm{T}} > 20\,\mathrm{GeV}$ and $|\eta| < 2.4$ for the decay leptons; the invariant mass of the pair must satisfy $66 < m_{\ell\ell} < 116\,\mathrm{GeV}$. In addition to the rapidity-inclusive measurement, the measurement is performed for $0 \leq |y_Z| < 1$, $1 \leq |y_Z| < 2$ and $2 \leq |y_Z| < 2.4$.

JHEP09(2014)145

The measurement is performed for three definitions of the particle-level final-state kinematics. The Born and bare kinematics are defined from the decay lepton kinematics before and after FSR, respectively. The dressed kinematics are defined by combining the bare momentum of each lepton with that of photons radiated within a distance smaller than $\Delta R = 0.1$. Conversion factors from the Born to the bare and dressed levels are defined from the ratio of the corresponding particle-level p_{T}^{Z} distributions and denoted by $k_{\mathrm{bare}}(p_{\mathrm{T}}^{Z})$ and $k_{\mathrm{dressed}}(p_{\mathrm{T}}^{Z})$, respectively.

The Z/γ^{*} transverse momentum is reconstructed from the measured lepton four-momenta. The p_{T}^{Z} range is divided into 26 bins of varying width between 0 GeV and 800 GeV, with finer granularity in the low-p_{T}^{Z} range, as shown in tables 1–3. The bin purity, defined as the fraction of reconstructed events for which p_{T}^{Z} falls in the same bin at reconstruction and particle level, is everywhere above 50%.

The total background is subtracted from the observed p_{T}^{Z} distribution. The electroweak background cross sections are assigned a 5% uncertainty derived by varying the PDFs within their uncertainties and from QCD renormalization and factorization scale variations; in addition, a relative uncertainty of 1.8% on the total integrated luminosity is taken into account. The normalization of the top background was verified comparing data and simulation at high missing transverse energy ($E_{\mathrm{T}}^{\mathrm{miss}}$), defined for each event as the total transverse momentum imbalance of the reconstructed objects. An uncertainty of 12% is assigned comparing data and simulation for $E_{\mathrm{T}}^{\mathrm{miss}} > 100\,\mathrm{GeV}$ and $20 < p_{\mathrm{T}}^{Z} < 120\,\mathrm{GeV}$, where this background contribution dominates. The multijet background uncertainty is discussed in section 6.

The p_{T}^{Z} distribution is subsequently corrected for resolution effects and QED final-state radiation back to the Born level, as well as for the differences between the reconstruction- and particle-level fiducial acceptance, with an iterative Bayesian unfolding method [45–47]; three iterations are used. The response matrix used for the unfolding is defined as a two-dimensional histogram correlating the Born-level and reconstructed p_{T}^{Z} distributions. The prior probability distribution for the Born-level p_{T}^{Z} distribution is defined from the modified POWHEG+PYTHIA6 prediction described in section 4, and matches that of PYTHIA6-AMBT1.

The statistical uncertainty on the unfolded spectrum is obtained by generating random replicas of the reconstruction-level p_{T}^{Z} distribution. For each trial, Poisson-distributed fluctuations are applied to the number of entries in each bin, and the measurement procedure is repeated. The obtained ensemble of fluctuated measurement results is used to fill a covariance matrix, including correlations between the bins introduced by the unfolding and normalization procedure. The relative statistical uncertainty remains below 0.6% for $p_{\mathrm{T}}^{Z} < 30\,\mathrm{GeV}$ in both channels, and below 1.1% up to 150 GeV. The uncertainty induced by the size of the MC samples is determined by applying the same method to the response matrix, and stays below 0.4% and 0.5% up to $p_{\mathrm{T}}^{Z} = 150$ GeV in the muon and electron channel, respectively, reaching 2% for the bin $300 < p_{\mathrm{T}}^{Z} < 800$ GeV.

Systematic uncertainties from experimental sources such as trigger, reconstruction and identification efficiency corrections, energy scale and resolution corrections, and the background normalization and p_{T} distribution are evaluated by repeating the analysis varying

JHEP09(2014)145

the corresponding parameters within their uncertainties and comparing to the nominal result. For each channel, the impact of a given source of uncertainty is evaluated preserving correlations across the measurement range. The uncertainty on the normalization of the electroweak and top quark backgrounds is treated as fully correlated between the two channels. The electron- and muon-specific uncertainties are uncorrelated between channels.

In the electron channel, the uncertainties on the trigger, reconstruction and identification efficiency corrections are propagated preserving their correlations across lepton η and p_{T}. These sources contribute a relative uncertainty of the order of 10^{-4} up to $p_{\mathrm{T}}^{Z} = 100$ GeV and less than 0.2% over the full measurement range. The uncertainty induced by the background subtraction is typically 0.1%, except around $p_{\mathrm{T}}^{Z} = 100$ GeV where it reaches 0.3% because of the top quark background contribution. The uncertainty induced by charge misidentification, estimated from the difference between the results obtained with and without an opposite-sign requirement on the leptons, amounts to less than 0.2% over the whole p_{T}^{Z} range. The dominant experimental uncertainties in the electron channel arise from the electron energy scale, resolution, mis-modelling of the electron energy tails caused by uncertainties in the treatment of electron multiple scattering in GEANT4 and in passive detector material. The combined contribution from energy scale and resolution uncertainties to the total systematic uncertainty is typically 0.3% per bin between 4 GeV and 70 GeV, and reaches about 2% at the end of the spectrum. The uncertainty from the energy tails amounts to 0.8% at most, contributing mainly at very low p_{T}^{Z} and at very high p_{T}^{Z} where the statistical uncertainty dominates.

In the muon channel, the trigger, reconstruction and isolation efficiency corrections contribute an uncertainty of 0.6% on average, spanning 0.2% to 1.7% across the measurement range. The momentum scale and resolution uncertainties amount to 0.2%, except in the last three p_{T}^{Z} bins where they stay below 1.5%. The uncertainty contributed by the background subtraction is below 0.1% over the whole p_{T}^{Z} range except around $p_{\mathrm{T}}^{Z} = 100$ GeV where it reaches 0.13% because of the top quark background contribution.

The dominant contribution to the systematic uncertainties for both channels comes from the unfolding method. Two effects are addressed: the bias of the result towards the prior, and the dependence of the result on the theoretical calculation used to determine the response matrix. The first item is evaluated by repeating the measurement using the nominal result as the prior. The difference between the nominal result and this iteration is less than 0.1% up to 100 GeV, and less than 1.3% for the rest of the distribution. The second effect is evaluated by unfolding the p_{T}^{Z} distribution using an alternative response matrix, constructed from a $Z/\gamma^{*} \to \ell^{+}\ell^{-}$ sample obtained with MC@NLO instead of POWHEG, and modified to match the PYTHIA6-AMBT1 spectrum as it was done for POWHEG. A systematic uncertainty of about 0.3% over the whole p_{T}^{Z} range is assigned from the difference between the two results. The PDF uncertainties are estimated by reweighting the baseline sample to each of the CT10 PDF error sets [30] and repeating the unfolding. In each bin, the sum in quadrature of deviations with respect to the nominal result is used to define the associated uncertainty, which is below 0.1% up to 60 GeV and below 0.3% over the remaining p_{T}^{Z} range. The unfolding systematic uncertainties are assumed to be fully correlated between the electron and muon channels.

JHEP09(2014)145

The uncertainty arising from the accuracy of the theoretical description of QED FSR is obtained by comparing $k_{\text{bare}}(p_{\text{T}}^{Z})$ and $k_{\text{dressed}}(p_{\text{T}}^{Z})$ as predicted by PHOTOS and SHERPA. The differences obtained for $k_{\text{bare}}(p_{\text{T}}^{Z})$ are representative of the QED uncertainty in the muon channel, and amount to 0.3% across the p_{T}^{Z} distribution. From the differences obtained for $k_{\text{dressed}}(p_{\text{T}}^{Z})$, a 0.1% uncertainty is assigned to the electron channel. Photon-induced dilepton production is significant only in the lowest p_{T}^{Z} bin (0-2 GeV), where it contributes 0.4%. The cross sections obtained for this process when evaluating the MRST2004qed PDFs in the current and constituent quark mass schemes differ by 30%, and contribute an uncertainty of 0.1% to the measurement in this bin.

Figure 2 presents the contributions from the different uncertainties to the inclusive p_{T}^{Z} measurement integrated over the Z rapidity.

8 Results

The inclusive normalized cross sections $(1/\sigma^{\text{fid}})(\text{d}\sigma^{\text{fid}}/\text{d}p_{\text{T}}^{Z})$ measured in the $Z/\gamma^{*} \to e^{+}e^{-}$ and $Z/\gamma^{*} \to \mu^{+}\mu^{-}$ channels are presented in table 1 including statistical, uncorrelated and correlated systematic uncertainties. The sizes of the correlated uncertainties depend on the channel because of different resolutions and background levels. The measurement results are reported at Born level and factors k_{bare} and k_{dressed} are given to translate to the bare and dressed levels. In each channel, the total uncertainty is between 0.5% and 1% for $p_{\text{T}}^{Z} < 30$ GeV, below 1.5% per bin up to $p_{\text{T}}^{Z} = 150$ GeV and rises to 7% at the end of the spectrum.

The electron- and muon-channel cross sections are combined using χ^2 minimization, following the best linear unbiased estimator prescription (BLUE) [48, 49]. The combination is performed for the Born-level and dressed-level distributions. When building the χ^2, the measurement uncertainties are categorized into uncorrelated and correlated sources. Table 2 presents the combined results for the inclusive measurement for Born level and dressed lepton kinematics. The combined precision is between 0.5% and 1.1% for $p_{\text{T}}^{Z} < 150$ GeV, rising to 5.5% towards the end of the spectrum. The combination has $\chi^2/\text{dof} = 12.3/25$ (χ^2 per degree of freedom). The individual channels are compared to the combined result in figure 3.

The measurements are repeated in three exclusive boson rapidity bins, namely $0 \leq |y_Z| < 1$, $1 \leq |y_Z| < 2$ and $2 \leq |y_Z| < 2.4$. The combined results, corrected to the Born level, are given in table 3 with statistical, correlated and uncorrelated systematic uncertainties for the three rapidity bins. The measurement results in each channel and their combination are illustrated in figures 4–6.

9 Comparison to QCD predictions

In figure 7, the Born-level combined result is compared to theoretical predictions at fixed order from FEWZ and DYNNLO, to RESBOS and to the NNLO+NNLL calculation of ref. [21]. FEWZ, DYNNLO and RESBOS use the CT10 PDFs, while the NNLO+NNLL calculation of ref. [21] uses the CTEQ6m PDFs [50].

JHEP09(2014)145

	$Z/\gamma^* \to e^+e^-$					$Z/\gamma^* \to \mu^+\mu^-$					Common	
p_{T} range	$\frac{1}{\sigma^{\mathrm{fid}}}\frac{\mathrm{d}\sigma^{\mathrm{fid}}}{\mathrm{d}p_{\mathrm{T}}^Z}$ [1/ GeV]			δ_{Stat}	$\delta_{\mathrm{Syst}}^{\mathrm{uncor}}$	$\frac{1}{\sigma^{\mathrm{fid}}}\frac{\mathrm{d}\sigma^{\mathrm{fid}}}{\mathrm{d}p_{\mathrm{T}}^Z}$ [1/ GeV]			δ_{Stat}	$\delta_{\mathrm{Syst}}^{\mathrm{uncor}}$	$\delta_{\mathrm{Syst}}^{\mathrm{cor}}$	$\delta_{\mathrm{Syst}}^{\mathrm{cor}}$
[GeV]	Born	k_{bare}	k_{dressed}	[%]	[%]	Born	k_{bare}	k_{dressed}	[%]	[%]	ee [%]	$\mu\mu$ [%]
0–2	$2.811\ 10^{-2}$	0.916	0.974	0.42	0.85	$2.836\ 10^{-2}$	0.953	0.974	0.35	0.50	0.36	0.36
2–4	$5.840\ 10^{-2}$	0.935	0.980	0.26	0.76	$5.833\ 10^{-2}$	0.964	0.980	0.22	0.43	0.35	0.34
4–6	$5.806\ 10^{-2}$	0.969	0.990	0.26	0.39	$5.800\ 10^{-2}$	0.982	0.990	0.22	0.35	0.36	0.36
6–8	$4.908\ 10^{-2}$	1.002	1.000	0.28	0.31	$4.929\ 10^{-2}$	1.002	1.000	0.24	0.35	0.36	0.36
8–10	$4.074\ 10^{-2}$	1.025	1.007	0.31	0.43	$4.082\ 10^{-2}$	1.014	1.007	0.27	0.44	0.34	0.34
10–12	$3.381\ 10^{-2}$	1.040	1.012	0.35	0.49	$3.375\ 10^{-2}$	1.023	1.012	0.30	0.45	0.34	0.34
12–14	$2.815\ 10^{-2}$	1.055	1.016	0.37	0.42	$2.814\ 10^{-2}$	1.031	1.016	0.33	0.46	0.34	0.34
14–16	$2.374\ 10^{-2}$	1.060	1.017	0.42	0.38	$2.376\ 10^{-2}$	1.032	1.017	0.35	0.46	0.34	0.34
16–18	$2.014\ 10^{-2}$	1.060	1.017	0.47	0.38	$2.011\ 10^{-2}$	1.032	1.016	0.39	0.48	0.34	0.34
18–22	$1.598\ 10^{-2}$	1.052	1.016	0.40	0.32	$1.593\ 10^{-2}$	1.029	1.016	0.33	0.47	0.34	0.34
22–26	$1.199\ 10^{-2}$	1.033	1.010	0.48	0.31	$1.201\ 10^{-2}$	1.018	1.010	0.39	0.50	0.36	0.36
26–30	$9.164\ 10^{-3}$	1.021	1.006	0.54	0.33	$9.172\ 10^{-3}$	1.010	1.006	0.44	0.53	0.36	0.36
30–34	$7.236\ 10^{-3}$	1.007	1.003	0.62	0.38	$7.256\ 10^{-3}$	1.006	1.003	0.50	0.54	0.35	0.35
34–38	$5.806\ 10^{-3}$	0.997	1.000	0.70	0.40	$5.800\ 10^{-3}$	0.999	1.000	0.56	0.58	0.35	0.35
38–42	$4.666\ 10^{-3}$	0.992	0.999	0.78	0.45	$4.619\ 10^{-3}$	0.997	0.999	0.63	0.63	0.35	0.35
42–46	$3.760\ 10^{-3}$	0.990	0.998	0.84	0.49	$3.795\ 10^{-3}$	0.992	0.998	0.68	0.68	0.35	0.34
46–50	$3.216\ 10^{-3}$	0.977	0.995	0.90	0.53	$3.137\ 10^{-3}$	0.990	0.995	0.73	0.66	0.37	0.37
50–54	$2.604\ 10^{-3}$	0.982	0.996	1.04	0.59	$2.586\ 10^{-3}$	0.987	0.996	0.82	0.68	0.37	0.36
54–60	$2.097\ 10^{-3}$	0.972	0.994	0.98	0.55	$2.113\ 10^{-3}$	0.986	0.994	0.79	0.65	0.38	0.36
60–70	$1.501\ 10^{-3}$	0.966	0.992	0.86	0.52	$1.484\ 10^{-3}$	0.982	0.992	0.72	0.71	0.39	0.36
70–80	$9.820\ 10^{-4}$	0.959	0.989	1.08	0.56	$9.886\ 10^{-4}$	0.976	0.989	0.89	0.78	0.44	0.39
80–100	$5.599\ 10^{-4}$	0.955	0.991	0.96	0.50	$5.449\ 10^{-4}$	0.979	0.991	0.81	0.83	0.46	0.39
100–150	$1.920\ 10^{-4}$	0.957	0.991	0.96	0.74	$1.917\ 10^{-4}$	0.976	0.991	0.83	0.83	0.67	0.62
150–200	$4.809\ 10^{-5}$	0.953	0.994	1.86	1.02	$4.982\ 10^{-5}$	0.975	0.994	1.70	1.11	0.64	0.60
200–300	$1.085\ 10^{-5}$	0.950	0.995	2.76	2.51	$1.074\ 10^{-5}$	0.974	0.995	2.58	1.99	1.33	1.34
300–800	$3.910\ 10^{-7}$	0.949	0.995	6.05	3.12	$4.047\ 10^{-7}$	0.958	0.995	5.84	3.20	1.35	1.30

Table 1. The measured normalized cross section $(1/\sigma^{\mathrm{fid}})(\mathrm{d}\sigma^{\mathrm{fid}}/\mathrm{d}p_{\mathrm{T}}^Z)$ in bins of p_{T}^Z for the $Z/\gamma^* \to e^+e^-$ and $Z/\gamma^* \to \mu^+\mu^-$ channels, and correction factors to the bare- and dressed-level cross sections. The relative statistical and total uncorrelated systematic uncertainties are given for each channel as well as the correlated systematic uncertainties.

p_{T} range [GeV]	Born $\frac{1}{\sigma^{\mathrm{fid}}}\frac{\mathrm{d}\sigma^{\mathrm{fid}}}{\mathrm{d}p_{\mathrm{T}}^{Z}}$ [1/ GeV]	Dressed $\frac{1}{\sigma^{\mathrm{fid}}}\frac{\mathrm{d}\sigma^{\mathrm{fid}}}{\mathrm{d}p_{\mathrm{T}}^{Z}}$ [1/ GeV]	δ_{Stat} [%]	$\delta_{\mathrm{Syst}}^{\mathrm{uncor}}$ [%]	$\delta_{\mathrm{Syst}}^{\mathrm{cor}}$ [%]
0–2	$2.822\ 10^{-2}$	$2.750\ 10^{-2}$	0.27	0.37	0.36
2–4	$5.840\ 10^{-2}$	$5.723\ 10^{-2}$	0.17	0.32	0.35
4–6	$5.805\ 10^{-2}$	$5.749\ 10^{-2}$	0.17	0.23	0.36
6–8	$4.917\ 10^{-2}$	$4.920\ 10^{-2}$	0.18	0.22	0.36
8–10	$4.076\ 10^{-2}$	$4.103\ 10^{-2}$	0.20	0.24	0.34
10–12	$3.380\ 10^{-2}$	$3.420\ 10^{-2}$	0.23	0.26	0.34
12–14	$2.815\ 10^{-2}$	$2.860\ 10^{-2}$	0.25	0.26	0.34
14–16	$2.375\ 10^{-2}$	$2.415\ 10^{-2}$	0.27	0.26	0.34
16–18	$2.012\ 10^{-2}$	$2.046\ 10^{-2}$	0.30	0.27	0.34
18–22	$1.595\ 10^{-2}$	$1.621\ 10^{-2}$	0.25	0.25	0.34
22–26	$1.200\ 10^{-2}$	$1.212\ 10^{-2}$	0.30	0.28	0.36
26–30	$9.166\ 10^{-3}$	$9.223\ 10^{-3}$	0.34	0.31	0.36
30–34	$7.242\ 10^{-3}$	$7.267\ 10^{-3}$	0.39	0.33	0.35
34–38	$5.802\ 10^{-3}$	$5.803\ 10^{-3}$	0.44	0.35	0.35
38–42	$4.641\ 10^{-3}$	$4.636\ 10^{-3}$	0.49	0.39	0.35
42–46	$3.777\ 10^{-3}$	$3.769\ 10^{-3}$	0.53	0.43	0.35
46–50	$3.172\ 10^{-3}$	$3.157\ 10^{-3}$	0.57	0.43	0.37
50–54	$2.593\ 10^{-3}$	$2.582\ 10^{-3}$	0.64	0.46	0.37
54–60	$2.104\ 10^{-3}$	$2.091\ 10^{-3}$	0.61	0.43	0.37
60–70	$1.492\ 10^{-3}$	$1.480\ 10^{-3}$	0.55	0.44	0.38
70–80	$9.851\ 10^{-4}$	$9.738\ 10^{-4}$	0.69	0.49	0.43
80–100	$5.525\ 10^{-4}$	$5.474\ 10^{-4}$	0.62	0.49	0.44
100–150	$1.918\ 10^{-4}$	$1.901\ 10^{-4}$	0.63	0.53	0.65
150–200	$4.891\ 10^{-5}$	$4.860\ 10^{-5}$	1.26	0.72	0.63
200–300	$1.081\ 10^{-5}$	$1.075\ 10^{-5}$	1.88	1.40	1.33
300–800	$3.985\ 10^{-7}$	$3.966\ 10^{-7}$	4.20	2.04	1.32

Table 2. The measured normalized combined (electron and muon channels) cross section $(1/\sigma^{\mathrm{fid}})(\mathrm{d}\sigma^{\mathrm{fid}}/\mathrm{d}p_{\mathrm{T}}^{Z})$, inclusive in rapidity. The cross sections at Born and dressed levels are given as well as the relative statistical (δ_{Stat}) and total systematic (δ_{Syst}) for uncorrelated and correlated sources.

JHEP09(2014)145

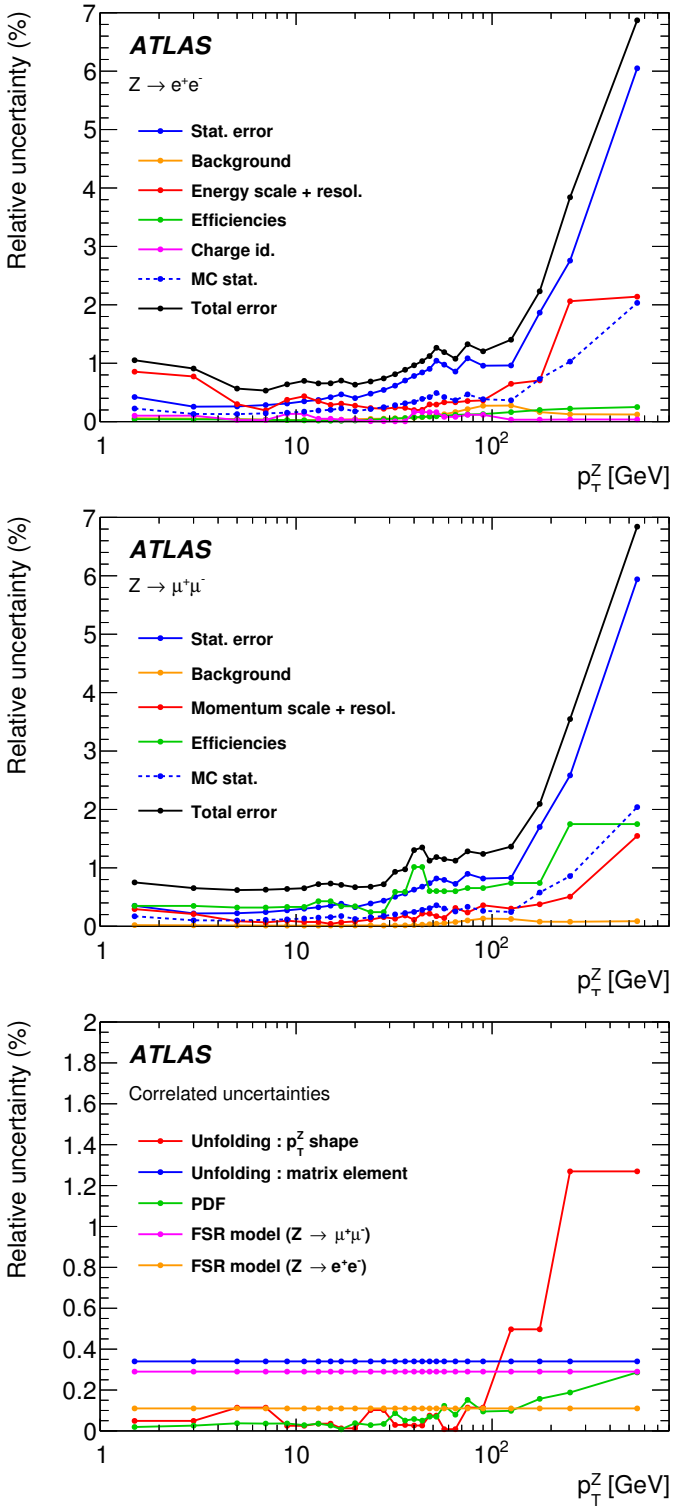

Figure 2. Summary of uncertainties for the y_Z-integrated measurement, given as a percentage of the central value of the bin. Electron channel (top), muon channel (middle), correlated uncertainties (bottom).

JHEP09(2014)145

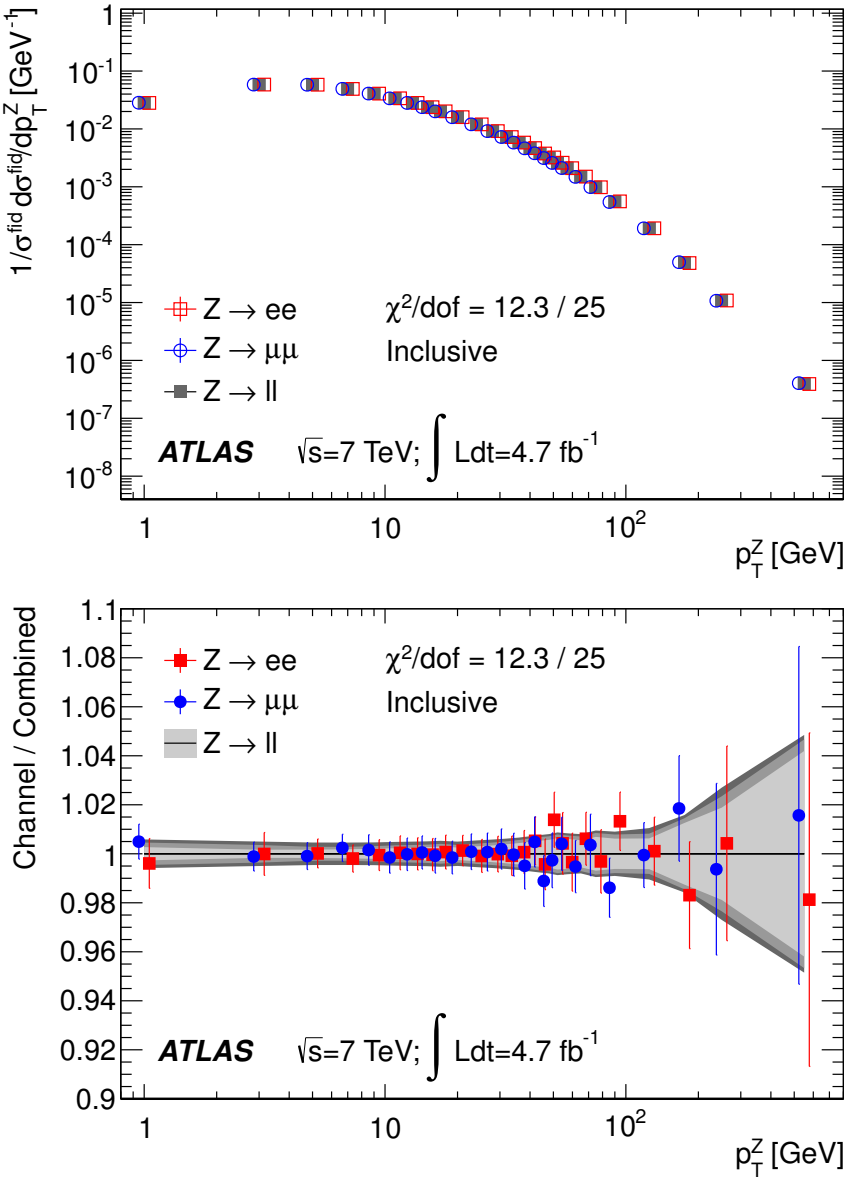

Figure 3. The measured inclusive normalized cross section $(1/\sigma^{\mathrm{fid}})(\mathrm{d}\sigma^{\mathrm{fid}}/\mathrm{d}p_{\mathrm{T}}^{Z})$ as a function of p_{T}^{Z} for the electron and muon channels and the combined result (top). Ratio of the electron and muon channels to the combined result (bottom). The uncertainty bands represent the statistical, total uncorrelated and total uncertainties, from light gray to dark gray respectively.

JHEP09(2014)145

p_T range	$0 \leq \|y_Z\| < 1$					$1 \leq \|y_Z\| < 2$					$2 \leq \|y_Z\| < 2.4$				
	Born $\frac{1}{\sigma^{fid}}\frac{d\sigma^{fid}}{dp_T^Z}$	Dressed $\frac{1}{\sigma^{fid}}\frac{d\sigma^{fid}}{dp_T^Z}$	δ_{Stat}	δ_{Syst}^{uncor}	δ_{Syst}^{cor}	Born $\frac{1}{\sigma^{fid}}\frac{d\sigma^{fid}}{dp_T^Z}$	Dressed $\frac{1}{\sigma^{fid}}\frac{d\sigma^{fid}}{dp_T^Z}$	δ_{Stat}	δ_{Syst}^{uncor}	δ_{Syst}^{cor}	Born $\frac{1}{\sigma^{fid}}\frac{d\sigma^{fid}}{dp_T^Z}$	Dressed $\frac{1}{\sigma^{fid}}\frac{d\sigma^{fid}}{dp_T^Z}$	δ_{Stat}	δ_{Syst}^{uncor}	δ_{Syst}^{cor}
[GeV]	[1/ GeV]	[1/ GeV]	[%]	[%]	[%]	[1/ GeV]	[1/ GeV]	[%]	[%]	[%]	[1/ GeV]	[1/ GeV]	[%]	[%]	[%]
0–2	$2.861\ 10^{-2}$	$2.792\ 10^{-2}$	0.37	0.34	0.36	$2.781\ 10^{-2}$	$2.704\ 10^{-2}$	0.42	0.48	0.37	$2.71\ 10^{-2}$	$2.63\ 10^{-2}$	1.3	1.0	0.5
2–4	$5.874\ 10^{-2}$	$5.763\ 10^{-2}$	0.23	0.31	0.34	$5.802\ 10^{-2}$	$5.680\ 10^{-2}$	0.26	0.39	0.35	$5.68\ 10^{-2}$	$5.53\ 10^{-2}$	0.8	0.7	0.4
4–6	$5.834\ 10^{-2}$	$5.784\ 10^{-2}$	0.23	0.23	0.35	$5.782\ 10^{-2}$	$5.720\ 10^{-2}$	0.25	0.27	0.39	$5.64\ 10^{-2}$	$5.56\ 10^{-2}$	0.8	0.5	0.5
6–8	$4.972\ 10^{-2}$	$4.974\ 10^{-2}$	0.26	0.22	0.34	$4.868\ 10^{-2}$	$4.872\ 10^{-2}$	0.28	0.27	0.38	$4.71\ 10^{-2}$	$4.70\ 10^{-2}$	0.8	0.6	0.5
8–10	$4.106\ 10^{-2}$	$4.134\ 10^{-2}$	0.28	0.24	0.34	$4.047\ 10^{-2}$	$4.074\ 10^{-2}$	0.31	0.30	0.34	$3.95\ 10^{-2}$	$3.97\ 10^{-2}$	0.9	0.6	0.4
10–12	$3.385\ 10^{-2}$	$3.424\ 10^{-2}$	0.31	0.26	0.35	$3.381\ 10^{-2}$	$3.423\ 10^{-2}$	0.34	0.32	0.34	$3.22\ 10^{-2}$	$3.27\ 10^{-2}$	1.0	0.7	0.4
12–14	$2.819\ 10^{-2}$	$2.859\ 10^{-2}$	0.35	0.27	0.34	$2.823\ 10^{-2}$	$2.876\ 10^{-2}$	0.38	0.32	0.35	$2.66\ 10^{-2}$	$2.71\ 10^{-2}$	1.1	0.7	0.4
14–16	$2.375\ 10^{-2}$	$2.412\ 10^{-2}$	0.37	0.27	0.35	$2.385\ 10^{-2}$	$2.427\ 10^{-2}$	0.40	0.32	0.34	$2.27\ 10^{-2}$	$2.33\ 10^{-2}$	1.3	0.7	0.5
16–18	$1.997\ 10^{-2}$	$2.028\ 10^{-2}$	0.42	0.29	0.35	$2.034\ 10^{-2}$	$2.070\ 10^{-2}$	0.44	0.35	0.35	$1.99\ 10^{-2}$	$2.03\ 10^{-2}$	1.4	0.8	0.5
18–22	$1.587\ 10^{-2}$	$1.609\ 10^{-2}$	0.35	0.27	0.34	$1.606\ 10^{-2}$	$1.634\ 10^{-2}$	0.39	0.32	0.35	$1.60\ 10^{-2}$	$1.64\ 10^{-2}$	1.2	0.6	0.5
22–26	$1.187\ 10^{-2}$	$1.199\ 10^{-2}$	0.41	0.29	0.35	$1.217\ 10^{-2}$	$1.228\ 10^{-2}$	0.47	0.36	0.36	$1.23\ 10^{-2}$	$1.24\ 10^{-2}$	1.4	0.8	0.6
26–30	$9.065\ 10^{-3}$	$9.113\ 10^{-3}$	0.46	0.31	0.35	$9.275\ 10^{-3}$	$9.340\ 10^{-3}$	0.52	0.41	0.35	$9.68\ 10^{-3}$	$9.81\ 10^{-3}$	1.7	0.8	0.6
30–34	$7.143\ 10^{-3}$	$7.165\ 10^{-3}$	0.53	0.35	0.35	$7.339\ 10^{-3}$	$7.363\ 10^{-3}$	0.59	0.46	0.35	$7.82\ 10^{-3}$	$7.90\ 10^{-3}$	1.8	0.9	0.5
34–38	$5.707\ 10^{-3}$	$5.707\ 10^{-3}$	0.59	0.38	0.34	$5.880\ 10^{-3}$	$5.883\ 10^{-3}$	0.66	0.49	0.35	$6.34\ 10^{-3}$	$6.34\ 10^{-3}$	2.0	1.0	0.5
38–42	$4.559\ 10^{-3}$	$4.554\ 10^{-3}$	0.66	0.44	0.35	$4.709\ 10^{-3}$	$4.704\ 10^{-3}$	0.74	0.51	0.35	$5.09\ 10^{-3}$	$5.09\ 10^{-3}$	2.2	1.2	0.4
42–46	$3.757\ 10^{-3}$	$3.747\ 10^{-3}$	0.73	0.47	0.35	$3.745\ 10^{-3}$	$3.739\ 10^{-3}$	0.82	0.57	0.38	$4.38\ 10^{-3}$	$4.40\ 10^{-3}$	2.4	1.2	0.4
46–50	$3.150\ 10^{-3}$	$3.140\ 10^{-3}$	0.79	0.48	0.38	$3.156\ 10^{-3}$	$3.134\ 10^{-3}$	0.86	0.62	0.37	$3.57\ 10^{-3}$	$3.55\ 10^{-3}$	2.6	1.4	0.4
50–54	$2.584\ 10^{-3}$	$2.575\ 10^{-3}$	0.88	0.52	0.36	$2.568\ 10^{-3}$	$2.556\ 10^{-3}$	0.99	0.67	0.36	$3.00\ 10^{-3}$	$2.99\ 10^{-3}$	2.9	1.5	0.6
54–60	$2.052\ 10^{-3}$	$2.040\ 10^{-3}$	0.81	0.48	0.37	$2.125\ 10^{-3}$	$2.110\ 10^{-3}$	0.92	0.59	0.35	$2.66\ 10^{-3}$	$2.65\ 10^{-3}$	2.7	1.3	0.4
60–70	$1.466\ 10^{-3}$	$1.457\ 10^{-3}$	0.73	0.46	0.39	$1.494\ 10^{-3}$	$1.481\ 10^{-3}$	0.87	0.64	0.39	$1.82\ 10^{-3}$	$1.80\ 10^{-3}$	2.5	1.3	0.4
70–80	$9.646\ 10^{-4}$	$9.557\ 10^{-4}$	0.92	0.55	0.43	$9.979\ 10^{-4}$	$9.845\ 10^{-4}$	1.08	0.71	0.40	$1.14\ 10^{-3}$	$1.12\ 10^{-3}$	3.3	1.6	0.7
80–100	$5.458\ 10^{-4}$	$5.413\ 10^{-4}$	0.83	0.53	0.47	$5.566\ 10^{-4}$	$5.509\ 10^{-4}$	0.99	0.69	0.48	$5.96\ 10^{-4}$	$5.89\ 10^{-4}$	3.1	1.4	0.8
100–150	$1.874\ 10^{-4}$	$1.859\ 10^{-4}$	0.83	0.54	0.57	$1.974\ 10^{-4}$	$1.954\ 10^{-4}$	1.00	0.70	0.71	$1.98\ 10^{-4}$	$1.96\ 10^{-4}$	3.3	1.5	2.1
150–200	$4.826\ 10^{-5}$	$4.794\ 10^{-5}$	1.67	0.74	0.51	$4.990\ 10^{-5}$	$4.959\ 10^{-5}$	2.03	0.99	0.69	$5.08\ 10^{-5}$	$5.05\ 10^{-5}$	6.7	2.8	2.2
200–300	$1.126\ 10^{-5}$	$1.124\ 10^{-5}$	2.38	1.40	1.43	$1.018\ 10^{-5}$	$1.011\ 10^{-5}$	3.17	2.05	1.20	$9.09\ 10^{-6}$	$9.12\ 10^{-6}$	10.9	4.4	0.8
300–800	$4.783\ 10^{-7}$	$4.768\ 10^{-7}$	5.02	2.00	1.50	$3.048\ 10^{-7}$	$3.028\ 10^{-7}$	8.02	3.67	1.03	$1.47\ 10^{-7}$	$1.45\ 10^{-7}$	34.0	15.8	0.9

Table 3. The measured normalized combined (electron and muon channels) cross section $(1/\sigma^{fid})(d\sigma^{fid}/dp_T^Z)$, for $0 \leq |y_Z| < 1$, $1 \leq |y_Z| < 2$ and $2 \leq |y_Z| < 2.4$. The cross sections at Born and dressed levels are given as well as the relative statistical (δ_{Stat}) and systematic (δ_{Syst}) uncertainties for uncorrelated and correlated sources.

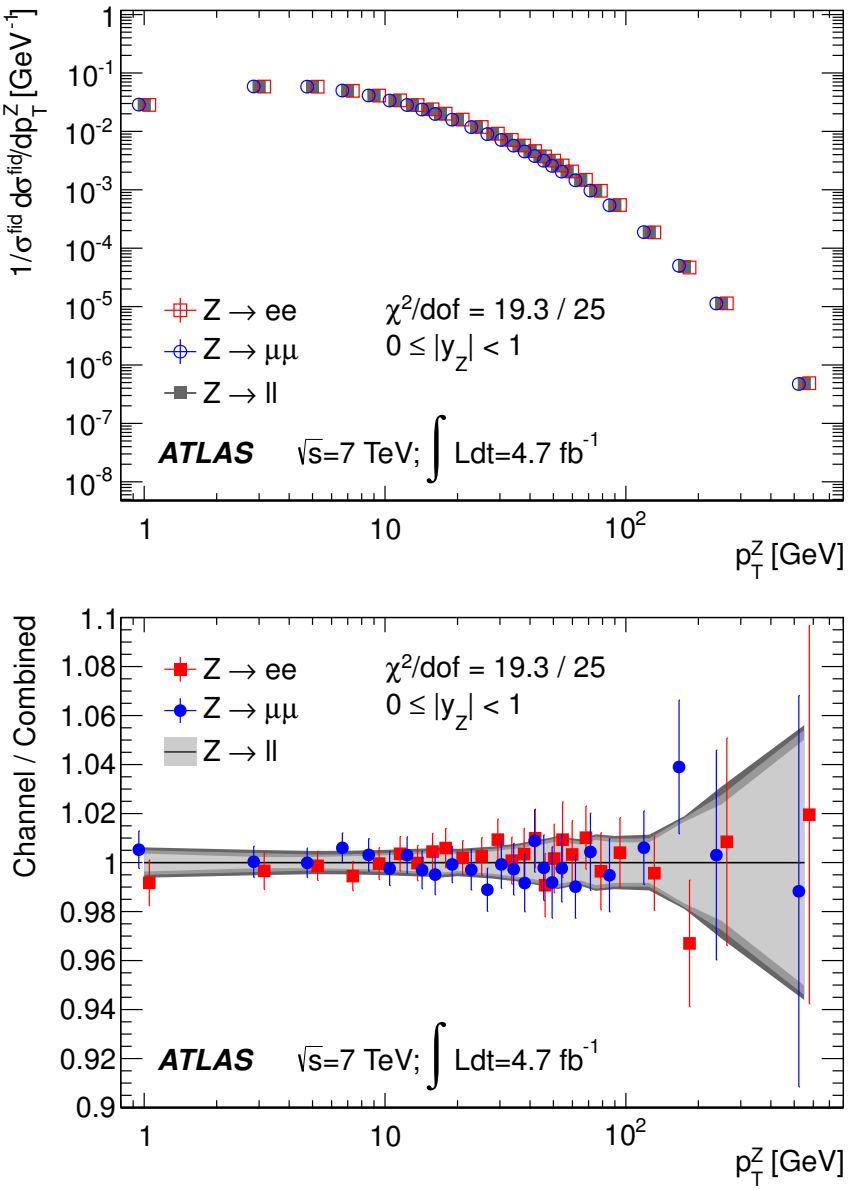

Figure 4. The measured normalized cross section $(1/\sigma^{\rm fid})(\mathrm{d}\sigma^{\rm fid}/\mathrm{d}p_{\rm T}^{Z})$ for $0 \leq |y_Z| < 1$, as a function of $p_{\rm T}^{Z}$ for the electron and muon channels and the combined result (top). Ratio of the electron and muon channels to the combined result (bottom). The uncertainty bands represent the statistical, total uncorrelated and total uncertainties, from light gray to dark gray respectively.

JHEP09(2014)145

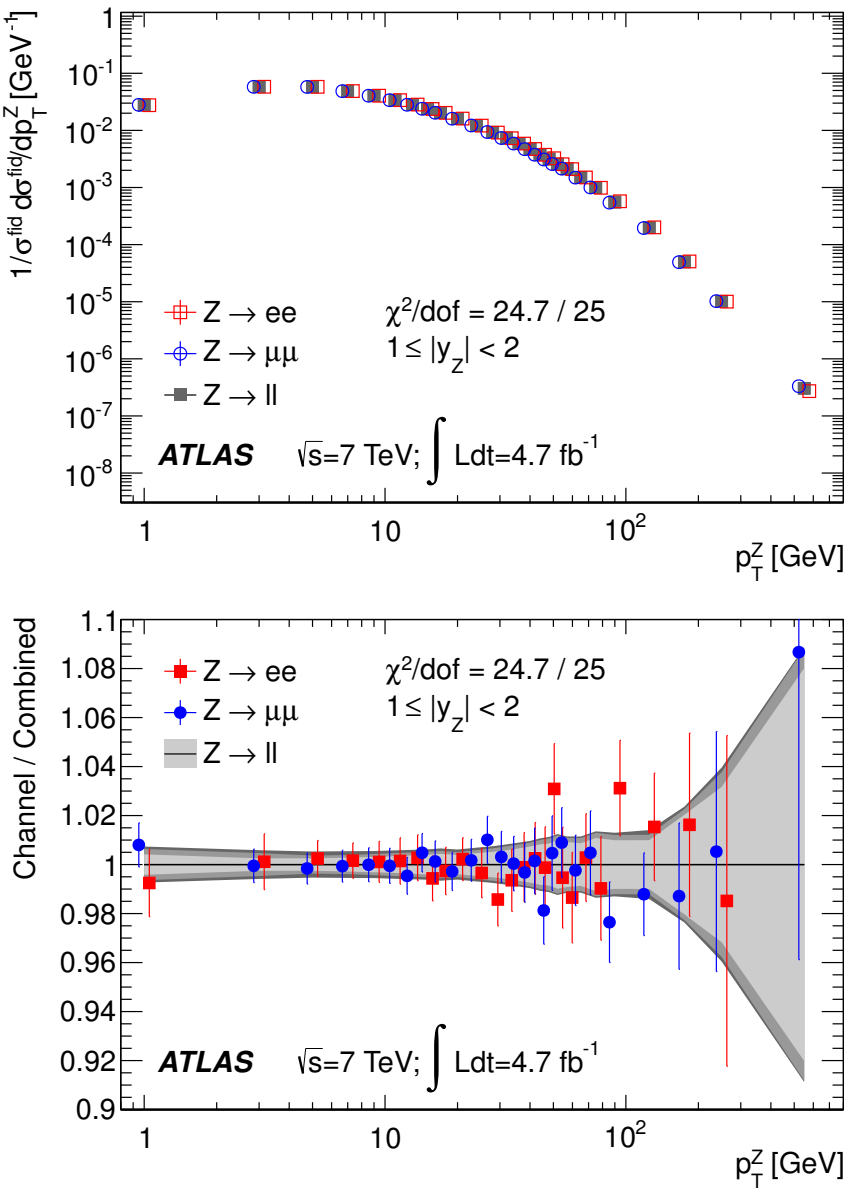

Figure 5. The measured normalized cross section $(1/\sigma^{\text{fid}})(\mathrm{d}\sigma^{\text{fid}}/\mathrm{d}p_{\text{T}}^{Z})$ for $1 \leq |y_Z| < 2$, as a function of p_{T}^{Z} for the electron and muon channels and the combined result (top). Ratio of the electron and muon channels to the combined result (bottom). The uncertainty bands represent the statistical, total uncorrelated and total uncertainties, from light gray to dark gray respectively.

JHEP09(2014)145

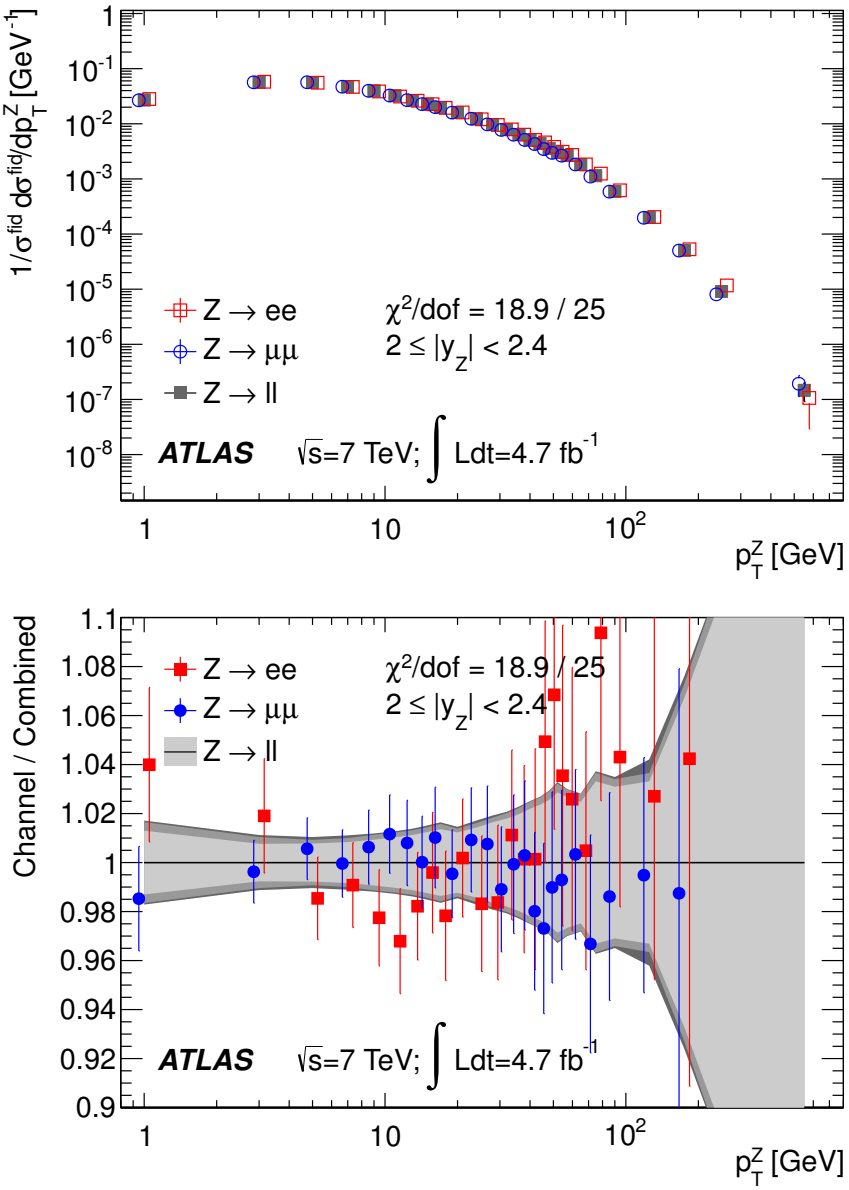

Figure 6. The measured normalized cross section $(1/\sigma^{\text{fid}})(\mathrm{d}\sigma^{\text{fid}}/\mathrm{d}p_{\mathrm{T}}^{Z})$ for $2 \leq |y_Z| < 2.4$, as a function of p_{T}^{Z} for the electron and muon channels and the combined result (top). Ratio of the electron and muon channels to the combined result (bottom). The uncertainty bands represent the statistical, total uncorrelated and total uncertainties, from light gray to dark gray respectively.

JHEP09(2014)145

The uncertainty on the predictions, estimated from the PDF uncertainties and renormalization and factorization scale variations, are in all cases much larger than the measurement uncertainties. The disagreement between the data and the FEWZ and DYNNLO predictions is larger than the data uncertainties, reaching 10% around 50 GeV and diverging at low p_{T}^{Z} as expected from the absence of resummation effects in these calculations. FEWZ and DYNNLO agree with each other when using QCD renormalization and factorization scales, μ_{R} and μ_{F}, defined as $\mu_{\mathrm{R}} = \mu_{\mathrm{F}} = m_Z$ and leading-order electroweak perturbative accuracy. The influence of the QCD scale choice is studied with DYNNLO by using the alternative dynamic scale E_{T}^{Z}, defined as the sum in quadrature of m_Z and p_{T}^{Z}. The resulting p_{T}^{Z} shape is in better agreement with the data for $p_{\mathrm{T}}^{Z} > 30\,\mathrm{GeV}$, but the normalization remains low by 10% in this region. NLO electroweak corrections to Z+jet production [51] are applied to the dynamic-scale DYNNLO prediction and lead to a decrease of the cross section of 10% in the highest p_{T}^{Z} bin.

The RESBOS-GNW prediction agrees with the data within 5–7%; the prediction uncertainties are defined from PDF, renormalization scale and factorization scale variations. The RESBOS-BLNY prediction, to which the previous ATLAS measurements [8, 9, 16] were compared, is included for reference. The NNLO+NNLL calculation following ref. [21] matches the data within 10–12%. The uncertainties on this prediction are defined from resummation, renormalization and factorization scale variations; PDF uncertainties are neglected. In both cases, the prediction uncertainties are almost sufficient to cover the difference with the data.

Figure 8 shows the ratio of the p_{T}^{Z} distributions predicted by different generators to the combined measurements performed inclusively in Z rapidity, and in the three exclusive Z rapidity bins described above. The PYTHIA and POWHEG generators agree with the data to within 5% in the $2 < p_{\mathrm{T}}^{Z} < 60$ GeV range, and to within 20% over the full range. MC@NLO shows a similar level of agreement with the data for $p_{\mathrm{T}}^{Z} < 30\,\mathrm{GeV}$ but develops a discrepancy up to around 40% at the end of the spectrum. SHERPA and ALPGEN agree with the data to within about 5% for $5 < p_{\mathrm{T}}^{Z} < 200$ GeV, but tend to overestimate the distribution near the end of the spectrum.

10 Tuning of PYTHIA8 and POWHEG + PYTHIA8

The parton shower tunes presented below are performed to determine the sensitivity of the measured p_{T}^{Z} cross sections presented here to parton shower model parameters in state-of-the-art MC generators, and to constrain the models by trying to achieve precise predictions of vector boson production. The ATLAS $\phi_{\eta}^{\star}$ measurement [16] is also exploited as it is highly correlated to p_{T}^{Z} and is hence sensitive to the same model components.

The PYTHIA8 generator with the p_{T}-ordered, interleaved parton shower is chosen for these studies. PYTHIA8 is used in standalone mode and in a configuration interfaced to POWHEG. To minimize dependence on QED final-state corrections, the tunes use the dressed-level measurement results. The study is restricted to the low p_{T}^{Z} range, where parton shower effects dominate. The tunes are performed for $p_{\mathrm{T}}^{Z} < 26\,\mathrm{GeV}$, which is found to be most sensitive to the model parameters described below, and $\phi_{\eta}^{\star} < 0.29$, which covers

JHEP09(2014)145

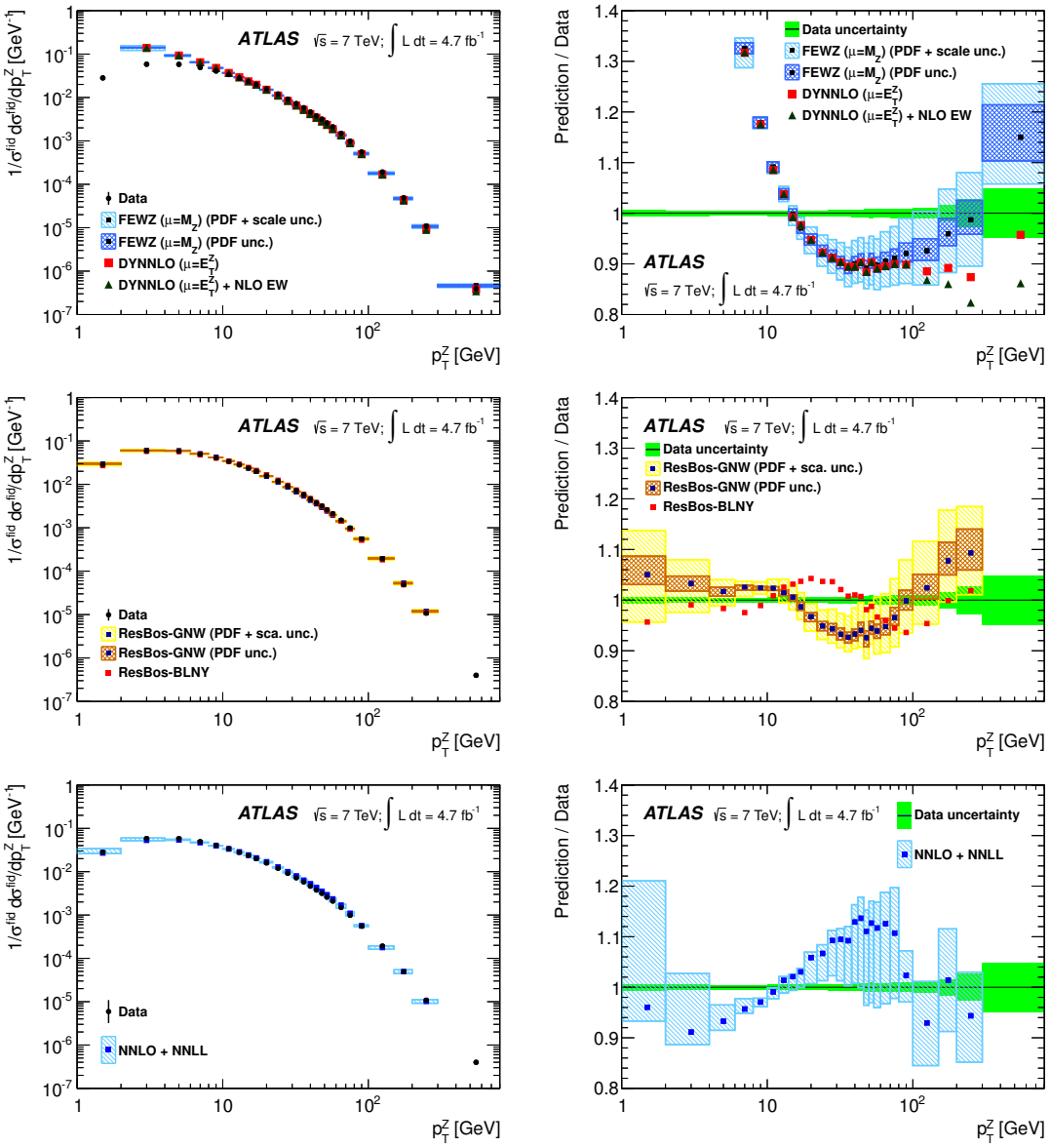

Figure 7. Left: comparison of the p_{T}^{Z} distributions predicted by different computations: FEWZ and DYNNLO (top), RESBOS (middle) and the NNLO+NNLL calculation of ref. [21] (bottom) with the Born-level combined measurement, inclusively in y_Z. Right: ratios between these predictions and the combined measurement.

a similar transverse momentum range. The measurement inclusive in rapidity is used for the tuning, and the compatibility of the tuned predictions with the data in the separate rapidity bins is then evaluated.

For PYTHIA8, the parton shower model components under consideration include the strong coupling constant used for the parton shower evolution $\alpha_{\mathrm{S}}^{\mathrm{ISR}}(m_Z)$, and the parton shower lower cut-off p_{T0} in the non-perturbative regime, implemented as a smooth damping factor $p_{\mathrm{T}}^2/(p_{\mathrm{T0}}^2 + p_{\mathrm{T}}^2)$. To populate the region below p_{T0}, the partons initiating the hard scattering process are assumed to have a primordial transverse momentum k_{T} following

JHEP09(2014)145

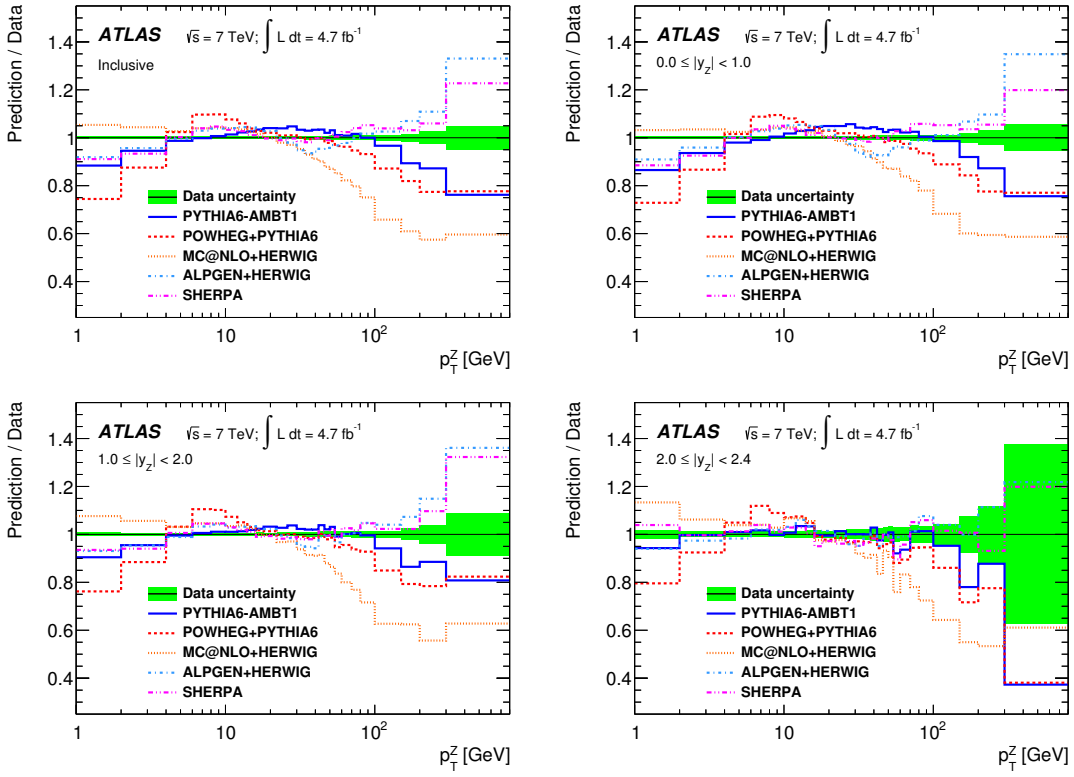

Figure 8. Ratio of the p_{T}^{Z} distribution predicted by different MC generators to the Born-level combined measurement, for the inclusive measurement and for $0 \leq |y_Z| < 1$, $1 \leq |y_Z| < 2$ and $2 \leq |y_Z| < 2.4$.

a Gaussian distribution with tunable width. The PYTHIA8 parton shower also includes QED emissions, but the corresponding cut-off values and coupling strength are left to the program defaults. The steerable parameters not used in the tuning are set to the values defined by the tune 4C [35].

POWHEG calculates the hardest (highest p_{T}) QCD radiation provided that it is above a transverse momentum threshold $p_{\mathrm{T,min}}^{2}$, which is a steerable parameter in the program. Below $p_{\mathrm{T,min}}^{2}$, POWHEG generates events without extra radiation and the phase space is populated by PYTHIA8. Therefore, the upper limit of the PYTHIA8 parton shower should match the POWHEG cut-off value. The tunes are performed using $p_{\mathrm{T,min}}^{2} = 4\,\mathrm{GeV}^2$, corresponding to $p_{\mathrm{T}}^{Z} = 2\,\mathrm{GeV}$. In addition, in order to avoid discontinuities in the matched spectrum, the $\alpha_{\mathrm{S}}(m_Z)$ value used to calculate the QCD radiation in POWHEG should match $\alpha_{\mathrm{S}}^{\mathrm{ISR}}(m_Z)$ in PYTHIA; $\alpha_{\mathrm{S}}(m_Z) = 0.118$ is used as in the CT10 PDFs. Correspondingly the running of α_{S} in the parton shower calculation is set to NLO. The tuning of POWHEG+PYTHIA8 hence only varies the shower cut-off and the primordial k_{T} in PYTHIA8. The other steerable parameters not used in the tuning are set to the values defined by the 4C tune.

The tunes are performed using the Professor [52] package, which interpolates the dependence of MC predictions on the model parameters as originally proposed in ref. [53]. Predictions for the p_{T}^{Z} distribution are generated at randomly chosen parameter settings

JHEP09(2014)145

Parameter	Variation Range PYTHIA8 tune	Variation Range PYTHIA8+POWHEG tune
Primordial k_{T} [GeV]	1.0–2.5	0.5–2.5
ISR $\alpha_{\mathrm{S}}^{\mathrm{ISR}}(m_Z)$	0.120–0.140	0.118
ISR cut-off [GeV]	0.5–2.5	0.5–3.0
ISR α_{S} order	LO	NLO
PYTHIA8 base tune	tune 4C	tune 4C
POWHEG cut-off [GeV^2]	—	4.0

Table 4. Parameter ranges and model switches used in the tuning of PYTHIA8 and PYTHIA8+POWHEG described in section 10.

	PYTHIA8		POWHEG+PYTHIA8	
	p_{T}^Z	$\phi_\eta^\star$	p_{T}^Z	$\phi_\eta^\star$
Primordial k_{T} [GeV]	1.74 ± 0.03	1.73 ± 0.03	1.75 ± 0.03	1.75 ± 0.04
ISR $\alpha_{\mathrm{S}}^{\mathrm{ISR}}(m_Z)$	0.1233 ± 0.0003	0.1238 ± 0.0002	0.118 (fixed)	0.118 (fixed)
ISR cut-off [GeV]	0.66 ± 0.14	0.58 ± 0.07	2.06 ± 0.12	1.88 ± 0.12
χ^2_{min}/dof	23.9/19	59.9/45	18.5/20	68.2/46

Table 5. Results of the PYTHIA8 and POWHEG+PYTHIA8 tuning to the p_{T}^Z and $\phi_\eta^\star$ data.

(anchor points) in the ranges indicated in table 4. A fourth-order polynomial is used to approximate the generator predictions between the anchor points. The optimal parameter values are determined using a χ^2 minimization between the interpolated generator response and the data.

The sensitivity of the generator parameters to the p_{T}^Z and $\phi_\eta^\star$ measurements is probed by performing tunes of PYTHIA8 and POWHEG+PYTHIA8 to each measurement separately. As shown in table 5 both measurements have comparable sensitivity and yield compatible tuned parameter values. As a further check of the compatibility between the p_{T}^Z and $\phi_\eta^\star$ measurements, the p_{T}^Z-tuned and $\phi_\eta^\star$-tuned predictions are compared to the measured p_{T}^Z distribution. The tuning uncertainty is obtained from variations of the eigenvector components of the parameters error matrix over a range covering $\Delta\chi^2 = \chi^2_{\mathrm{min}}/\mathrm{dof}$. Figure 9 shows that the tuned predictions agree with the measured cross sections within 2% for $p_{\mathrm{T}}^Z < 50\,\mathrm{GeV}$, and with each other within the tuned parameter uncertainties.

Since the p_{T}^Z and $\phi_\eta^\star$ observables provide similar sensitivity to the parton shower parameters and to avoid correlations between these measurements, the final tune optimally combines the most precise independent single measurements, namely the muon channel p_{T}^Z measurement, and the electron channel $\phi_\eta^\star$ measurement. The same tuning range is used. Table 6 shows the tune results and figure 10 shows the comparison of the tuned predictions to the data. The final tunes are referred to as AZ and AZNLO for PYTHIA8 and POWHEG+PYTHIA8 respectively. The tuned predictions agree with the measurement

JHEP09(2014)145

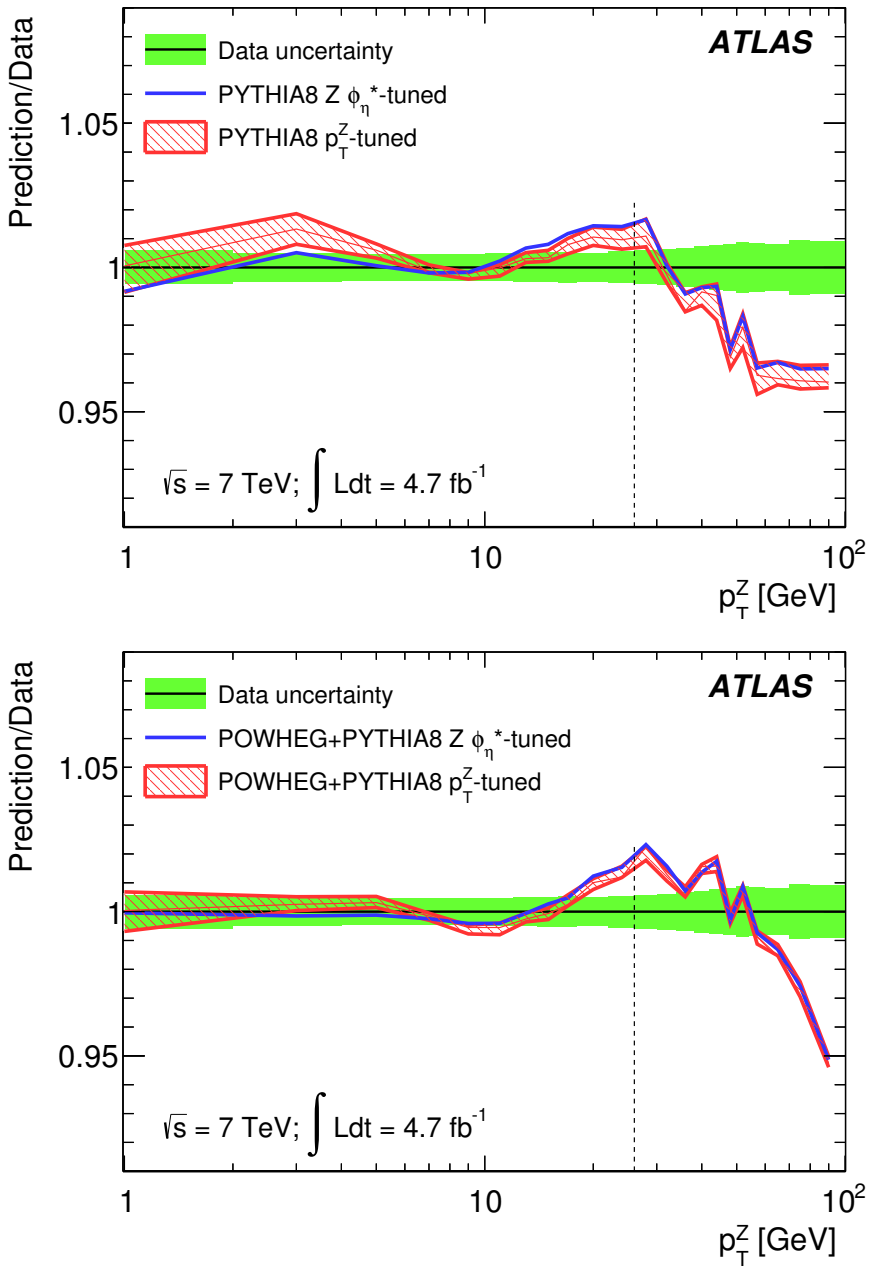

Figure 9. Comparison of the PYTHIA8 (top) and POWHEG+PYTHIA8 (bottom) tuned predictions based on the $\phi_\eta^\star$ and p_{T}^Z measurements with the data, for dressed kinematics. The vertical dashed lines show the upper limit of the tuning range.

to better than 2% in the range used for the tuning, and below $p_{\mathrm{T}}^Z = 50$ GeV. The primordial k_{T} and ISR cut-off parameters are essentially constrained by the data in the region $p_{\mathrm{T}}^Z < 12\,\mathrm{GeV}$ and not affected by the choice of upper bound for the tuning range. In contrast, $\alpha_{\mathrm{S}}^{\mathrm{ISR}}(m_Z)$ is tightly constrained for a given choice of range but its tuned value varies by 2% when increasing the upper bound to 50 GeV. At higher transverse momentum, discrepancies of around 15% for PYTHIA8 and 20% for POWHEG+PYTHIA8 remain,

JHEP09(2014)145

	PYTHIA8	POWHEG+PYTHIA8	Base tune
Tune Name	AZ	AZNLO	4C
Primordial k_{T} [GeV]	1.71 ± 0.03	1.75 ± 0.03	2.0
ISR $\alpha_{\mathrm{S}}^{\mathrm{ISR}}(m_Z)$	0.1237 ± 0.0002	0.118 (fixed)	0.137
ISR cut-off [GeV]	0.59 ± 0.08	1.92 ± 0.12	2.0
χ^2_{min}/dof	45.4/32	46.0/33	—

Table 6. Final PYTHIA8 and POWHEG+PYTHIA8 tuning results, and comparison to the PYTHIA8 base tune.

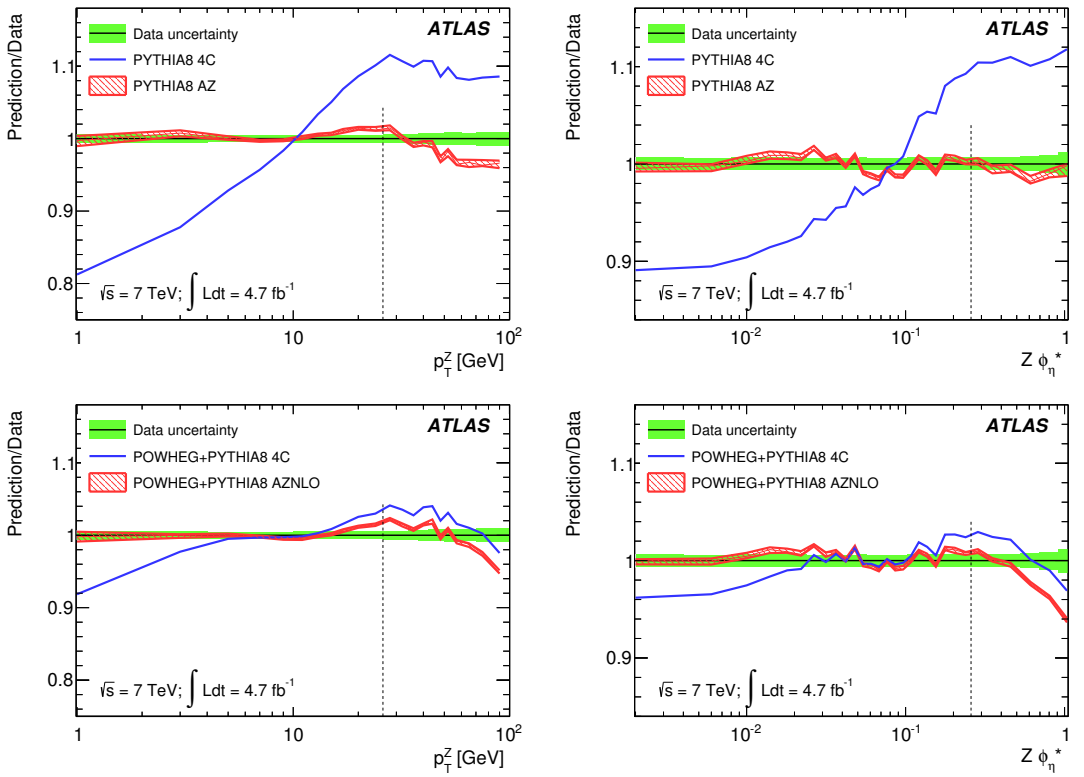

Figure 10. Comparison of tuned predictions to the p_{T}^Z and $\phi_\eta^\star$ differential cross sections, for dressed kinematics and in the full rapidity range. Comparison of the PYTHIA8 generator with the 4C and AZ tunes to the muon-channel p_{T}^Z data and electron-channel $\phi_\eta^\star$ data (top). Comparison of the POWHEG+PYTHIA8 set-up with the 4C and AZNLO tunes to the same data (bottom). The vertical dashed lines show the upper limit of the tuning range.

indicating the limited accuracy of the NLO signal matrix element and suggesting the need for contributions from higher parton multiplicity.

Tuned predictions based on the parameter values given in table 6 are produced in the different Z rapidity bins and compared to the measured cross sections with the aim of assessing how accurately the tune based on the inclusive measurement reproduces the data in each Z rapidity bin. The results are shown in figure 11. A satisfactory description

JHEP09(2014)145

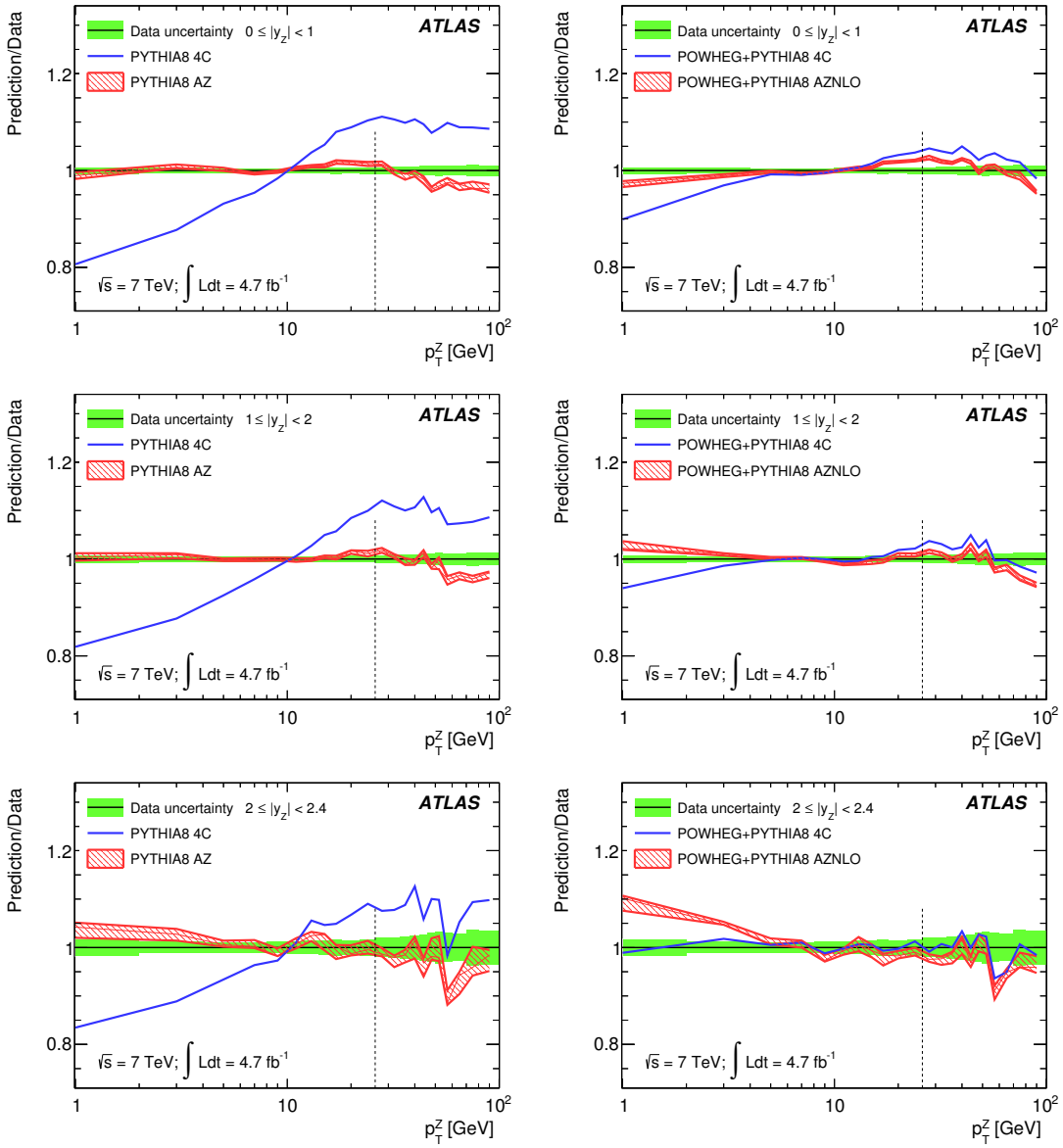

Figure 11. Tuned predictions based on table 6 for PYTHIA8 (left) and POWHEG+PYTHIA8 (right) for $0 \leq |y_Z| < 1$ (top), $1 \leq |y_Z| < 2$ (middle) and $2 \leq |y_Z| < 2.4$ (bottom), compared to the corresponding combined measurements, for dressed kinematics. The vertical dashed lines show the upper limit of the tuning range.

across rapidity is obtained in the case of PYTHIA8; in the case of POWHEG+PYTHIA8, the prediction at low p_{T}^{Z} undershoots the data for $0 \leq |y_Z| < 1$, and overshoots the data for $2 \leq |y_Z| < 2.4$. The inclusive tune thus appears as a compromise between the different $|y_Z|$ regions in this case.

The sensitivity of the parton shower tune to other model components provided in PYTHIA8, such as multiple parton interactions (MPI), which affect the event overall hadronic activity, was studied by varying the corresponding parameters. No effect on

JHEP09(2014)145

the parton shower parameters is found. In order to compensate for the changes in energy and particle flow induced by the modifications in the parton shower and primordial k_{T} parameters, the p_{T} threshold for the QCD $2 \to 2$ scattering processes used in MPI is changed from 2.085 GeV (tune 4C) to 2.18 GeV for Pythia8, following the underlying event data measured in Drell-Yan events by ATLAS [54]. For the Powheg+Pythia8 configuration, the interleaving of MPI in the parton shower model in Pythia8 is adapted to also properly take into account the Powheg emissions. It is tuned in the same way as Pythia8 in standalone mode and an optimized value of 2.00 for the low-p_{T} regularization of MPI is found. Finally, comparing tunes based on the native Pythia8 QED final-state corrections with Pythia8 results using Photos for QED final-state radiation, the results are found insensitive to the differences in the QED FSR implementations.

A consistent description of the p_{T}^{Z} and $\phi_{\eta}^{\star}$ data is reached with a single tune. Both observables are also found to provide similar sensitivity to the parameters of interest. The inclusive tune provides an accurate description of the different rapidity bins in the case of Pythia8, while the agreement versus $|y_Z|$ is slightly worse in the case of Powheg+Pythia8.

11 Conclusion

A measurement of the Z/γ^* transverse momentum spectrum in the $Z/\gamma^* \to e^+e^-$ and $Z/\gamma^* \to \mu^+\mu^-$ channels with the ATLAS detector is presented, using 4.7 fb^{-1} of LHC proton-proton collision data at a centre-of-mass energy of $\sqrt{s} = 7$ TeV. Normalized differential cross sections as a function of p_{T}^{Z} are measured for the range $0 < p_{\mathrm{T}}^{Z} < 800$ GeV and the individual channel results are combined. The measurement is performed inclusively in rapidity, and for $0 \leq |y_Z| < 1$, $1 \leq |y_Z| < 2$ and $2 \leq |y_Z| < 2.4$. The large data sample allows a fine binning in p_{T}^{Z} with a typical uncertainty on the combined result better than 1% for $p_{\mathrm{T}}^{Z} < 100$ GeV, rising to 5% towards the end of the spectrum.

The cross-section measurements are compared to pQCD and resummed predictions. While Fewz and Dynnlo do not include resummation and the observed disagreement at low p_{T}^{Z} is expected, ResBos and the NNLO+NNLL prediction of ref. [21] marginally agree with the data given the large uncertainties on these predictions. The data are also compared to predictions from Pythia6-AUET2B, Powheg+Pythia6-AUET2B, MC@NLO, Alpgen and Sherpa. The Pythia and Powheg generators agree with the data to within 5% in the range $2 < p_{\mathrm{T}}^{Z} < 60$ GeV and to within 20% over the full range, whereas Mc@nlo shows a deficit of about 40% at the end of the measured spectrum. Alpgen and Sherpa provide good agreement over a larger range, $p_{\mathrm{T}}^{Z} < 200$ GeV, but overestimate the high end of the distribution. These patterns are compatible with what was observed for the $\phi_{\eta}^{\star}$ measurement. Electroweak corrections and the choice of a dynamic QCD scale were found to have a significant impact on the predictions at high p_{T}^{Z}; incorporating these improvements provides a better description of the measured distribution in the high p_{T}^{Z} region.

The p_{T}^{Z} and $\phi_{\eta}^{\star}$ measurements were used to tune the Pythia8 and Powheg+Pythia8 generators. Both measurements can be interpreted consistently in terms of the Z/γ^* bosons

JHEP09(2014)145

transverse momentum distribution and provide similar sensitivity to parton shower model parameters. The tuned predictions are in agreement with the data within 2% for p_{T}^{Z} below 50 GeV. The best description is provided by Pythia8, which is also able to describe the different rapidity intervals with a single tune.

Acknowledgments

We thank CERN for the very successful operation of the LHC, as well as the support staff from our institutions without whom ATLAS could not be operated efficiently.

We acknowledge the support of ANPCyT, Argentina; YerPhI, Armenia; ARC, Australia; BMWF and FWF, Austria; ANAS, Azerbaijan; SSTC, Belarus; CNPq and FAPESP, Brazil; NSERC, NRC and CFI, Canada; CERN; CONICYT, Chile; CAS, MOST and NSFC, China; COLCIENCIAS, Colombia; MSMT CR, MPO CR and VSC CR, Czech Republic; DNRF, DNSRC and Lundbeck Foundation, Denmark; EPLANET, ERC and NSRF, European Union; IN2P3-CNRS, CEA-DSM/IRFU, France; GNSF, Georgia; BMBF, DFG, HGF, MPG and AvH Foundation, Germany; GSRT and NSRF, Greece; ISF, MINERVA, GIF, I-CORE and Benoziyo Center, Israel; INFN, Italy; MEXT and JSPS, Japan; CNRST, Morocco; FOM and NWO, Netherlands; BRF and RCN, Norway; MNiSW and NCN, Poland; GRICES and FCT, Portugal; MNE/IFA, Romania; MES of Russia and ROSATOM, Russian Federation; JINR; MSTD, Serbia; MSSR, Slovakia; ARRS and MIZŠ, Slovenia; DST/NRF, South Africa; MINECO, Spain; SRC and Wallenberg Foundation, Sweden; SER, SNSF and Cantons of Bern and Geneva, Switzerland; NSC, Taiwan; TAEK, Turkey; STFC, the Royal Society and Leverhulme Trust, United Kingdom; DOE and NSF, United States of America.

The crucial computing support from all WLCG partners is acknowledged gratefully, in particular from CERN and the ATLAS Tier-1 facilities at TRIUMF (Canada), NDGF (Denmark, Norway, Sweden), CC-IN2P3 (France), KIT/GridKA (Germany), INFN-CNAF (Italy), NL-T1 (Netherlands), PIC (Spain), ASGC (Taiwan), RAL (U.K.) and BNL (U.S.A.) and in the Tier-2 facilities worldwide.

References

[1] C. Balázs and C.P. Yuan, *Soft gluon effects on lepton pairs at hadron colliders*, *Phys. Rev.* **D 56** (1997) 5558 [hep-ph/9704258] [INSPIRE].

[2] T. Sjöstrand, S. Mrenna and P.Z. Skands, *PYTHIA 6.4 physics and manual*, *JHEP* **05** (2006) 026 [hep-ph/0603175] [INSPIRE].

[3] G. Corcella et al., *HERWIG 6: an event generator for hadron emission reactions with interfering gluons (including supersymmetric processes)*, *JHEP* **01** (2001) 010 [hep-ph/0011363] [INSPIRE].

JHEP09(2014)145

[4] K. Melnikov and F. Petriello, *Electroweak gauge boson production at hadron colliders through* $O(\alpha_s^2)$, *Phys. Rev.* **D 74** (2006) 114017 [hep-ph/0609070] [INSPIRE].

[5] R. Gavin, Y. Li, F. Petriello and S. Quackenbush, *FEWZ 2.0: a code for hadronic Z production at next-to-next-to-leading order*, *Comput. Phys. Commun.* **182** (2011) 2388 [arXiv:1011.3540] [INSPIRE].

[6] Y. Li and F. Petriello, *Combining QCD and electroweak corrections to dilepton production in FEWZ*, *Phys. Rev.* **D 86** (2012) 094034 [arXiv:1208.5967] [INSPIRE].

[7] M. Klasen and M. Brandt, *Parton densities from LHC vector boson production at small and large transverse momenta*, *Phys. Rev.* **D 88** (2013) 054002 [arXiv:1305.5677] [INSPIRE].

[8] ATLAS collaboration, *Measurement of the transverse momentum distribution of Z/gamma* bosons in proton-proton collisions at* $\sqrt{s} = 7$ *TeV with the ATLAS detector*, *Phys. Lett.* **B 705** (2011) 415 [arXiv:1107.2381] [INSPIRE].

[9] ATLAS collaboration, *Measurement of the transverse momentum distribution of W bosons in pp collisions at* $\sqrt{s} = 7$ *TeV with the ATLAS detector*, *Phys. Rev.* **D 85** (2012) 012005 [arXiv:1108.6308] [INSPIRE].

[10] CMS collaboration, *Measurement of the rapidity and transverse momentum distributions of Z bosons in pp collisions at* $\sqrt{s} = 7$ *TeV*, *Phys. Rev.* **D 85** (2012) 032002 [arXiv:1110.4973] [INSPIRE].

[11] ATLAS collaboration, *Improved luminosity determination in pp collisions at* $\sqrt{s} = 7$ *TeV using the ATLAS detector at the LHC*, *Eur. Phys. J.* **C 73** (2013) 2518 [arXiv:1302.4393] [INSPIRE].

[12] A. Banfi, S. Redford, M. Vesterinen, P. Waller and T.R. Wyatt, *Optimisation of variables for studying dilepton transverse momentum distributions at hadron colliders*, *Eur. Phys. J.* **C 71** (2011) 1600 [arXiv:1009.1580] [INSPIRE].

[13] D0 collaboration, V.M. Abazov et al., *Measurement of the shape of the boson transverse momentum distribution in* $p\bar{p} \to Z/\gamma^* \to e^+e^- + X$ *events produced at* $\sqrt{s} = 1.96$ *TeV*, *Phys. Rev. Lett.* **100** (2008) 102002 [arXiv:0712.0803] [INSPIRE].

[14] D0 collaboration, V.M. Abazov et al., *Measurement of the normalized* $Z/\gamma^* \to \mu^+\mu^-$ *transverse momentum distribution in* $p\bar{p}$ *collisions at* $\sqrt{s} = 1.96$ *TeV*, *Phys. Lett.* **B 693** (2010) 522 [arXiv:1006.0618] [INSPIRE].

[15] CDF collaboration, T. Aaltonen et al., *Transverse momentum cross section of* e^+e^- *pairs in the Z-boson region from* $p\bar{p}$ *collisions at* $\sqrt{s} = 1.96$ *TeV*, *Phys. Rev.* **D 86** (2012) 052010 [arXiv:1207.7138] [INSPIRE].

[16] ATLAS collaboration, *Measurement of angular correlations in Drell-Yan lepton pairs to probe* Z/γ^* *boson transverse momentum at* $\sqrt{s} = 7$ *TeV with the ATLAS detector*, *Phys. Lett.* **B 720** (2013) 32 [arXiv:1211.6899] [INSPIRE].

[17] LHCb collaboration, *Measurement of the cross-section for* $Z \to e^+e^-$ *production in pp collisions at* $\sqrt{s} = 7$ *TeV*, *JHEP* **02** (2013) 106 [arXiv:1212.4620] [INSPIRE].

[18] S. Catani, L. Cieri, G. Ferrera, D. de Florian and M. Grazzini, *Vector boson production at hadron colliders: a fully exclusive QCD calculation at NNLO*, *Phys. Rev. Lett.* **103** (2009) 082001 [arXiv:0903.2120] [INSPIRE].

[19] S. Catani and M. Grazzini, *An NNLO subtraction formalism in hadron collisions and its application to Higgs boson production at the LHC*, *Phys. Rev. Lett.* **98** (2007) 222002 [hep-ph/0703012] [INSPIRE].

JHEP09(2014)145

[20] M. Guzzi, P.M. Nadolsky and B. Wang, *Nonperturbative contributions to a resummed leptonic angular distribution in inclusive neutral vector boson production*, *Phys. Rev.* **D 90** (2014) 014030 [arXiv:1309.1393] [INSPIRE].

[21] A. Banfi, M. Dasgupta, S. Marzani and L. Tomlinson, *Predictions for Drell-Yan ϕ^* and Q_T observables at the LHC*, *Phys. Lett.* **B 715** (2012) 152 [arXiv:1205.4760] [INSPIRE].

[22] S. Frixione and B.R. Webber, *Matching NLO QCD computations and parton shower simulations*, *JHEP* **06** (2002) 029 [hep-ph/0204244] [INSPIRE].

[23] S. Alioli, P. Nason, C. Oleari and E. Re, *NLO vector-boson production matched with shower in POWHEG*, *JHEP* **07** (2008) 060 [arXiv:0805.4802] [INSPIRE].

[24] M.L. Mangano, M. Moretti, F. Piccinini, R. Pittau and A.D. Polosa, *ALPGEN, a generator for hard multiparton processes in hadronic collisions*, *JHEP* **07** (2003) 001 [hep-ph/0206293] [INSPIRE].

[25] T. Gleisberg et al., *Event generation with SHERPA 1.1*, *JHEP* **02** (2009) 007 [arXiv:0811.4622] [INSPIRE].

[26] ATLAS collaboration, *The ATLAS experiment at the CERN Large Hadron Collider*, 2008 *JINST* **3** S08003 [INSPIRE].

[27] ATLAS collaboration, *The ATLAS simulation infrastructure*, *Eur. Phys. J.* **C 70** (2010) 823 [arXiv:1005.4568] [INSPIRE].

[28] GEANT4 collaboration, S. Agostinelli et al., *GEANT4: a simulation toolkit*, *Nucl. Instrum. Meth.* **A 506** (2003) 250 [INSPIRE].

[29] ATLAS collaboration, *ATLAS tunes of PYTHIA 6 and PYTHIA 8 for MC11*, ATL-PHYS-PUB-2011-009 (2011).

[30] H.-L. Lai et al., *New parton distributions for collider physics*, *Phys. Rev.* **D 82** (2010) 074024 [arXiv:1007.2241] [INSPIRE].

[31] ATLAS collaboration, *Charged particle multiplicities in pp interactions at $\sqrt{s}$ = 0.9 and 7 TeV in a diffractive limited phase-space measured with the ATLAS detector at the LHC and new PYTHIA6 tune*, ATLAS-CONF-2010-031 (2010).

[32] A. Sherstnev and R.S. Thorne, *Parton distributions for LO generators*, *Eur. Phys. J.* **C 55** (2008) 553 [arXiv:0711.2473] [INSPIRE].

[33] J.M. Butterworth, J.R. Forshaw and M.H. Seymour, *Multiparton interactions in photoproduction at HERA*, *Z. Phys.* **C 72** (1996) 637 [hep-ph/9601371] [INSPIRE].

[34] ATLAS collaboration, *New ATLAS event generator tunes to 2010 data*, ATL-PHYS-PUB-2011-008 (2011).

[35] R. Corke and T. Sjöstrand, *Interleaved parton showers and tuning prospects*, *JHEP* **03** (2011) 032 [arXiv:1011.1759] [INSPIRE].

[36] T. Sjöstrand, S. Mrenna and P.Z. Skands, *A brief introduction to PYTHIA 8.1*, *Comput. Phys. Commun.* **178** (2008) 852 [arXiv:0710.3820] [INSPIRE].

[37] P. Golonka and Z. Was, *PHOTOS Monte Carlo: a precision tool for QED corrections in Z and W decays*, *Eur. Phys. J.* **C 45** (2006) 97 [hep-ph/0506026] [INSPIRE].

[38] S. Jadach, Z. Was, R. Decker and J.H. Kuhn, *The τ decay library TAUOLA: version 2.4*, *Comput. Phys. Commun.* **76** (1993) 361 [INSPIRE].

[39] C.M. Carloni Calame, G. Montagna, O. Nicrosini and A. Vicini, *Precision electroweak calculation of the production of a high transverse-momentum lepton pair at hadron colliders*, *JHEP* **10** (2007) 109 [arXiv:0710.1722] [INSPIRE].

JHEP09(2014)145

[40] M. Bahr et al., *HERWIG++ physics and manual*, *Eur. Phys. J.* **C 58** (2008) 639 [arXiv:0803.0883] [INSPIRE].

[41] A.D. Martin, R.G. Roberts, W.J. Stirling and R.S. Thorne, *Parton distributions incorporating QED contributions*, *Eur. Phys. J.* **C 39** (2005) 155 [hep-ph/0411040] [INSPIRE].

[42] ATLAS collaboration, *Electron reconstruction and identification efficiency measurements with the ATLAS detector using the 2011 LHC proton-proton collision data*, *Eur. Phys. J.* **C 74** (2014) 2941 [arXiv:1404.2240] [INSPIRE].

[43] ATLAS collaboration, *Electron performance measurements with the ATLAS detector using the 2010 LHC proton-proton collision data*, *Eur. Phys. J.* **C 72** (2012) 1909 [arXiv:1110.3174] [INSPIRE].

[44] ATLAS collaboration, *Muon reconstruction efficiency and momentum resolution of the ATLAS experiment in proton-proton collisions at* $\sqrt{s} = 7$ *TeV in 2010*, arXiv:1404.4562 [INSPIRE].

[45] G. D'Agostini, *A multidimensional unfolding method based on Bayes' theorem*, *Nucl. Instrum. Meth.* **A 362** (1995) 487 [INSPIRE].

[46] G. D'Agostini, *Improved iterative bayesian unfolding*, arXiv:1010.0632.

[47] T. Adye, *Unfolding algorithms and tests using RooUnfold*, arXiv:1105.1160 [INSPIRE].

[48] L. Lyons, D. Gibaut and P. Clifford, *How to combine correlated estimates of a single physical quantity*, *Nucl. Instrum. Meth.* **A 270** (1988) 110 [INSPIRE].

[49] A. Valassi, *Combining correlated measurements of several different physical quantities*, *Nucl. Instrum. Meth.* **A 500** (2003) 391 [INSPIRE].

[50] J. Pumplin et al., *New generation of parton distributions with uncertainties from global QCD analysis*, *JHEP* **07** (2002) 012 [hep-ph/0201195] [INSPIRE].

[51] A. Denner, S. Dittmaier, T. Kasprzik and A. Muck, *Electroweak corrections to dilepton + jet production at hadron colliders*, *JHEP* **06** (2011) 069 [arXiv:1103.0914] [INSPIRE].

[52] A. Buckley, H. Hoeth, H. Lacker, H. Schulz and J.E. von Seggern, *Systematic event generator tuning for the LHC*, *Eur. Phys. J.* **C 65** (2010) 331 [arXiv:0907.2973] [INSPIRE].

[53] DELPHI collaboration, *Tuning and test of fragmentation models based on identified particles and precision event shape data*, *Z. Phys.* **C 73** (1996) 11.

[54] ATLAS collaboration, *Measurement of observables sensitive to the underlying event in inclusive Z-boson production at proton-proton collisions at* $\sqrt{s} = 7$ *TeV*, arXiv: 1409.3433 [INSPIRE].

The ATLAS collaboration

G. Aad[84], B. Abbott[112], J. Abdallah[152], S. Abdel Khalek[116], O. Abdinov[11], R. Aben[106], B. Abi[113], M. Abolins[89], O.S. AbouZeid[159], H. Abramowicz[154], H. Abreu[153], R. Abreu[30], Y. Abulaiti[147a,147b], B.S. Acharya[165a,165b,a], L. Adamczyk[38a], D.L. Adams[25], J. Adelman[177], S. Adomeit[99], T. Adye[130], T. Agatonovic-Jovin[13a], J.A. Aguilar-Saavedra[125a,125f], M. Agustoni[17], S.P. Ahlen[22], F. Ahmadov[64,b], G. Aielli[134a,134b], H. Akerstedt[147a,147b], T.P.A. Åkesson[80], G. Akimoto[156], A.V. Akimov[95], G.L. Alberghi[20a,20b], J. Albert[170], S. Albrand[55], M.J. Alconada Verzini[70], M. Aleksa[30], I.N. Aleksandrov[64], C. Alexa[26a], G. Alexander[154], G. Alexandre[49], T. Alexopoulos[10], M. Alhroob[165a,165c], G. Alimonti[90a], L. Alio[84], J. Alison[31], B.M.M. Allbrooke[18], L.J. Allison[71], P.P. Allport[73], J. Almond[83], A. Aloisio[103a,103b], A. Alonso[36], F. Alonso[70], C. Alpigiani[75], A. Altheimer[35], B. Alvarez Gonzalez[89], M.G. Alviggi[103a,103b], K. Amako[65], Y. Amaral Coutinho[24a], C. Amelung[23], D. Amidei[88], S.P. Amor Dos Santos[125a,125c], A. Amorim[125a,125b], S. Amoroso[48], N. Amram[154], G. Amundsen[23], C. Anastopoulos[140], L.S. Ancu[49], N. Andari[30], T. Andeen[35], C.F. Anders[58b], G. Anders[30], K.J. Anderson[31], A. Andreazza[90a,90b], V. Andrei[58a], X.S. Anduaga[70], S. Angelidakis[9], I. Angelozzi[106], P. Anger[44], A. Angerami[35], F. Anghinolfi[30], A.V. Anisenkov[108], N. Anjos[125a], A. Annovi[47], A. Antonaki[9], M. Antonelli[47], A. Antonov[97], J. Antos[145b], F. Anulli[133a], M. Aoki[65], L. Aperio Bella[18], R. Apolle[119,c], G. Arabidze[89], I. Aracena[144], Y. Arai[65], J.P. Araque[125a], A.T.H. Arce[45], J-F. Arguin[94], S. Argyropoulos[42], M. Arik[19a], A.J. Armbruster[30], O. Arnaez[30], V. Arnal[81], H. Arnold[48], M. Arratia[28], O. Arslan[21], A. Artamonov[96], G. Artoni[23], S. Asai[156], N. Asbah[42], A. Ashkenazi[154], B. Åsman[147a,147b], L. Asquith[6], K. Assamagan[25], R. Astalos[145a], M. Atkinson[166], N.B. Atlay[142], B. Auerbach[6], K. Augsten[127], M. Aurousseau[146b], G. Avolio[30], G. Azuelos[94,d], Y. Azuma[156], M.A. Baak[30], C. Bacci[135a,135b], H. Bachacou[137], K. Bachas[155], M. Backes[30], M. Backhaus[30], J. Backus Mayes[144], E. Badescu[26a], P. Bagiacchi[133a,133b], P. Bagnaia[133a,133b], Y. Bai[33a], T. Bain[35], J.T. Baines[130], O.K. Baker[177], S. Baker[77], P. Balek[128], F. Balli[137], E. Banas[39], Sw. Banerjee[174], A.A.E. Bannoura[176], V. Bansal[170], H.S. Bansil[18], L. Barak[173], S.P. Baranov[95], E.L. Barberio[87], D. Barberis[50a,50b], M. Barbero[84], T. Barillari[100], M. Barisonzi[176], T. Barklow[144], N. Barlow[28], B.M. Barnett[130], R.M. Barnett[15], Z. Barnovska[5], A. Baroncelli[135a], G. Barone[49], A.J. Barr[119], F. Barreiro[81], J. Barreiro Guimarães da Costa[57], R. Bartoldus[144], A.E. Barton[71], P. Bartos[145a], V. Bartsch[150], A. Bassalat[116], A. Basye[166], R.L. Bates[53], L. Batkova[145a], J.R. Batley[28], M. Battaglia[138], M. Battistin[30], F. Bauer[137], H.S. Bawa[144,e], T. Beau[79], P.H. Beauchemin[162], R. Beccherle[123a,123b], P. Bechtle[21], H.P. Beck[17], K. Becker[176], S. Becker[99], M. Beckingham[139], C. Becot[116], A.J. Beddall[19c], A. Beddall[19c], S. Bedikian[177], V.A. Bednyakov[64], C.P. Bee[149], L.J. Beemster[106], T.A. Beermann[176], M. Begel[25], K. Behr[119], C. Belanger-Champagne[86], P.J. Bell[49], W.H. Bell[49], G. Bella[154], L. Bellagamba[20a], A. Bellerive[29], M. Bellomo[85], K. Belotskiy[97], O. Beltramello[30], O. Benary[154], D. Benchekroun[136a], K. Bendtz[147a,147b], N. Benekos[166], Y. Benhammou[154], E. Benhar Noccioli[49], J.A. Benitez Garcia[160b], D.P. Benjamin[45], J.R. Bensinger[23], K. Benslama[131], S. Bentvelsen[106], D. Berge[106], E. Bergeaas Kuutmann[16], N. Berger[5], F. Berghaus[170], E. Berglund[106], J. Beringer[15], C. Bernard[22], P. Bernat[77], C. Bernius[78], F.U. Bernlochner[170], T. Berry[76], P. Berta[128], C. Bertella[84], G. Bertoli[147a,147b], F. Bertolucci[123a,123b], D. Bertsche[112], M.I. Besana[90a], G.J. Besjes[105], O. Bessidskaia[147a,147b], M.F. Bessner[42], N. Besson[137], C. Betancourt[48], S. Bethke[100], W. Bhimji[46], R.M. Bianchi[124], L. Bianchini[23], M. Bianco[30], O. Biebel[99], S.P. Bieniek[77], K. Bierwagen[54], J. Biesiada[15], M. Biglietti[135a], J. Bilbao De Mendizabal[49], H. Bilokon[47], M. Bindi[54], S. Binet[116], A. Bingul[19c], C. Bini[133a,133b], C.W. Black[151], J.E. Black[144], K.M. Black[22], D. Blackburn[139], R.E. Blair[6], J.-B. Blanchard[137], T. Blazek[145a], I. Bloch[42], C. Blocker[23], W. Blum[82,*], U. Blumenschein[54], G.J. Bobbink[106], V.S. Bobrovnikov[108], S.S. Bocchetta[80], A. Bocci[45], C. Bock[99], C.R. Boddy[119], M. Boehler[48], J. Boek[176], T.T. Boek[176], J.A. Bogaerts[30], A.G. Bogdanchikov[108], A. Bogouch[91,*], C. Bohm[147a], J. Bohm[126], V. Boisvert[76], T. Bold[38a], V. Boldea[26a], A.S. Boldyrev[98], M. Bomben[79], M. Bona[75], M. Boonekamp[137], A. Borisov[129], G. Borissov[71], M. Borri[83], S. Borroni[42], J. Bortfeldt[99], V. Bortolotto[135a,135b], K. Bos[106], D. Boscherini[20a], M. Bosman[12], H. Boterenbrood[106], J. Boudreau[124], J. Bouffard[2],

JHEP09(2014)145

E.V. Bouhova-Thacker[71], D. Boumediene[34], C. Bourdarios[116], N. Bousson[113], S. Boutouil[136d], A. Boveia[31], J. Boyd[30], I.R. Boyko[64], I. Bozovic-Jelisavcic[13b], J. Bracinik[18], A. Brandt[8], G. Brandt[15], O. Brandt[58a], U. Bratzler[157], B. Brau[85], J.E. Brau[115], H.M. Braun[176,*], S.F. Brazzale[165a,165c], B. Brelier[159], K. Brendlinger[121], A.J. Brennan[87], R. Brenner[167], S. Bressler[173], K. Bristow[146c], T.M. Bristow[46], D. Britton[53], F.M. Brochu[28], I. Brock[21], R. Brock[89], C. Bromberg[89], J. Bronner[100], G. Brooijmans[35], T. Brooks[76], W.K. Brooks[32b], J. Brosamer[15], E. Brost[115], G. Brown[83], J. Brown[55], P.A. Bruckman de Renstrom[39], D. Bruncko[145b], R. Bruneliere[48], S. Brunet[60], A. Bruni[20a], G. Bruni[20a], M. Bruschi[20a], L. Bryngemark[80], T. Buanes[14], Q. Buat[143], F. Bucci[49], P. Buchholz[142], R.M. Buckingham[119], A.G. Buckley[53], S.I. Buda[26a], I.A. Budagov[64], F. Buehrer[48], L. Bugge[118], M.K. Bugge[118], O. Bulekov[97], A.C. Bundock[73], H. Burckhart[30], S. Burdin[73], B. Burghgrave[107], S. Burke[130], I. Burmeister[43], E. Busato[34], D. Büscher[48], V. Büscher[82], P. Bussey[53], C.P. Buszello[167], B. Butler[57], J.M. Butler[22], A.I. Butt[3], C.M. Buttar[53], J.M. Butterworth[77], P. Butti[106], W. Buttinger[28], A. Buzatu[53], M. Byszewski[10], S. Cabrera Urbán[168], D. Caforio[20a,20b], O. Cakir[4a], P. Calafiura[15], A. Calandri[137], G. Calderini[79], P. Calfayan[99], R. Calkins[107], L.P. Caloba[24a], D. Calvet[34], S. Calvet[34], R. Camacho Toro[49], S. Camarda[42], D. Cameron[118], L.M. Caminada[15], R. Caminal Armadans[12], S. Campana[30], M. Campanelli[77], A. Campoverde[149], V. Canale[103a,103b], A. Canepa[160a], M. Cano Bret[75], J. Cantero[81], R. Cantrill[76], T. Cao[40], M.D.M. Capeans Garrido[30], I. Caprini[26a], M. Caprini[26a], M. Capua[37a,37b], R. Caputo[82], R. Cardarelli[134a], T. Carli[30], G. Carlino[103a], L. Carminati[90a,90b], S. Caron[105], E. Carquin[32a], G.D. Carrillo-Montoya[146c], J.R. Carter[28], J. Carvalho[125a,125c], D. Casadei[77], M.P. Casado[12], M. Casolino[12], E. Castaneda-Miranda[146b], A. Castelli[106], V. Castillo Gimenez[168], N.F. Castro[125a], P. Catastini[57], A. Catinaccio[30], J.R. Catmore[118], A. Cattai[30], G. Cattani[134a,134b], S. Caughron[89], V. Cavaliere[166], D. Cavalli[90a], M. Cavalli-Sforza[12], V. Cavasinni[123a,123b], F. Ceradini[135a,135b], B. Cerio[45], K. Cerny[128], A.S. Cerqueira[24b], A. Cerri[150], L. Cerrito[75], F. Cerutti[15], M. Cerv[30], A. Cervelli[17], S.A. Cetin[19b], A. Chafaq[136a], D. Chakraborty[107], I. Chalupkova[128], P. Chang[166], B. Chapleau[86], J.D. Chapman[28], D. Charfeddine[116], D.G. Charlton[18], C.C. Chau[159], C.A. Chavez Barajas[150], S. Cheatham[86], A. Chegwidden[89], S. Chekanov[6], S.V. Chekulaev[160a], G.A. Chelkov[64], M.A. Chelstowska[88], C. Chen[63], H. Chen[25], K. Chen[149], L. Chen[33d,f], S. Chen[33c], X. Chen[146c], Y. Chen[35], H.C. Cheng[88], Y. Cheng[31], A. Cheplakov[64], R. Cherkaoui El Moursli[136e], V. Chernyatin[25,*], E. Cheu[7], L. Chevalier[137], V. Chiarella[47], G. Chiefari[103a,103b], J.T. Childers[6], A. Chilingarov[71], G. Chiodini[72a], A.S. Chisholm[18], R.T. Chislett[77], A. Chitan[26a], M.V. Chizhov[64], S. Chouridou[9], B.K.B. Chow[99], D. Chromek-Burckhart[30], M.L. Chu[152], J. Chudoba[126], J.J. Chwastowski[39], L. Chytka[114], G. Ciapetti[133a,133b], A.K. Ciftci[4a], R. Ciftci[4a], D. Cinca[62], V. Cindro[74], A. Ciocio[15], P. Cirkovic[13b], Z.H. Citron[173], M. Citterio[90a], M. Ciubancan[26a], A. Clark[49], P.J. Clark[46], R.N. Clarke[15], W. Cleland[124], J.C. Clemens[84], C. Clement[147a,147b], Y. Coadou[84], M. Cobal[165a,165c], A. Coccaro[139], J. Cochran[63], L. Coffey[23], J.G. Cogan[144], J. Coggeshall[166], B. Cole[35], S. Cole[107], A.P. Colijn[106], J. Collot[55], T. Colombo[58c], G. Colon[85], G. Compostella[100], P. Conde Muiño[125a,125b], E. Coniavitis[167], M.C. Conidi[12], S.H. Connell[146b], I.A. Connelly[76], S.M. Consonni[90a,90b], V. Consorti[48], S. Constantinescu[26a], C. Conta[120a,120b], G. Conti[57], F. Conventi[103a,g], M. Cooke[15], B.D. Cooper[77], A.M. Cooper-Sarkar[119], N.J. Cooper-Smith[76], K. Copic[15], T. Cornelissen[176], M. Corradi[20a], F. Corriveau[86,h], A. Corso-Radu[164], A. Cortes-Gonzalez[12], G. Cortiana[100], G. Costa[90a], M.J. Costa[168], D. Costanzo[140], D. Côté[8], G. Cottin[28], G. Cowan[76], B.E. Cox[83], K. Cranmer[109], G. Cree[29], S. Crépé-Renaudin[55], F. Crescioli[79], W.A. Cribbs[147a,147b], M. Crispin Ortuzar[119], M. Cristinziani[21], V. Croft[105], G. Crosetti[37a,37b], C.-M. Cuciuc[26a], T. Cuhadar Donszelmann[140], J. Cummings[177], M. Curatolo[47], C. Cuthbert[151], H. Czirr[142], P. Czodrowski[3], Z. Czyczula[177], S. D'Auria[53], M. D'Onofrio[73], M.J. Da Cunha Sargedas De Sousa[125a,125b], C. Da Via[83], W. Dabrowski[38a], A. Dafinca[119], T. Dai[88], O. Dale[14], F. Dallaire[94], C. Dallapiccola[85], M. Dam[36], A.C. Daniells[18], M. Dano Hoffmann[137], V. Dao[105], G. Darbo[50a], S. Darmora[8], J.A. Dassoulas[42], A. Dattagupta[60], W. Davey[21], C. David[170], T. Davidek[128], E. Davies[119,c], M. Davies[154], O. Davignon[79],

JHEP09(2014)145

A.R. Davison[77], P. Davison[77], Y. Davygora[58a], E. Dawe[143], I. Dawson[140], R.K. Daya-Ishmukhametova[85], K. De[8], R. de Asmundis[103a], S. De Castro[20a,20b], S. De Cecco[79], N. De Groot[105], P. de Jong[106], H. De la Torre[81], F. De Lorenzi[63], L. De Nooij[106], D. De Pedis[133a], A. De Salvo[133a], U. De Sanctis[165a,165b], A. De Santo[150], J.B. De Vivie De Regie[116], W.J. Dearnaley[71], R. Debbe[25], C. Debenedetti[46], B. Dechenaux[55], D.V. Dedovich[64], I. Deigaard[106], J. Del Peso[81], T. Del Prete[123a,123b], F. Deliot[137], C.M. Delitzsch[49], M. Deliyergiyev[74], A. Dell'Acqua[30], L. Dell'Asta[22], M. Dell'Orso[123a,123b], M. Della Pietra[103a,g], D. della Volpe[49], M. Delmastro[5], P.A. Delsart[55], C. Deluca[106], S. Demers[177], M. Demichev[64], A. Demilly[79], S.P. Denisov[129], D. Derendarz[39], J.E. Derkaoui[136d], F. Derue[79], P. Dervan[73], K. Desch[21], C. Deterre[42], P.O. Deviveiros[106], A. Dewhurst[130], S. Dhaliwal[106], A. Di Ciaccio[134a,134b], L. Di Ciaccio[5], A. Di Domenico[133a,133b], C. Di Donato[103a,103b], A. Di Girolamo[30], B. Di Girolamo[30], A. Di Mattia[153], B. Di Micco[135a,135b], R. Di Nardo[47], A. Di Simone[48], R. Di Sipio[20a,20b], D. Di Valentino[29], M.A. Diaz[32a], E.B. Diehl[88], J. Dietrich[42], T.A. Dietzsch[58a], S. Diglio[84], A. Dimitrievska[13a], J. Dingfelder[21], C. Dionisi[133a,133b], P. Dita[26a], S. Dita[26a], F. Dittus[30], F. Djama[84], T. Djobava[51b], M.A.B. do Vale[24c], A. Do Valle Wemans[125a,125g], T.K.O. Doan[5], D. Dobos[30], C. Doglioni[49], T. Doherty[53], T. Dohmae[156], J. Dolejsi[128], Z. Dolezal[128], B.A. Dolgoshein[97,*], M. Donadelli[24d], S. Donati[123a,123b], P. Dondero[120a,120b], J. Donini[34], J. Dopke[30], A. Doria[103a], M.T. Dova[70], A.T. Doyle[53], M. Dris[10], J. Dubbert[88], S. Dube[15], E. Dubreuil[34], E. Duchovni[173], G. Duckeck[99], O.A. Ducu[26a], D. Duda[176], A. Dudarev[30], F. Dudziak[63], L. Duflot[116], L. Duguid[76], M. Dührssen[30], M. Dunford[58a], H. Duran Yildiz[4a], M. Düren[52], A. Durglishvili[51b], M. Dwuznik[38a], M. Dyndal[38a], J. Ebke[99], W. Edson[2], N.C. Edwards[46], W. Ehrenfeld[21], T. Eifert[144], G. Eigen[14], K. Einsweiler[15], T. Ekelof[167], M. El Kacimi[136c], M. Ellert[167], S. Elles[5], F. Ellinghaus[82], N. Ellis[30], J. Elmsheuser[99], M. Elsing[30], D. Emeliyanov[130], Y. Enari[156], O.C. Endner[82], M. Endo[117], R. Engelmann[149], J. Erdmann[177], A. Ereditato[17], D. Eriksson[147a], G. Ernis[176], J. Ernst[2], M. Ernst[25], J. Ernwein[137], D. Errede[166], S. Errede[166], E. Ertel[82], M. Escalier[116], H. Esch[43], C. Escobar[124], B. Esposito[47], A.I. Etienvre[137], E. Etzion[154], H. Evans[60], A. Ezhilov[122], L. Fabbri[20a,20b], G. Facini[31], R.M. Fakhrutdinov[129], S. Falciano[133a], R.J. Falla[77], J. Faltova[128], Y. Fang[33a], M. Fanti[90a,90b], A. Farbin[8], A. Farilla[135a], T. Farooque[12], S. Farrell[164], S.M. Farrington[171], P. Farthouat[30], F. Fassi[168], P. Fassnacht[30], D. Fassouliotis[9], A. Favareto[50a,50b], L. Fayard[116], P. Federic[145a], O.L. Fedin[122,i], W. Fedorko[169], M. Fehling-Kaschek[48], S. Feigl[30], L. Feligioni[84], C. Feng[33d], E.J. Feng[6], H. Feng[88], A.B. Fenyuk[129], S. Fernandez Perez[30], S. Ferrag[53], J. Ferrando[53], A. Ferrari[167], P. Ferrari[106], R. Ferrari[120a], D.E. Ferreira de Lima[53], A. Ferrer[168], D. Ferrere[49], C. Ferretti[88], A. Ferretto Parodi[50a,50b], M. Fiascaris[31], F. Fiedler[82], A. Filipčič[74], M. Filipuzzi[42], F. Filthaut[105], M. Fincke-Keeler[170], K.D. Finelli[151], M.C.N. Fiolhais[125a,125c], L. Fiorini[168], A. Firan[40], J. Fischer[176], W.C. Fisher[89], E.A. Fitzgerald[23], M. Flechl[48], I. Fleck[142], P. Fleischmann[88], S. Fleischmann[176], G.T. Fletcher[140], G. Fletcher[75], T. Flick[176], A. Floderus[80], L.R. Flores Castillo[174,j], A.C. Florez Bustos[160b], M.J. Flowerdew[100], A. Formica[137], A. Forti[83], D. Fortin[160a], D. Fournier[116], H. Fox[71], S. Fracchia[12], P. Francavilla[79], M. Franchini[20a,20b], S. Franchino[30], D. Francis[30], M. Franklin[57], S. Franz[61], M. Fraternali[120a,120b], S.T. French[28], C. Friedrich[42], F. Friedrich[44], D. Froidevaux[30], J.A. Frost[28], C. Fukunaga[157], E. Fullana Torregrosa[82], B.G. Fulsom[144], J. Fuster[168], C. Gabaldon[55], O. Gabizon[173], A. Gabrielli[20a,20b], A. Gabrielli[133a,133b], S. Gadatsch[106], S. Gadomski[49], G. Gagliardi[50a,50b], P. Gagnon[60], C. Galea[105], B. Galhardo[125a,125c], E.J. Gallas[119], V. Gallo[17], B.J. Gallop[130], P. Gallus[127], G. Galster[36], K.K. Gan[110], R.P. Gandrajula[62], J. Gao[33b,f], Y.S. Gao[144,e], F.M. Garay Walls[46], F. Garberson[177], C. García[168], J.E. García Navarro[168], M. Garcia-Sciveres[15], R.W. Gardner[31], N. Garelli[144], V. Garonne[30], C. Gatti[47], G. Gaudio[120a], B. Gaur[142], L. Gauthier[94], P. Gauzzi[133a,133b], I.L. Gavrilenko[95], C. Gay[169], G. Gaycken[21], E.N. Gazis[10], P. Ge[33d], Z. Gecse[169], C.N.P. Gee[130], D.A.A. Geerts[106], Ch. Geich-Gimbel[21], K. Gellerstedt[147a,147b], C. Gemme[50a], A. Gemmell[53], M.H. Genest[55], S. Gentile[133a,133b], M. George[54], S. George[76], D. Gerbaudo[164], A. Gershon[154], H. Ghazlane[136b], N. Ghodbane[34],

JHEP09(2014)145

B. Giacobbe[20a], S. Giagu[133a,133b], V. Giangiobbe[12], P. Giannetti[123a,123b], F. Gianotti[30], B. Gibbard[25], S.M. Gibson[76], M. Gilchriese[15], T.P.S. Gillam[28], D. Gillberg[30], G. Gilles[34], D.M. Gingrich[3,d], N. Giokaris[9], M.P. Giordani[165a,165c], R. Giordano[103a,103b], F.M. Giorgi[20a], F.M. Giorgi[16], P.F. Giraud[137], D. Giugni[90a], C. Giuliani[48], M. Giulini[58b], B.K. Gjelsten[118], S. Gkaitatzis[155], I. Gkialas[155,k], L.K. Gladilin[98], C. Glasman[81], J. Glatzer[30], P.C.F. Glaysher[46], A. Glazov[42], G.L. Glonti[64], M. Goblirsch-Kolb[100], J.R. Goddard[75], J. Godfrey[143], J. Godlewski[30], C. Goeringer[82], S. Goldfarb[88], T. Golling[177], D. Golubkov[129], A. Gomes[125a,125b,125d], L.S. Gomez Fajardo[42], R. Gonçalo[125a], J. Goncalves Pinto Firmino Da Costa[137], L. Gonella[21], S. González de la Hoz[168], G. Gonzalez Parra[12], S. Gonzalez-Sevilla[49], L. Goossens[30], P.A. Gorbounov[96], H.A. Gordon[25], I. Gorelov[104], B. Gorini[30], E. Gorini[72a,72b], A. Gorišek[74], E. Gornicki[39], A.T. Goshaw[6], C. Gössling[43], M.I. Gostkin[64], M. Gouighri[136a], D. Goujdami[136c], M.P. Goulette[49], A.G. Goussiou[139], C. Goy[5], S. Gozpinar[23], H.M.X. Grabas[137], L. Graber[54], I. Grabowska-Bold[38a], P. Grafström[20a,20b], K-J. Grahn[42], J. Gramling[49], E. Gramstad[118], S. Grancagnolo[16], V. Grassi[149], V. Gratchev[122], H.M. Gray[30], E. Graziani[135a], O.G. Grebenyuk[122], Z.D. Greenwood[78,l], K. Gregersen[77], I.M. Gregor[42], P. Grenier[144], J. Griffiths[8], A.A. Grillo[138], K. Grimm[71], S. Grinstein[12,m], Ph. Gris[34], Y.V. Grishkevich[98], J.-F. Grivaz[116], J.P. Grohs[44], A. Grohsjean[42], E. Gross[173], J. Grosse-Knetter[54], G.C. Grossi[134a,134b], J. Groth-Jensen[173], Z.J. Grout[150], L. Guan[33b], F. Guescini[49], D. Guest[177], O. Gueta[154], C. Guicheney[34], E. Guido[50a,50b], T. Guillemin[116], S. Guindon[2], U. Gul[53], C. Gumpert[44], J. Gunther[127], J. Guo[35], S. Gupta[119], P. Gutierrez[112], N.G. Gutierrez Ortiz[53], C. Gutschow[77], N. Guttman[154], C. Guyot[137], C. Gwenlan[119], C.B. Gwilliam[73], A. Haas[109], C. Haber[15], H.K. Hadavand[8], N. Haddad[136e], P. Haefner[21], S. Hageböck[21], Z. Hajduk[39], H. Hakobyan[178], M. Haleem[42], D. Hall[119], G. Halladjian[89], K. Hamacher[176], P. Hamal[114], K. Hamano[170], M. Hamer[54], A. Hamilton[146a], S. Hamilton[162], P.G. Hamnett[42], L. Han[33b], K. Hanagaki[117], K. Hanawa[156], M. Hance[15], P. Hanke[58a], R. Hanna[137], J.B. Hansen[36], J.D. Hansen[36], P.H. Hansen[36], K. Hara[161], A.S. Hard[174], T. Harenberg[176], F. Hariri[116], S. Harkusha[91], D. Harper[88], R.D. Harrington[46], O.M. Harris[139], P.F. Harrison[171], F. Hartjes[106], S. Hasegawa[102], Y. Hasegawa[141], A. Hasib[112], S. Hassani[137], S. Haug[17], M. Hauschild[30], R. Hauser[89], M. Havranek[126], C.M. Hawkes[18], R.J. Hawkings[30], A.D. Hawkins[80], T. Hayashi[161], D. Hayden[89], C.P. Hays[119], H.S. Hayward[73], S.J. Haywood[130], S.J. Head[18], T. Heck[82], V. Hedberg[80], L. Heelan[8], S. Heim[121], T. Heim[176], B. Heinemann[15], L. Heinrich[109], S. Heisterkamp[36], J. Hejbal[126], L. Helary[22], C. Heller[99], M. Heller[30], S. Hellman[147a,147b], D. Hellmich[21], C. Helsens[30], J. Henderson[119], R.C.W. Henderson[71], C. Hengler[42], A. Henrichs[177], A.M. Henriques Correia[30], S. Henrot-Versille[116], C. Hensel[54], G.H. Herbert[16], Y. Hernández Jiménez[168], R. Herrberg-Schubert[16], G. Herten[48], R. Hertenberger[99], L. Hervas[30], G.G. Hesketh[77], N.P. Hessey[106], R. Hickling[75], E. Higón-Rodriguez[168], E. Hill[170], J.C. Hill[28], K.H. Hiller[42], S. Hillert[21], S.J. Hillier[18], I. Hinchliffe[15], E. Hines[121], M. Hirose[158], D. Hirschbuehl[176], J. Hobbs[149], N. Hod[106], M.C. Hodgkinson[140], P. Hodgson[140], A. Hoecker[30], M.R. Hoeferkamp[104], J. Hoffman[40], D. Hoffmann[84], J.I. Hofmann[58a], M. Hohlfeld[82], T.R. Holmes[15], T.M. Hong[121], L. Hooft van Huysduynen[109], J-Y. Hostachy[55], S. Hou[152], A. Hoummada[136a], J. Howard[119], J. Howarth[42], M. Hrabovsky[114], I. Hristova[16], J. Hrivnac[116], T. Hryn'ova[5], P.J. Hsu[82], S.-C. Hsu[139], D. Hu[35], X. Hu[25], Y. Huang[42], Z. Hubacek[30], F. Hubaut[84], F. Huegging[21], T.B. Huffman[119], E.W. Hughes[35], G. Hughes[71], M. Huhtinen[30], T.A. Hülsing[82], M. Hurwitz[15], N. Huseynov[64,b], J. Huston[89], J. Huth[57], G. Iacobucci[49], G. Iakovidis[10], I. Ibragimov[142], L. Iconomidou-Fayard[116], E. Ideal[177], P. Iengo[103a], O. Igonkina[106], T. Iizawa[172], Y. Ikegami[65], K. Ikematsu[142], M. Ikeno[65], Y. Ilchenko[31,aa], D. Iliadis[155], N. Ilic[159], Y. Inamaru[66], T. Ince[100], P. Ioannou[9], M. Iodice[135a], K. Iordanidou[9], V. Ippolito[57], A. Irles Quiles[168], C. Isaksson[167], M. Ishino[67], M. Ishitsuka[158], R. Ishmukhametov[110], C. Issever[119], S. Istin[19a], J.M. Iturbe Ponce[83], R. Iuppa[134a,134b], J. Ivarsson[80], W. Iwanski[39], H. Iwasaki[65], J.M. Izen[41], V. Izzo[103a], B. Jackson[121], M. Jackson[73], P. Jackson[1], M.R. Jaekel[30], V. Jain[2], K. Jakobs[48], S. Jakobsen[30], T. Jakoubek[126], J. Jakubek[127], D.O. Jamin[152], D.K. Jana[78], E. Jansen[77], H. Jansen[30], J. Janssen[21], M. Janus[171], G. Jarlskog[80], N. Javadov[64,b], T. Javůrek[48],

JHEP09(2014)145

L. Jeanty[15], J. Jejelava[51a,n], G.-Y. Jeng[151], D. Jennens[87], P. Jenni[48,o], J. Jentzsch[43], C. Jeske[171], S. Jézéquel[5], H. Ji[174], W. Ji[82], J. Jia[149], Y. Jiang[33b], M. Jimenez Belenguer[42], S. Jin[33a], A. Jinaru[26a], O. Jinnouchi[158], M.D. Joergensen[36], K.E. Johansson[147a], P. Johansson[140], K.A. Johns[7], K. Jon-And[147a,147b], G. Jones[171], R.W.L. Jones[71], T.J. Jones[73], J. Jongmanns[58a], P.M. Jorge[125a,125b], K.D. Joshi[83], J. Jovicevic[148], X. Ju[174], C.A. Jung[43], R.M. Jungst[30], P. Jussel[61], A. Juste Rozas[12,m], M. Kaci[168], A. Kaczmarska[39], M. Kado[116], H. Kagan[110], M. Kagan[144], E. Kajomovitz[45], C.W. Kalderon[119], S. Kama[40], A. Kamenshchikov[129], N. Kanaya[156], M. Kaneda[30], S. Kaneti[28], T. Kanno[158], V.A. Kantserov[97], J. Kanzaki[65], B. Kaplan[109], A. Kapliy[31], D. Kar[53], K. Karakostas[10], N. Karastathis[10], M. Karnevskiy[82], S.N. Karpov[64], K. Karthik[109], V. Kartvelishvili[71], A.N. Karyukhin[129], L. Kashif[174], G. Kasieczka[58b], R.D. Kass[110], A. Kastanas[14], Y. Kataoka[156], A. Katre[49], J. Katzy[42], V. Kaushik[7], K. Kawagoe[69], T. Kawamoto[156], G. Kawamura[54], S. Kazama[156], V.F. Kazanin[108], M.Y. Kazarinov[64], R. Keeler[170], R. Kehoe[40], M. Keil[54], J.S. Keller[42], J.J. Kempster[76], H. Keoshkerian[5], O. Kepka[126], B.P. Kerševan[74], S. Kersten[176], K. Kessoku[156], J. Keung[159], F. Khalil-zada[11], H. Khandanyan[147a,147b], A. Khanov[113], A. Khodinov[97], A. Khomich[58a], T.J. Khoo[28], G. Khoriauli[21], A. Khoroshilov[176], V. Khovanskiy[96], E. Khramov[64], J. Khubua[51b], H.Y. Kim[8], H. Kim[147a,147b], S.H. Kim[161], N. Kimura[172], O. Kind[16], B.T. King[73], M. King[168], R.S.B. King[119], S.B. King[169], J. Kirk[130], A.E. Kiryunin[100], T. Kishimoto[66], D. Kisielewska[38a], F. Kiss[48], T. Kitamura[66], T. Kittelmann[124], K. Kiuchi[161], E. Kladiva[145b], M. Klein[73], U. Klein[73], K. Kleinknecht[82], P. Klimek[147a,147b], A. Klimentov[25], R. Klingenberg[43], J.A. Klinger[83], T. Klioutchnikova[30], P.F. Klok[105], E.-E. Kluge[58a], P. Kluit[106], S. Kluth[100], E. Kneringer[61], E.B.F.G. Knoops[84], A. Knue[53], T. Kobayashi[156], M. Kobel[44], M. Kocian[144], P. Kodys[128], P. Koevesarki[21], T. Koffas[29], E. Koffeman[106], L.A. Kogan[119], S. Kohlmann[176], Z. Kohout[127], T. Kohriki[65], T. Koi[144], H. Kolanoski[16], I. Koletsou[5], J. Koll[89], A.A. Komar[95,*], Y. Komori[156], T. Kondo[65], N. Kondrashova[42], K. Köneke[48], A.C. König[105], S. König[82], T. Kono[65,p], R. Konoplich[109,q], N. Konstantinidis[77], R. Kopeliansky[153], S. Koperny[38a], L. Köpke[82], A.K. Kopp[48], K. Korcyl[39], K. Kordas[155], A. Korn[77], A.A. Korol[108,r], I. Korolkov[12], E.V. Korolkova[140], V.A. Korotkov[129], O. Kortner[100], S. Kortner[100], V.V. Kostyukhin[21], V.M. Kotov[64], A. Kotwal[45], C. Kourkoumelis[9], V. Kouskoura[155], A. Koutsman[160a], R. Kowalewski[170], T.Z. Kowalski[38a], W. Kozanecki[137], A.S. Kozhin[129], V. Kral[127], V.A. Kramarenko[98], G. Kramberger[74], D. Krasnopevtsev[97], M.W. Krasny[79], A. Krasznahorkay[30], J.K. Kraus[21], A. Kravchenko[25], S. Kreiss[109], M. Kretz[58c], J. Kretzschmar[73], K. Kreutzfeldt[52], P. Krieger[159], K. Kroeninger[54], H. Kroha[100], J. Kroll[121], J. Kroseberg[21], J. Krstic[13a], U. Kruchonak[64], H. Krüger[21], T. Kruker[17], N. Krumnack[63], Z.V. Krumshteyn[64], A. Kruse[174], M.C. Kruse[45], M. Kruskal[22], T. Kubota[87], S. Kuday[4a], S. Kuehn[48], A. Kugel[58c], A. Kuhl[138], T. Kuhl[42], V. Kukhtin[64], Y. Kulchitsky[91], S. Kuleshov[32b], M. Kuna[133a,133b], J. Kunkle[121], A. Kupco[126], H. Kurashige[66], Y.A. Kurochkin[91], R. Kurumida[66], V. Kus[126], E.S. Kuwertz[148], M. Kuze[158], J. Kvita[114], A. La Rosa[49], L. La Rotonda[37a,37b], C. Lacasta[168], F. Lacava[133a,133b], J. Lacey[29], H. Lacker[16], D. Lacour[79], V.R. Lacuesta[168], E. Ladygin[64], R. Lafaye[5], B. Laforge[79], T. Lagouri[177], S. Lai[48], H. Laier[58a], L. Lambourne[77], S. Lammers[60], C.L. Lampen[7], W. Lampl[7], E. Lançon[137], U. Landgraf[48], M.P.J. Landon[75], V.S. Lang[58a], C. Lange[42], A.J. Lankford[164], F. Lanni[25], K. Lantzsch[30], S. Laplace[79], C. Lapoire[21], J.F. Laporte[137], T. Lari[90a], M. Lassnig[30], P. Laurelli[47], W. Lavrijsen[15], A.T. Law[138], P. Laycock[73], B.T. Le[55], O. Le Dortz[79], E. Le Guirriec[84], E. Le Menedeu[12], T. LeCompte[6], F. Ledroit-Guillon[55], C.A. Lee[152], H. Lee[106], J.S.H. Lee[117], S.C. Lee[152], L. Lee[177], G. Lefebvre[79], M. Lefebvre[170], F. Legger[99], C. Leggett[15], A. Lehan[73], M. Lehmacher[21], G. Lehmann Miotto[30], X. Lei[7], W.A. Leight[29], A. Leisos[155], A.G. Leister[177], M.A.L. Leite[24d], R. Leitner[128], D. Lellouch[173], B. Lemmer[54], K.J.C. Leney[77], T. Lenz[106], G. Lenzen[176], B. Lenzi[30], R. Leone[7], S. Leone[123a,123b], K. Leonhardt[44], C. Leonidopoulos[46], S. Leontsinis[10], C. Leroy[94], C.G. Lester[28], C.M. Lester[121], M. Levchenko[122], J. Levêque[5], D. Levin[88], L.J. Levinson[173], M. Levy[18], A. Lewis[119], G.H. Lewis[109], A.M. Leyko[21], M. Leyton[41], B. Li[33b,s], B. Li[84], H. Li[149], H.L. Li[31], L. Li[45], L. Li[33e], S. Li[45], Y. Li[33c,t], Z. Liang[138], H. Liao[34], B. Liberti[134a], P. Lichard[30], K. Lie[166], J. Liebal[21], W. Liebig[14],

JHEP09(2014)145

C. Limbach[21], A. Limosani[87], S.C. Lin[152,u], T.H. Lin[82], F. Linde[106], B.E. Lindquist[149], J.T. Linnemann[89], E. Lipeles[121], A. Lipniacka[14], M. Lisovyi[42], T.M. Liss[166], D. Lissauer[25], A. Lister[169], A.M. Litke[138], B. Liu[152], D. Liu[152], J.B. Liu[33b], K. Liu[33b,v], L. Liu[88], M. Liu[45], M. Liu[33b], Y. Liu[33b], M. Livan[120a,120b], S.S.A. Livermore[119], A. Lleres[55], J. Llorente Merino[81], S.L. Lloyd[75], F. Lo Sterzo[152], E. Lobodzinska[42], P. Loch[7], W.S. Lockman[138], T. Loddenkoetter[21], F.K. Loebinger[83], A.E. Loevschall-Jensen[36], A. Loginov[177], C.W. Loh[169], T. Lohse[16], K. Lohwasser[42], M. Lokajicek[126], V.P. Lombardo[5], B.A. Long[22], J.D. Long[88], R.E. Long[71], L. Lopes[125a], D. Lopez Mateos[57], B. Lopez Paredes[140], I. Lopez Paz[12], J. Lorenz[99], N. Lorenzo Martinez[60], M. Losada[163], P. Loscutoff[15], X. Lou[41], A. Lounis[116], J. Love[6], P.A. Love[71], A.J. Lowe[144,e], F. Lu[33a], H.J. Lubatti[139], C. Luci[133a,133b], A. Lucotte[55], F. Luehring[60], W. Lukas[61], L. Luminari[133a], O. Lundberg[147a,147b], B. Lund-Jensen[148], M. Lungwitz[82], D. Lynn[25], R. Lysak[126], E. Lytken[80], H. Ma[25], L.L. Ma[33d], G. Maccarrone[47], A. Macchiolo[100], J. Machado Miguens[125a,125b], D. Macina[30], D. Madaffari[84], R. Madar[48], H.J. Maddocks[71], W.F. Mader[44], A. Madsen[167], M. Maeno[8], T. Maeno[25], E. Magradze[54], K. Mahboubi[48], J. Mahlstedt[106], S. Mahmoud[73], C. Maiani[137], C. Maidantchik[24a], A. Maio[125a,125b,125d], S. Majewski[115], Y. Makida[65], N. Makovec[116], P. Mal[137,w], B. Malaescu[79], Pa. Malecki[39], V.P. Maleev[122], F. Malek[55], U. Mallik[62], D. Malon[6], C. Malone[144], S. Maltezos[10], V.M. Malyshev[108], S. Malyukov[30], J. Mamuzic[13b], B. Mandelli[30], L. Mandelli[90a], I. Mandić[74], R. Mandrysch[62], J. Maneira[125a,125b], A. Manfredini[100], L. Manhaes de Andrade Filho[24b], J.A. Manjarres Ramos[160b], A. Mann[99], P.M. Manning[138], A. Manousakis-Katsikakis[9], B. Mansoulie[137], R. Mantifel[86], L. Mapelli[30], L. March[168], J.F. Marchand[29], G. Marchiori[79], M. Marcisovsky[126], C.P. Marino[170], M. Marjanovic[13a], C.N. Marques[125a], F. Marroquim[24a], S.P. Marsden[83], Z. Marshall[15], L.F. Marti[17], S. Marti-Garcia[168], B. Martin[30], B. Martin[89], T.A. Martin[171], V.J. Martin[46], B. Martin dit Latour[14], H. Martinez[137], M. Martinez[12,m], S. Martin-Haugh[130], A.C. Martyniuk[77], M. Marx[139], F. Marzano[133a], A. Marzin[30], L. Masetti[82], T. Mashimo[156], R. Mashinistov[95], J. Masik[83], A.L. Maslennikov[108], I. Massa[20a,20b], N. Massol[5], P. Mastrandrea[149], A. Mastroberardino[37a,37b], T. Masubuchi[156], T. Matsushita[66], P. Mättig[176], J. Mattmann[82], J. Maurer[26a], S.J. Maxfield[73], D.A. Maximov[108,r], R. Mazini[152], L. Mazzaferro[134a,134b], G. Mc Goldrick[159], S.P. Mc Kee[88], A. McCarn[88], R.L. McCarthy[149], T.G. McCarthy[29], N.A. McCubbin[130], K.W. McFarlane[56,*], J.A. Mcfayden[77], G. Mchedlidze[54], S.J. McMahon[130], R.A. McPherson[170,h], A. Meade[85], J. Mechnich[106], M. Medinnis[42], S. Meehan[31], S. Mehlhase[36], A. Mehta[73], K. Meier[58a], C. Meineck[99], B. Meirose[80], C. Melachrinos[31], B.R. Mellado Garcia[146c], F. Meloni[17], A. Mengarelli[20a,20b], S. Menke[100], E. Meoni[162], K.M. Mercurio[57], S. Mergelmeyer[21], N. Meric[137], P. Mermod[49], L. Merola[103a,103b], C. Meroni[90a], F.S. Merritt[31], H. Merritt[110], A. Messina[30,x], J. Metcalfe[25], A.S. Mete[164], C. Meyer[82], C. Meyer[31], J-P. Meyer[137], J. Meyer[30], R.P. Middleton[130], S. Migas[73], L. Mijović[21], G. Mikenberg[173], M. Mikestikova[126], M. Mikuž[74], D.W. Miller[31], C. Mills[46], A. Milov[173], D.A. Milstead[147a,147b], D. Milstein[173], A.A. Minaenko[129], I.A. Minashvili[64], A.I. Mincer[109], B. Mindur[38a], M. Mineev[64], Y. Ming[174], L.M. Mir[12], G. Mirabelli[133a], T. Mitani[172], J. Mitrevski[99], V.A. Mitsou[168], S. Mitsui[65], A. Miucci[49], P.S. Miyagawa[140], J.U. Mjörnmark[80], T. Moa[147a,147b], K. Mochizuki[84], V. Moeller[28], S. Mohapatra[35], W. Mohr[48], S. Molander[147a,147b], R. Moles-Valls[168], K. Mönig[42], C. Monini[55], J. Monk[36], E. Monnier[84], J. Montejo Berlingen[12], F. Monticelli[70], S. Monzani[133a,133b], R.W. Moore[3], A. Moraes[53], N. Morange[62], D. Moreno[82], M. Moreno Llácer[54], P. Morettini[50a], M. Morgenstern[44], M. Morii[57], S. Moritz[82], A.K. Morley[148], G. Mornacchi[30], J.D. Morris[75], L. Morvaj[102], H.G. Moser[100], M. Mosidze[51b], J. Moss[110], R. Mount[144], E. Mountricha[25], S.V. Mouraviev[95,*], E.J.W. Moyse[85], S. Muanza[84], R.D. Mudd[18], F. Mueller[58a], J. Mueller[124], K. Mueller[21], T. Mueller[28], T. Mueller[82], D. Muenstermann[49], Y. Munwes[154], J.A. Murillo Quijada[18], W.J. Murray[171,130], H. Musheghyan[54], E. Musto[153], A.G. Myagkov[129,y], M. Myska[127], O. Nackenhorst[54], J. Nadal[54], K. Nagai[61], R. Nagai[158], Y. Nagai[84], K. Nagano[65], A. Nagarkar[110], Y. Nagasaka[59], M. Nagel[100], A.M. Nairz[30], Y. Nakahama[30], K. Nakamura[65], T. Nakamura[156], I. Nakano[111], H. Namasivayam[41], G. Nanava[21], R. Narayan[58b], T. Nattermann[21], T. Naumann[42], G. Navarro[163], R. Nayyar[7], H.A. Neal[88],

JHEP09(2014)145

P.Yu. Nechaeva[95], T.J. Neep[83], A. Negri[120a,120b], G. Negri[30], M. Negrini[20a], S. Nektarijevic[49], A. Nelson[164], T.K. Nelson[144], S. Nemecek[126], P. Nemethy[109], A.A. Nepomuceno[24a], M. Nessi[30,z], M.S. Neubauer[166], M. Neumann[176], R.M. Neves[109], P. Nevski[25], P.R. Newman[18], D.H. Nguyen[6], R.B. Nickerson[119], R. Nicolaidou[137], B. Nicquevert[30], J. Nielsen[138], N. Nikiforou[35], A. Nikiforov[16], V. Nikolaenko[129,y], I. Nikolic-Audit[79], K. Nikolics[49], K. Nikolopoulos[18], P. Nilsson[8], Y. Ninomiya[156], A. Nisati[133a], R. Nisius[100], T. Nobe[158], L. Nodulman[6], M. Nomachi[117], I. Nomidis[155], S. Norberg[112], M. Nordberg[30], S. Nowak[100], M. Nozaki[65], L. Nozka[114], K. Ntekas[10], G. Nunes Hanninger[87], T. Nunnemann[99], E. Nurse[77], F. Nuti[87], B.J. O'Brien[46], F. O'grady[7], D.C. O'Neil[143], V. O'Shea[53], F.G. Oakham[29,d], H. Oberlack[100], T. Obermann[21], J. Ocariz[79], A. Ochi[66], M.I. Ochoa[77], S. Oda[69], S. Odaka[65], H. Ogren[60], A. Oh[83], S.H. Oh[45], C.C. Ohm[30], H. Ohman[167], T. Ohshima[102], W. Okamura[117], H. Okawa[25], Y. Okumura[31], T. Okuyama[156], A. Olariu[26a], A.G. Olchevski[64], S.A. Olivares Pino[46], D. Oliveira Damazio[25], E. Oliver Garcia[168], A. Olszewski[39], J. Olszowska[39], A. Onofre[125a,125e], P.U.E. Onyisi[31,aa], C.J. Oram[160a], M.J. Oreglia[31], Y. Oren[154], D. Orestano[135a,135b], N. Orlando[72a,72b], C. Oropeza Barrera[53], R.S. Orr[159], B. Osculati[50a,50b], R. Ospanov[121], G. Otero y Garzon[27], H. Otono[69], M. Ouchrif[136d], E.A. Ouellette[170], F. Ould-Saada[118], A. Ouraou[137], K.P. Oussoren[106], Q. Ouyang[33a], A. Ovcharova[15], M. Owen[83], V.E. Ozcan[19a], N. Ozturk[8], K. Pachal[119], A. Pacheco Pages[12], C. Padilla Aranda[12], M. Pagáčová[48], S. Pagan Griso[15], E. Paganis[140], C. Pahl[100], F. Paige[25], P. Pais[85], K. Pajchel[118], G. Palacino[160b], S. Palestini[30], M. Palka[38b], D. Pallin[34], A. Palma[125a,125b], J.D. Palmer[18], Y.B. Pan[174], E. Panagiotopoulou[10], J.G. Panduro Vazquez[76], P. Pani[106], N. Panikashvili[88], S. Panitkin[25], D. Pantea[26a], L. Paolozzi[134a,134b], Th.D. Papadopoulou[10], K. Papageorgiou[155,k], A. Paramonov[6], D. Paredes Hernandez[34], M.A. Parker[28], F. Parodi[50a,50b], J.A. Parsons[35], U. Parzefall[48], E. Pasqualucci[133a], S. Passaggio[50a], A. Passeri[135a], F. Pastore[135a,135b,*], Fr. Pastore[76], G. Pásztor[29], S. Pataraia[176], N.D. Patel[151], J.R. Pater[83], S. Patricelli[103a,103b], T. Pauly[30], J. Pearce[170], M. Pedersen[118], S. Pedraza Lopez[168], R. Pedro[125a,125b], S.V. Peleganchuk[108], D. Pelikan[167], H. Peng[33b], B. Penning[31], J. Penwell[60], D.V. Perepelitsa[25], E. Perez Codina[160a], M.T. Pérez García-Estañ[168], V. Perez Reale[35], L. Perini[90a,90b], H. Pernegger[30], R. Perrino[72a], R. Peschke[42], V.D. Peshekhonov[64], K. Peters[30], R.F.Y. Peters[83], B.A. Petersen[87], T.C. Petersen[36], E. Petit[42], A. Petridis[147a,147b], C. Petridou[155], E. Petrolo[133a], F. Petrucci[135a,135b], M. Petteni[143], N.E. Pettersson[158], R. Pezoa[32b], P.W. Phillips[130], G. Piacquadio[144], E. Pianori[171], A. Picazio[49], E. Piccaro[75], M. Piccinini[20a,20b], R. Piegaia[27], D.T. Pignotti[110], J.E. Pilcher[31], A.D. Pilkington[77], J. Pina[125a,125b,125d], M. Pinamonti[165a,165c,ab], A. Pinder[119], J.L. Pinfold[3], A. Pingel[36], B. Pinto[125a], S. Pires[79], M. Pitt[173], C. Pizio[90a,90b], L. Plazak[145a], M.-A. Pleier[25], V. Pleskot[128], E. Plotnikova[64], P. Plucinski[147a,147b], S. Poddar[58a], F. Podlyski[34], R. Poettgen[82], L. Poggioli[116], D. Pohl[21], M. Pohl[49], G. Polesello[120a], A. Policicchio[37a,37b], R. Polifka[159], A. Polini[20a], C.S. Pollard[45], V. Polychronakos[25], K. Pommès[30], L. Pontecorvo[133a], B.G. Pope[89], G.A. Popeneciu[26b], D.S. Popovic[13a], A. Poppleton[30], X. Portell Bueso[12], G.E. Pospelov[100], S. Pospisil[127], K. Potamianos[15], I.N. Potrap[64], C.J. Potter[150], C.T. Potter[115], G. Poulard[30], J. Poveda[60], V. Pozdnyakov[64], P. Pralavorio[84], A. Pranko[15], S. Prasad[30], R. Pravahan[8], S. Prell[63], D. Price[83], J. Price[73], L.E. Price[6], D. Prieur[124], M. Primavera[72a], M. Proissl[46], K. Prokofiev[47], F. Prokoshin[32b], E. Protopapadaki[137], S. Protopopescu[25], J. Proudfoot[6], M. Przybycien[38a], H. Przysiezniak[5], E. Ptacek[115], E. Pueschel[85], D. Puldon[149], M. Purohit[25,ac], P. Puzo[116], J. Qian[88], G. Qin[53], Y. Qin[83], A. Quadt[54], D.R. Quarrie[15], W.B. Quayle[165a,165b], M. Queitsch-Maitland[83], D. Quilty[53], A. Qureshi[160b], V. Radeka[25], V. Radescu[42], S.K. Radhakrishnan[149], P. Radloff[115], P. Rados[87], F. Ragusa[90a,90b], G. Rahal[179], S. Rajagopalan[25], M. Rammensee[30], A.S. Randle-Conde[40], C. Rangel-Smith[167], K. Rao[164], F. Rauscher[99], T.C. Rave[48], T. Ravenscroft[53], M. Raymond[30], A.L. Read[118], N.P. Readioff[73], D.M. Rebuzzi[120a,120b], A. Redelbach[175], G. Redlinger[25], R. Reece[138], K. Reeves[41], L. Rehnisch[16], H. Reisin[27], M. Relich[164], C. Rembser[30], H. Ren[33a], Z.L. Ren[152], A. Renaud[116], M. Rescigno[133a], S. Resconi[90a], O.L. Rezanova[108,r], P. Reznicek[128], R. Rezvani[94], R. Richter[100], M. Ridel[79], P. Rieck[16], J. Rieger[54], M. Rijssenbeek[149], A. Rimoldi[120a,120b], L. Rinaldi[20a], E. Ritsch[61],

JHEP09(2014)145

I. Riu[12], F. Rizatdinova[113], E. Rizvi[75], S.H. Robertson[86,h], A. Robichaud-Veronneau[86], D. Robinson[28], J.E.M. Robinson[83], A. Robson[53], C. Roda[123a,123b], L. Rodrigues[30], S. Roe[30], O. Røhne[118], S. Rolli[162], A. Romaniouk[97], M. Romano[20a,20b], E. Romero Adam[168], N. Rompotis[139], L. Roos[79], E. Ros[168], S. Rosati[133a], K. Rosbach[49], M. Rose[76], P.L. Rosendahl[14], O. Rosenthal[142], V. Rossetti[147a,147b], E. Rossi[103a,103b], L.P. Rossi[50a], R. Rosten[139], M. Rotaru[26a], I. Roth[173], J. Rothberg[139], D. Rousseau[116], C.R. Royon[137], A. Rozanov[84], Y. Rozen[153], X. Ruan[146c], F. Rubbo[12], I. Rubinskiy[42], V.I. Rud[98], C. Rudolph[44], M.S. Rudolph[159], F. Rühr[48], A. Ruiz-Martinez[30], Z. Rurikova[48], N.A. Rusakovich[64], A. Ruschke[99], J.P. Rutherfoord[7], N. Ruthmann[48], Y.F. Ryabov[122], M. Rybar[128], G. Rybkin[116], N.C. Ryder[119], A.F. Saavedra[151], S. Sacerdoti[27], A. Saddique[3], I. Sadeh[154], H.F-W. Sadrozinski[138], R. Sadykov[64], F. Safai Tehrani[133a], H. Sakamoto[156], Y. Sakurai[172], G. Salamanna[75], A. Salamon[134a], M. Saleem[112], D. Salek[106], P.H. Sales De Bruin[139], D. Salihagic[100], A. Salnikov[144], J. Salt[168], B.M. Salvachua Ferrando[6], D. Salvatore[37a,37b], F. Salvatore[150], A. Salvucci[105], A. Salzburger[30], D. Sampsonidis[155], A. Sanchez[103a,103b], J. Sánchez[168], V. Sanchez Martinez[168], H. Sandaker[14], R.L. Sandbach[75], H.G. Sander[82], M.P. Sanders[99], M. Sandhoff[176], T. Sandoval[28], C. Sandoval[163], R. Sandstroem[100], D.P.C. Sankey[130], A. Sansoni[47], C. Santoni[34], R. Santonico[134a,134b], H. Santos[125a], I. Santoyo Castillo[150], K. Sapp[124], A. Sapronov[64], J.G. Saraiva[125a,125d], B. Sarrazin[21], G. Sartisohn[176], O. Sasaki[65], Y. Sasaki[156], G. Sauvage[5,*], E. Sauvan[5], P. Savard[159,d], D.O. Savu[30], C. Sawyer[119], L. Sawyer[78,l], D.H. Saxon[53], J. Saxon[121], C. Sbarra[20a], A. Sbrizzi[3], T. Scanlon[77], D.A. Scannicchio[164], M. Scarcella[151], J. Schaarschmidt[173], P. Schacht[100], D. Schaefer[121], R. Schaefer[42], S. Schaepe[21], S. Schaetzel[58b], U. Schäfer[82], A.C. Schaffer[116], D. Schaile[99], R.D. Schamberger[149], V. Scharf[58a], V.A. Schegelsky[122], D. Scheirich[128], M. Schernau[164], M.I. Scherzer[35], C. Schiavi[50a,50b], J. Schieck[99], C. Schillo[48], M. Schioppa[37a,37b], S. Schlenker[30], E. Schmidt[48], K. Schmieden[30], C. Schmitt[82], C. Schmitt[99], S. Schmitt[58b], B. Schneider[17], Y.J. Schnellbach[73], U. Schnoor[44], L. Schoeffel[137], A. Schoening[58b], B.D. Schoenrock[89], A.L.S. Schorlemmer[54], M. Schott[82], D. Schouten[160a], J. Schovancova[25], S. Schramm[159], M. Schreyer[175], C. Schroeder[82], N. Schuh[82], M.J. Schultens[21], H.-C. Schultz-Coulon[58a], H. Schulz[16], M. Schumacher[48], B.A. Schumm[138], Ph. Schune[137], C. Schwanenberger[83], A. Schwartzman[144], Ph. Schwegler[100], Ph. Schwemling[137], R. Schwienhorst[89], J. Schwindling[137], T. Schwindt[21], M. Schwoerer[5], F.G. Sciacca[17], E. Scifo[116], G. Sciolla[23], W.G. Scott[130], F. Scuri[123a,123b], F. Scutti[21], J. Searcy[88], G. Sedov[42], E. Sedykh[122], S.C. Seidel[104], A. Seiden[138], F. Seifert[127], J.M. Seixas[24a], G. Sekhniaidze[103a], S.J. Sekula[40], K.E. Selbach[46], D.M. Seliverstov[122,*], G. Sellers[73], N. Semprini-Cesari[20a,20b], C. Serfon[30], L. Serin[116], L. Serkin[54], T. Serre[84], R. Seuster[160a], H. Severini[112], T. Sfiligoj[74], F. Sforza[100], A. Sfyrla[30], E. Shabalina[54], M. Shamim[115], L.Y. Shan[33a], R. Shang[166], J.T. Shank[22], M. Shapiro[15], P.B. Shatalov[96], K. Shaw[165a,165b], C.Y. Shehu[150], P. Sherwood[77], L. Shi[152,ad], S. Shimizu[66], C.O. Shimmin[164], M. Shimojima[101], M. Shiyakova[64], A. Shmeleva[95], M.J. Shochet[31], D. Short[119], S. Shrestha[63], E. Shulga[97], M.A. Shupe[7], S. Shushkevich[42], P. Sicho[126], O. Sidiropoulou[155], D. Sidorov[113], A. Sidoti[133a], F. Siegert[44], Dj. Sijacki[13a], J. Silva[125a,125d], Y. Silver[154], D. Silverstein[144], S.B. Silverstein[147a], V. Simak[127], O. Simard[5], Lj. Simic[13a], S. Simion[116], E. Simioni[82], B. Simmons[77], R. Simoniello[90a,90b], M. Simonyan[36], P. Sinervo[159], N.B. Sinev[115], V. Sipica[142], G. Siragusa[175], A. Sircar[78], A.N. Sisakyan[64,*], S.Yu. Sivoklokov[98], J. Sjölin[147a,147b], T.B. Sjursen[14], H.P. Skottowe[57], K.Yu. Skovpen[108], P. Skubic[112], M. Slater[18], T. Slavicek[127], K. Sliwa[162], V. Smakhtin[173], B.H. Smart[46], L. Smestad[14], S.Yu. Smirnov[97], Y. Smirnov[97], L.N. Smirnova[98,ae], O. Smirnova[80], K.M. Smith[53], M. Smizanska[71], K. Smolek[127], A.A. Snesarev[95], G. Snidero[75], S. Snyder[25], R. Sobie[170,h], F. Socher[44], A. Soffer[154], D.A. Soh[152,ad], C.A. Solans[30], M. Solar[127], J. Solc[127], E.Yu. Soldatov[97], U. Soldevila[168], E. Solfaroli Camillocci[133a,133b], A.A. Solodkov[129], A. Soloshenko[64], O.V. Solovyanov[129], V. Solovyev[122], P. Sommer[48], H.Y. Song[33b], N. Soni[1], A. Sood[15], A. Sopczak[127], B. Sopko[127], V. Sopko[127], V. Sorin[12], M. Sosebee[8], R. Soualah[165a,165c], P. Soueid[94], A.M. Soukharev[108], D. South[42], S. Spagnolo[72a,72b], F. Spanò[76], W.R. Spearman[57], R. Spighi[20a], G. Spigo[30], M. Spousta[128], T. Spreitzer[159], B. Spurlock[8], R.D. St. Denis[53,*],

JHEP09(2014)145

S. Staerz[44], J. Stahlman[121], R. Stamen[58a], E. Stanecka[39], R.W. Stanek[6], C. Stanescu[135a], M. Stanescu-Bellu[42], M.M. Stanitzki[42], S. Stapnes[118], E.A. Starchenko[129], J. Stark[55], P. Staroba[126], P. Starovoitov[42], R. Staszewski[39], P. Stavina[145a,*], P. Steinberg[25], B. Stelzer[143], H.J. Stelzer[30], O. Stelzer-Chilton[160a], H. Stenzel[52], S. Stern[100], G.A. Stewart[53], J.A. Stillings[21], M.C. Stockton[86], M. Stoebe[86], G. Stoicea[26a], P. Stolte[54], S. Stonjek[100], A.R. Stradling[8], A. Straessner[44], M.E. Stramaglia[17], J. Strandberg[148], S. Strandberg[147a,147b], A. Strandlie[118], E. Strauss[144], M. Strauss[112], P. Strizenec[145b], R. Ströhmer[175], D.M. Strom[115], R. Stroynowski[40], S.A. Stucci[17], B. Stugu[14], N.A. Styles[42], D. Su[144], J. Su[124], HS. Subramania[3], R. Subramaniam[78], A. Succurro[12], Y. Sugaya[117], C. Suhr[107], M. Suk[127], V.V. Sulin[95], S. Sultansoy[4c], T. Sumida[67], X. Sun[33a], J.E. Sundermann[48], K. Suruliz[140], G. Susinno[37a,37b], M.R. Sutton[150], Y. Suzuki[65], M. Svatos[126], S. Swedish[169], M. Swiatlowski[144], I. Sykora[145a], T. Sykora[128], D. Ta[89], K. Tackmann[42], J. Taenzer[159], A. Taffard[164], R. Tafirout[160a], N. Taiblum[154], Y. Takahashi[102], H. Takai[25], R. Takashima[68], H. Takeda[66], T. Takeshita[141], Y. Takubo[65], M. Talby[84], A.A. Talyshev[108,r], J.Y.C. Tam[175], K.G. Tan[87], J. Tanaka[156], R. Tanaka[116], S. Tanaka[132], S. Tanaka[65], A.J. Tanasijczuk[143], K. Tani[66], N. Tannoury[21], S. Tapprogge[82], S. Tarem[153], F. Tarrade[29], G.F. Tartarelli[90a], P. Tas[128], M. Tasevsky[126], T. Tashiro[67], E. Tassi[37a,37b], A. Tavares Delgado[125a,125b], Y. Tayalati[136d], F.E. Taylor[93], G.N. Taylor[87], W. Taylor[160b], F.A. Teischinger[30], M. Teixeira Dias Castanheira[75], P. Teixeira-Dias[76], K.K. Temming[48], H. Ten Kate[30], P.K. Teng[152], J.J. Teoh[117], S. Terada[65], K. Terashi[156], J. Terron[81], S. Terzo[100], M. Testa[47], R.J. Teuscher[159,h], J. Therhaag[21], T. Theveneaux-Pelzer[34], J.P. Thomas[18], J. Thomas-Wilsker[76], E.N. Thompson[35], P.D. Thompson[18], P.D. Thompson[159], A.S. Thompson[53], L.A. Thomsen[36], E. Thomson[121], M. Thomson[28], W.M. Thong[87], R.P. Thun[88,*], F. Tian[35], M.J. Tibbetts[15], V.O. Tikhomirov[95,af], Yu.A. Tikhonov[108,r], S. Timoshenko[97], E. Tiouchichine[84], P. Tipton[177], S. Tisserant[84], T. Todorov[5], S. Todorova-Nova[128], B. Toggerson[7], J. Tojo[69], S. Tokár[145a], K. Tokushuku[65], K. Tollefson[89], L. Tomlinson[83], M. Tomoto[102], L. Tompkins[31], K. Toms[104], N.D. Topilin[64], E. Torrence[115], H. Torres[143], E. Torró Pastor[168], J. Toth[84,ag], F. Touchard[84], D.R. Tovey[140], H.L. Tran[116], T. Trefzger[175], L. Tremblet[30], A. Tricoli[30], I.M. Trigger[160a], S. Trincaz-Duvoid[79], M.F. Tripiana[70], N. Triplett[25], W. Trischuk[159], B. Trocmé[55], C. Troncon[90a], M. Trottier-McDonald[143], M. Trovatelli[135a,135b], P. True[89], M. Trzebinski[39], A. Trzupek[39], C. Tsarouchas[30], J.C-L. Tseng[119], P.V. Tsiareshka[91], D. Tsionou[137], G. Tsipolitis[10], N. Tsirintanis[9], S. Tsiskaridze[12], V. Tsiskaridze[48], E.G. Tskhadadze[51a], I.I. Tsukerman[96], V. Tsulaia[15], S. Tsuno[65], D. Tsybychev[149], A. Tudorache[26a], V. Tudorache[26a], A.N. Tuna[121], S.A. Tupputi[20a,20b], S. Turchikhin[98,ae], D. Turecek[127], I. Turk Cakir[4d], R. Turra[90a,90b], P.M. Tuts[35], A. Tykhonov[74], M. Tylmad[147a,147b], M. Tyndel[130], K. Uchida[21], I. Ueda[156], R. Ueno[29], M. Ughetto[84], M. Ugland[14], M. Uhlenbrock[21], F. Ukegawa[161], G. Unal[30], A. Undrus[25], G. Unel[164], F.C. Ungaro[48], Y. Unno[65], D. Urbaniec[35], P. Urquijo[87], G. Usai[8], A. Usanova[61], L. Vacavant[84], V. Vacek[127], B. Vachon[86], N. Valencic[106], S. Valentinetti[20a,20b], A. Valero[168], L. Valery[34], S. Valkar[128], E. Valladolid Gallego[168], S. Vallecorsa[49], J.A. Valls Ferrer[168], P.C. Van Der Deijl[106], R. van der Geer[106], H. van der Graaf[106], R. Van Der Leeuw[106], D. van der Ster[30], N. van Eldik[30], P. van Gemmeren[6], J. Van Nieuwkoop[143], I. van Vulpen[106], M.C. van Woerden[30], M. Vanadia[133a,133b], W. Vandelli[30], R. Vanguri[121], A. Vaniachine[6], P. Vankov[42], F. Vannucci[79], G. Vardanyan[178], R. Vari[133a], E.W. Varnes[7], T. Varol[85], D. Varouchas[79], A. Vartapetian[8], K.E. Varvell[151], F. Vazeille[34], T. Vazquez Schroeder[54], J. Veatch[7], F. Veloso[125a,125c], S. Veneziano[133a], A. Ventura[72a,72b], D. Ventura[85], M. Venturi[170], N. Venturi[159], A. Venturini[23], V. Vercesi[120a], M. Verducci[139], W. Verkerke[106], J.C. Vermeulen[106], A. Vest[44], M.C. Vetterli[143,d], O. Viazlo[80], I. Vichou[166], T. Vickey[146c,ah], O.E. Vickey Boeriu[146c], G.H.A. Viehhauser[119], S. Viel[169], R. Vigne[30], M. Villa[20a,20b], M. Villaplana Perez[90a,90b], E. Vilucchi[47], M.G. Vincter[29], V.B. Vinogradov[64], J. Virzi[15], I. Vivarelli[150], F. Vives Vaque[3], S. Vlachos[10], D. Vladoiu[99], M. Vlasak[127], A. Vogel[21], M. Vogel[32a], P. Vokac[127], G. Volpi[123a,123b], M. Volpi[87], H. von der Schmitt[100], H. von Radziewski[48], E. von Toerne[21], V. Vorobel[128], K. Vorobev[97], M. Vos[168], R. Voss[30], J.H. Vossebeld[73], N. Vranjes[137], M. Vranjes Milosavljevic[106], V. Vrba[126], M. Vreeswijk[106],

JHEP09(2014)145

T. Vu Anh[48], R. Vuillermet[30], I. Vukotic[31], Z. Vykydal[127], P. Wagner[21], W. Wagner[176], H. Wahlberg[70], S. Wahrmund[44], J. Wakabayashi[102], J. Walder[71], R. Walker[99], W. Walkowiak[142], R. Wall[177], P. Waller[73], B. Walsh[177], C. Wang[152,ai], C. Wang[45], F. Wang[174], H. Wang[15], H. Wang[40], J. Wang[42], J. Wang[33a], K. Wang[86], R. Wang[104], S.M. Wang[152], T. Wang[21], X. Wang[177], C. Wanotayaroj[115], A. Warburton[86], C.P. Ward[28], D.R. Wardrope[77], M. Warsinsky[48], A. Washbrook[46], C. Wasicki[42], I. Watanabe[66], P.M. Watkins[18], A.T. Watson[18], I.J. Watson[151], M.F. Watson[18], G. Watts[139], S. Watts[83], B.M. Waugh[77], S. Webb[83], M.S. Weber[17], S.W. Weber[175], J.S. Webster[31], A.R. Weidberg[119], P. Weigell[100], B. Weinert[60], J. Weingarten[54], C. Weiser[48], H. Weits[106], P.S. Wells[30], T. Wenaus[25], D. Wendland[16], Z. Weng[152,ad], T. Wengler[30], S. Wenig[30], N. Wermes[21], M. Werner[48], P. Werner[30], M. Wessels[58a], J. Wetter[162], K. Whalen[29], A. White[8], M.J. White[1], R. White[32b], S. White[123a,123b], D. Whiteson[164], D. Wicke[176], F.J. Wickens[130], W. Wiedenmann[174], M. Wielers[130], P. Wienemann[21], C. Wiglesworth[36], L.A.M. Wiik-Fuchs[21], P.A. Wijeratne[77], A. Wildauer[100], M.A. Wildt[42,aj], H.G. Wilkens[30], J.Z. Will[99], H.H. Williams[121], S. Williams[28], C. Willis[89], S. Willocq[85], A. Wilson[88], J.A. Wilson[18], I. Wingerter-Seez[5], F. Winklmeier[115], B.T. Winter[21], M. Wittgen[144], T. Wittig[43], J. Wittkowski[99], S.J. Wollstadt[82], M.W. Wolter[39], H. Wolters[125a,125c], B.K. Wosiek[39], J. Wotschack[30], M.J. Woudstra[83], K.W. Wozniak[39], M. Wright[53], M. Wu[55], S.L. Wu[174], X. Wu[49], Y. Wu[88], E. Wulf[35], T.R. Wyatt[83], B.M. Wynne[46], S. Xella[36], M. Xiao[137], D. Xu[33a], L. Xu[33b,ak], B. Yabsley[151], S. Yacoob[146b,al], M. Yamada[65], H. Yamaguchi[156], Y. Yamaguchi[156], A. Yamamoto[65], K. Yamamoto[63], S. Yamamoto[156], T. Yamamura[156], T. Yamanaka[156], K. Yamauchi[102], Y. Yamazaki[66], Z. Yan[22], H. Yang[33e], H. Yang[174], U.K. Yang[83], Y. Yang[110], S. Yanush[92], L. Yao[33a], W-M. Yao[15], Y. Yasu[65], E. Yatsenko[42], K.H. Yau Wong[21], J. Ye[40], S. Ye[25], A.L. Yen[57], E. Yildirim[42], M. Yilmaz[4b], R. Yoosoofmiya[124], K. Yorita[172], R. Yoshida[6], K. Yoshihara[156], C. Young[144], C.J.S. Young[30], S. Youssef[22], D.R. Yu[15], J. Yu[8], J.M. Yu[88], J. Yu[113], L. Yuan[66], A. Yurkewicz[107], B. Zabinski[39], R. Zaidan[62], A.M. Zaitsev[129,y], A. Zaman[149], S. Zambito[23], L. Zanello[133a,133b], D. Zanzi[100], C. Zeitnitz[176], M. Zeman[127], A. Zemla[38a], K. Zengel[23], O. Zenin[129], T. Ženiš[145a], D. Zerwas[116], G. Zevi della Porta[57], D. Zhang[88], F. Zhang[174], H. Zhang[89], J. Zhang[6], L. Zhang[152], X. Zhang[33d], Z. Zhang[116], Z. Zhao[33b], A. Zhemchugov[64], J. Zhong[119], B. Zhou[88], L. Zhou[35], N. Zhou[164], C.G. Zhu[33d], H. Zhu[33a], J. Zhu[88], Y. Zhu[33b], X. Zhuang[33a], K. Zhukov[95], A. Zibell[175], D. Zieminska[60], N.I. Zimine[64], C. Zimmermann[82], R. Zimmermann[21], S. Zimmermann[21], S. Zimmermann[48], Z. Zinonos[54], M. Ziolkowski[142], G. Zobernig[174], A. Zoccoli[20a,20b], M. zur Nedden[16], G. Zurzolo[103a,103b], V. Zutshi[107], L. Zwalinski[30]

[1] Department of Physics, University of Adelaide, Adelaide, Australia
[2] Physics Department, SUNY Albany, Albany NY, United States of America
[3] Department of Physics, University of Alberta, Edmonton AB, Canada
[4] [(a)] Department of Physics, Ankara University, Ankara; [(b)] Department of Physics, Gazi University, Ankara; [(c)] Division of Physics, TOBB University of Economics and Technology, Ankara; [(d)] Turkish Atomic Energy Authority, Ankara, Turkey
[5] LAPP, CNRS/IN2P3 and Université de Savoie, Annecy-le-Vieux, France
[6] High Energy Physics Division, Argonne National Laboratory, Argonne IL, United States of America
[7] Department of Physics, University of Arizona, Tucson AZ, United States of America
[8] Department of Physics, The University of Texas at Arlington, Arlington TX, United States of America
[9] Physics Department, University of Athens, Athens, Greece
[10] Physics Department, National Technical University of Athens, Zografou, Greece
[11] Institute of Physics, Azerbaijan Academy of Sciences, Baku, Azerbaijan
[12] Institut de Física d'Altes Energies and Departament de Física de la Universitat Autònoma de Barcelona, Barcelona, Spain
[13] [(a)] Institute of Physics, University of Belgrade, Belgrade; [(b)] Vinca Institute of Nuclear Sciences, University of Belgrade, Belgrade, Serbia
[14] Department for Physics and Technology, University of Bergen, Bergen, Norway

JHEP09(2014)145

[15] Physics Division, Lawrence Berkeley National Laboratory and University of California, Berkeley CA, United States of America
[16] Department of Physics, Humboldt University, Berlin, Germany
[17] Albert Einstein Center for Fundamental Physics and Laboratory for High Energy Physics, University of Bern, Bern, Switzerland
[18] School of Physics and Astronomy, University of Birmingham, Birmingham, United Kingdom
[19] [(a)] Department of Physics, Bogazici University, Istanbul; [(b)] Department of Physics, Dogus University, Istanbul; [(c)] Department of Physics Engineering, Gaziantep University, Gaziantep, Turkey
[20] [(a)] INFN Sezione di Bologna; [(b)] Dipartimento di Fisica e Astronomia, Università di Bologna, Bologna, Italy
[21] Physikalisches Institut, University of Bonn, Bonn, Germany
[22] Department of Physics, Boston University, Boston MA, United States of America
[23] Department of Physics, Brandeis University, Waltham MA, United States of America
[24] [(a)] Universidade Federal do Rio De Janeiro COPPE/EE/IF, Rio de Janeiro; [(b)] Federal University of Juiz de Fora (UFJF), Juiz de Fora; [(c)] Federal University of Sao Joao del Rei (UFSJ), Sao Joao del Rei; [(d)] Instituto de Fisica, Universidade de Sao Paulo, Sao Paulo, Brazil
[25] Physics Department, Brookhaven National Laboratory, Upton NY, United States of America
[26] [(a)] National Institute of Physics and Nuclear Engineering, Bucharest; [(b)] National Institute for Research and Development of Isotopic and Molecular Technologies, Physics Department, Cluj Napoca; [(c)] University Politehnica Bucharest, Bucharest; [(d)] West University in Timisoara, Timisoara, Romania
[27] Departamento de Física, Universidad de Buenos Aires, Buenos Aires, Argentina
[28] Cavendish Laboratory, University of Cambridge, Cambridge, United Kingdom
[29] Department of Physics, Carleton University, Ottawa ON, Canada
[30] CERN, Geneva, Switzerland
[31] Enrico Fermi Institute, University of Chicago, Chicago IL, United States of America
[32] [(a)] Departamento de Física, Pontificia Universidad Católica de Chile, Santiago; [(b)] Departamento de Física, Universidad Técnica Federico Santa María, Valparaíso, Chile
[33] [(a)] Institute of High Energy Physics, Chinese Academy of Sciences, Beijing; [(b)] Department of Modern Physics, University of Science and Technology of China, Anhui; [(c)] Department of Physics, Nanjing University, Jiangsu; [(d)] School of Physics, Shandong University, Shandong; [(e)] Physics Department, Shanghai Jiao Tong University, Shanghai, China
[34] Laboratoire de Physique Corpusculaire, Clermont Université and Université Blaise Pascal and CNRS/IN2P3, Clermont-Ferrand, France
[35] Nevis Laboratory, Columbia University, Irvington NY, United States of America
[36] Niels Bohr Institute, University of Copenhagen, Kobenhavn, Denmark
[37] [(a)] INFN Gruppo Collegato di Cosenza, Laboratori Nazionali di Frascati; [(b)] Dipartimento di Fisica, Università della Calabria, Rende, Italy
[38] [(a)] AGH University of Science and Technology, Faculty of Physics and Applied Computer Science, Krakow; [(b)] Marian Smoluchowski Institute of Physics, Jagiellonian University, Krakow, Poland
[39] The Henryk Niewodniczanski Institute of Nuclear Physics, Polish Academy of Sciences, Krakow, Poland
[40] Physics Department, Southern Methodist University, Dallas TX, United States of America
[41] Physics Department, University of Texas at Dallas, Richardson TX, United States of America
[42] DESY, Hamburg and Zeuthen, Germany
[43] Institut für Experimentelle Physik IV, Technische Universität Dortmund, Dortmund, Germany
[44] Institut für Kern- und Teilchenphysik, Technische Universität Dresden, Dresden, Germany
[45] Department of Physics, Duke University, Durham NC, United States of America
[46] SUPA - School of Physics and Astronomy, University of Edinburgh, Edinburgh, United Kingdom
[47] INFN Laboratori Nazionali di Frascati, Frascati, Italy
[48] Fakultät für Mathematik und Physik, Albert-Ludwigs-Universität, Freiburg, Germany

JHEP09(2014)145

[49] Section de Physique, Université de Genève, Geneva, Switzerland
[50] [(a)] INFN Sezione di Genova; [(b)] Dipartimento di Fisica, Università di Genova, Genova, Italy
[51] [(a)] E. Andronikashvili Institute of Physics, Iv. Javakhishvili Tbilisi State University, Tbilisi; [(b)] High Energy Physics Institute, Tbilisi State University, Tbilisi, Georgia
[52] II Physikalisches Institut, Justus-Liebig-Universität Giessen, Giessen, Germany
[53] SUPA - School of Physics and Astronomy, University of Glasgow, Glasgow, United Kingdom
[54] II Physikalisches Institut, Georg-August-Universität, Göttingen, Germany
[55] Laboratoire de Physique Subatomique et de Cosmologie, Université Grenoble-Alpes, CNRS/IN2P3, Grenoble, France
[56] Department of Physics, Hampton University, Hampton VA, United States of America
[57] Laboratory for Particle Physics and Cosmology, Harvard University, Cambridge MA, United States of America
[58] [(a)] Kirchhoff-Institut für Physik, Ruprecht-Karls-Universität Heidelberg, Heidelberg; [(b)] Physikalisches Institut, Ruprecht-Karls-Universität Heidelberg, Heidelberg; [(c)] ZITI Institut für technische Informatik, Ruprecht-Karls-Universität Heidelberg, Mannheim, Germany
[59] Faculty of Applied Information Science, Hiroshima Institute of Technology, Hiroshima, Japan
[60] Department of Physics, Indiana University, Bloomington IN, United States of America
[61] Institut für Astro- und Teilchenphysik, Leopold-Franzens-Universität, Innsbruck, Austria
[62] University of Iowa, Iowa City IA, United States of America
[63] Department of Physics and Astronomy, Iowa State University, Ames IA, United States of America
[64] Joint Institute for Nuclear Research, JINR Dubna, Dubna, Russia
[65] KEK, High Energy Accelerator Research Organization, Tsukuba, Japan
[66] Graduate School of Science, Kobe University, Kobe, Japan
[67] Faculty of Science, Kyoto University, Kyoto, Japan
[68] Kyoto University of Education, Kyoto, Japan
[69] Department of Physics, Kyushu University, Fukuoka, Japan
[70] Instituto de Física La Plata, Universidad Nacional de La Plata and CONICET, La Plata, Argentina
[71] Physics Department, Lancaster University, Lancaster, United Kingdom
[72] [(a)] INFN Sezione di Lecce; [(b)] Dipartimento di Matematica e Fisica, Università del Salento, Lecce, Italy
[73] Oliver Lodge Laboratory, University of Liverpool, Liverpool, United Kingdom
[74] Department of Physics, Jožef Stefan Institute and University of Ljubljana, Ljubljana, Slovenia
[75] School of Physics and Astronomy, Queen Mary University of London, London, United Kingdom
[76] Department of Physics, Royal Holloway University of London, Surrey, United Kingdom
[77] Department of Physics and Astronomy, University College London, London, United Kingdom
[78] Louisiana Tech University, Ruston LA, United States of America
[79] Laboratoire de Physique Nucléaire et de Hautes Energies, UPMC and Université Paris-Diderot and CNRS/IN2P3, Paris, France
[80] Fysiska institutionen, Lunds universitet, Lund, Sweden
[81] Departamento de Fisica Teorica C-15, Universidad Autonoma de Madrid, Madrid, Spain
[82] Institut für Physik, Universität Mainz, Mainz, Germany
[83] School of Physics and Astronomy, University of Manchester, Manchester, United Kingdom
[84] CPPM, Aix-Marseille Université and CNRS/IN2P3, Marseille, France
[85] Department of Physics, University of Massachusetts, Amherst MA, United States of America
[86] Department of Physics, McGill University, Montreal QC, Canada
[87] School of Physics, University of Melbourne, Victoria, Australia
[88] Department of Physics, The University of Michigan, Ann Arbor MI, United States of America
[89] Department of Physics and Astronomy, Michigan State University, East Lansing MI, United States of America
[90] [(a)] INFN Sezione di Milano; [(b)] Dipartimento di Fisica, Università di Milano, Milano, Italy
[91] B.I. Stepanov Institute of Physics, National Academy of Sciences of Belarus, Minsk, Republic of Belarus

JHEP09(2014)145

[92] National Scientific and Educational Centre for Particle and High Energy Physics, Minsk, Republic of Belarus
[93] Department of Physics, Massachusetts Institute of Technology, Cambridge MA, United States of America
[94] Group of Particle Physics, University of Montreal, Montreal QC, Canada
[95] P.N. Lebedev Institute of Physics, Academy of Sciences, Moscow, Russia
[96] Institute for Theoretical and Experimental Physics (ITEP), Moscow, Russia
[97] Moscow Engineering and Physics Institute (MEPhI), Moscow, Russia
[98] D.V.Skobeltsyn Institute of Nuclear Physics, M.V.Lomonosov Moscow State University, Moscow, Russia
[99] Fakultät für Physik, Ludwig-Maximilians-Universität München, München, Germany
[100] Max-Planck-Institut für Physik (Werner-Heisenberg-Institut), München, Germany
[101] Nagasaki Institute of Applied Science, Nagasaki, Japan
[102] Graduate School of Science and Kobayashi-Maskawa Institute, Nagoya University, Nagoya, Japan
[103] [(a)] INFN Sezione di Napoli; [(b)] Dipartimento di Fisica, Università di Napoli, Napoli, Italy
[104] Department of Physics and Astronomy, University of New Mexico, Albuquerque NM, United States of America
[105] Institute for Mathematics, Astrophysics and Particle Physics, Radboud University Nijmegen/Nikhef, Nijmegen, Netherlands
[106] Nikhef National Institute for Subatomic Physics and University of Amsterdam, Amsterdam, Netherlands
[107] Department of Physics, Northern Illinois University, DeKalb IL, United States of America
[108] Budker Institute of Nuclear Physics, SB RAS, Novosibirsk, Russia
[109] Department of Physics, New York University, New York NY, United States of America
[110] Ohio State University, Columbus OH, United States of America
[111] Faculty of Science, Okayama University, Okayama, Japan
[112] Homer L. Dodge Department of Physics and Astronomy, University of Oklahoma, Norman OK, United States of America
[113] Department of Physics, Oklahoma State University, Stillwater OK, United States of America
[114] Palacký University, RCPTM, Olomouc, Czech Republic
[115] Center for High Energy Physics, University of Oregon, Eugene OR, United States of America
[116] LAL, Université Paris-Sud and CNRS/IN2P3, Orsay, France
[117] Graduate School of Science, Osaka University, Osaka, Japan
[118] Department of Physics, University of Oslo, Oslo, Norway
[119] Department of Physics, Oxford University, Oxford, United Kingdom
[120] [(a)] INFN Sezione di Pavia; [(b)] Dipartimento di Fisica, Università di Pavia, Pavia, Italy
[121] Department of Physics, University of Pennsylvania, Philadelphia PA, United States of America
[122] Petersburg Nuclear Physics Institute, Gatchina, Russia
[123] [(a)] INFN Sezione di Pisa; [(b)] Dipartimento di Fisica E. Fermi, Università di Pisa, Pisa, Italy
[124] Department of Physics and Astronomy, University of Pittsburgh, Pittsburgh PA, United States of America
[125] [(a)] Laboratorio de Instrumentacao e Fisica Experimental de Particulas - LIP, Lisboa; [(b)] Faculdade de Ciências, Universidade de Lisboa, Lisboa; [(c)] Department of Physics, University of Coimbra, Coimbra; [(d)] Centro de Física Nuclear da Universidade de Lisboa, Lisboa; [(e)] Departamento de Fisica, Universidade do Minho, Braga; [(f)] Departamento de Fisica Teorica y del Cosmos and CAFPE, Universidad de Granada, Granada (Spain); [(g)] Dep Fisica and CEFITEC of Faculdade de Ciencias e Tecnologia, Universidade Nova de Lisboa, Caparica, Portugal
[126] Institute of Physics, Academy of Sciences of the Czech Republic, Praha, Czech Republic
[127] Czech Technical University in Prague, Praha, Czech Republic
[128] Faculty of Mathematics and Physics, Charles University in Prague, Praha, Czech Republic
[129] State Research Center Institute for High Energy Physics, Protvino, Russia
[130] Particle Physics Department, Rutherford Appleton Laboratory, Didcot, United Kingdom

JHEP09(2014)145

[131] Physics Department, University of Regina, Regina SK, Canada
[132] Ritsumeikan University, Kusatsu, Shiga, Japan
[133] [(a)] INFN Sezione di Roma; [(b)] Dipartimento di Fisica, Sapienza Università di Roma, Roma, Italy
[134] [(a)] INFN Sezione di Roma Tor Vergata; [(b)] Dipartimento di Fisica, Università di Roma Tor Vergata, Roma, Italy
[135] [(a)] INFN Sezione di Roma Tre; [(b)] Dipartimento di Matematica e Fisica, Università Roma Tre, Roma, Italy
[136] [(a)] Faculté des Sciences Ain Chock, Réseau Universitaire de Physique des Hautes Energies - Université Hassan II, Casablanca; [(b)] Centre National de l'Energie des Sciences Techniques Nucleaires, Rabat; [(c)] Faculté des Sciences Semlalia, Université Cadi Ayyad, LPHEA-Marrakech; [(d)] Faculté des Sciences, Université Mohamed Premier and LPTPM, Oujda; [(e)] Faculté des sciences, Université Mohammed V-Agdal, Rabat, Morocco
[137] DSM/IRFU (Institut de Recherches sur les Lois Fondamentales de l'Univers), CEA Saclay (Commissariat à l'Energie Atomique et aux Energies Alternatives), Gif-sur-Yvette, France
[138] Santa Cruz Institute for Particle Physics, University of California Santa Cruz, Santa Cruz CA, United States of America
[139] Department of Physics, University of Washington, Seattle WA, United States of America
[140] Department of Physics and Astronomy, University of Sheffield, Sheffield, United Kingdom
[141] Department of Physics, Shinshu University, Nagano, Japan
[142] Fachbereich Physik, Universität Siegen, Siegen, Germany
[143] Department of Physics, Simon Fraser University, Burnaby BC, Canada
[144] SLAC National Accelerator Laboratory, Stanford CA, United States of America
[145] [(a)] Faculty of Mathematics, Physics & Informatics, Comenius University, Bratislava; [(b)] Department of Subnuclear Physics, Institute of Experimental Physics of the Slovak Academy of Sciences, Kosice, Slovak Republic
[146] [(a)] Department of Physics, University of Cape Town, Cape Town; [(b)] Department of Physics, University of Johannesburg, Johannesburg; [(c)] School of Physics, University of the Witwatersrand, Johannesburg, South Africa
[147] [(a)] Department of Physics, Stockholm University; [(b)] The Oskar Klein Centre, Stockholm, Sweden
[148] Physics Department, Royal Institute of Technology, Stockholm, Sweden
[149] Departments of Physics & Astronomy and Chemistry, Stony Brook University, Stony Brook NY, United States of America
[150] Department of Physics and Astronomy, University of Sussex, Brighton, United Kingdom
[151] School of Physics, University of Sydney, Sydney, Australia
[152] Institute of Physics, Academia Sinica, Taipei, Taiwan
[153] Department of Physics, Technion: Israel Institute of Technology, Haifa, Israel
[154] Raymond and Beverly Sackler School of Physics and Astronomy, Tel Aviv University, Tel Aviv, Israel
[155] Department of Physics, Aristotle University of Thessaloniki, Thessaloniki, Greece
[156] International Center for Elementary Particle Physics and Department of Physics, The University of Tokyo, Tokyo, Japan
[157] Graduate School of Science and Technology, Tokyo Metropolitan University, Tokyo, Japan
[158] Department of Physics, Tokyo Institute of Technology, Tokyo, Japan
[159] Department of Physics, University of Toronto, Toronto ON, Canada
[160] [(a)] TRIUMF, Vancouver BC; [(b)] Department of Physics and Astronomy, York University, Toronto ON, Canada
[161] Faculty of Pure and Applied Sciences, University of Tsukuba, Tsukuba, Japan
[162] Department of Physics and Astronomy, Tufts University, Medford MA, United States of America
[163] Centro de Investigaciones, Universidad Antonio Narino, Bogota, Colombia
[164] Department of Physics and Astronomy, University of California Irvine, Irvine CA, United States of America
[165] [(a)] INFN Gruppo Collegato di Udine, Sezione di Trieste, Udine; [(b)] ICTP, Trieste; [(c)] Dipartimento di Chimica, Fisica e Ambiente, Università di Udine, Udine, Italy

JHEP09(2014)145

[166] Department of Physics, University of Illinois, Urbana IL, United States of America
[167] Department of Physics and Astronomy, University of Uppsala, Uppsala, Sweden
[168] Instituto de Física Corpuscular (IFIC) and Departamento de Física Atómica, Molecular y Nuclear and Departamento de Ingeniería Electrónica and Instituto de Microelectrónica de Barcelona (IMB-CNM), University of Valencia and CSIC, Valencia, Spain
[169] Department of Physics, University of British Columbia, Vancouver BC, Canada
[170] Department of Physics and Astronomy, University of Victoria, Victoria BC, Canada
[171] Department of Physics, University of Warwick, Coventry, United Kingdom
[172] Waseda University, Tokyo, Japan
[173] Department of Particle Physics, The Weizmann Institute of Science, Rehovot, Israel
[174] Department of Physics, University of Wisconsin, Madison WI, United States of America
[175] Fakultät für Physik und Astronomie, Julius-Maximilians-Universität, Würzburg, Germany
[176] Fachbereich C Physik, Bergische Universität Wuppertal, Wuppertal, Germany
[177] Department of Physics, Yale University, New Haven CT, United States of America
[178] Yerevan Physics Institute, Yerevan, Armenia
[179] Centre de Calcul de l'Institut National de Physique Nucléaire et de Physique des Particules (IN2P3), Villeurbanne, France

[a] Also at Department of Physics, King's College London, London, United Kingdom
[b] Also at Institute of Physics, Azerbaijan Academy of Sciences, Baku, Azerbaijan
[c] Also at Particle Physics Department, Rutherford Appleton Laboratory, Didcot, United Kingdom
[d] Also at TRIUMF, Vancouver BC, Canada
[e] Also at Department of Physics, California State University, Fresno CA, United States of America
[f] Also at CPPM, Aix-Marseille Université and CNRS/IN2P3, Marseille, France
[g] Also at Università di Napoli Parthenope, Napoli, Italy
[h] Also at Institute of Particle Physics (IPP), Canada
[i] Also at Department of Physics, St. Petersburg State Polytechnical University, St. Petersburg, Russia
[j] Also at Chinese University of Hong Kong, China
[k] Also at Department of Financial and Management Engineering, University of the Aegean, Chios, Greece
[l] Also at Louisiana Tech University, Ruston LA, United States of America
[m] Also at Institucio Catalana de Recerca i Estudis Avancats, ICREA, Barcelona, Spain
[n] Also at Institute of Theoretical Physics, Ilia State University, Tbilisi, Georgia
[o] Also at CERN, Geneva, Switzerland
[p] Also at Ochadai Academic Production, Ochanomizu University, Tokyo, Japan
[q] Also at Manhattan College, New York NY, United States of America
[r] Also at Novosibirsk State University, Novosibirsk, Russia
[s] Also at Institute of Physics, Academia Sinica, Taipei, Taiwan
[t] Also at LAL, Université Paris-Sud and CNRS/IN2P3, Orsay, France
[u] Also at Academia Sinica Grid Computing, Institute of Physics, Academia Sinica, Taipei, Taiwan
[v] Also at Laboratoire de Physique Nucléaire et de Hautes Energies, UPMC and Université Paris-Diderot and CNRS/IN2P3, Paris, France
[w] Also at School of Physical Sciences, National Institute of Science Education and Research, Bhubaneswar, India
[x] Also at Dipartimento di Fisica, Sapienza Università di Roma, Roma, Italy
[y] Also at Moscow Institute of Physics and Technology State University, Dolgoprudny, Russia
[z] Also at Section de Physique, Université de Genève, Geneva, Switzerland
[aa] Also at Department of Physics, The University of Texas at Austin, Austin TX, United States of America
[ab] Also at International School for Advanced Studies (SISSA), Trieste, Italy
[ac] Also at Department of Physics and Astronomy, University of South Carolina, Columbia SC, United States of America

JHEP09(2014)145

[ad] Also at School of Physics and Engineering, Sun Yat-sen University, Guangzhou, China
[ae] Also at Faculty of Physics, M.V.Lomonosov Moscow State University, Moscow, Russia
[af] Also at Moscow Engineering and Physics Institute (MEPhI), Moscow, Russia
[ag] Also at Institute for Particle and Nuclear Physics, Wigner Research Centre for Physics, Budapest, Hungary
[ah] Also at Department of Physics, Oxford University, Oxford, United Kingdom
[ai] Also at Department of Physics, Nanjing University, Jiangsu, China
[aj] Also at Institut für Experimentalphysik, Universität Hamburg, Hamburg, Germany
[ak] Also at Department of Physics, The University of Michigan, Ann Arbor MI, United States of America
[al] Also at Discipline of Physics, University of KwaZulu-Natal, Durban, South Africa
[*] Deceased

JHEP09(2014)145